ERJ open research
THE BEST IN OPEN ACCESS BASIC, TRANSLATIONAL & CLINICAL RESPIRATORY RESEARCH

Early View

Original research article

Impact of computed tomographic patterns and extent on clinical management and outcomes of patients with organizing pneumonia

Tang-Hsiu Huang, Sheng-Huan Wei, Li-Ting Huang, Hong-Ping Er, Yu-Ting Yu, Chung-Ta Lee, Yau-Lin Tseng, Chao-Liang Wu

Please cite this article as: Huang T-H, Wei S-H, Huang L-T, *et al*. Impact of computed tomographic patterns and extent on clinical management and outcomes of patients with organizing pneumonia. *ERJ Open Res* 2022; in press (https://doi.org/10.1183/23120541.00505-2022).

This manuscript has recently been accepted for publication in the *ERJ Open Research*. It is published here in its accepted form prior to copyediting and typesetting by our production team. After these production processes are complete and the authors have approved the resulting proofs, the article will move to the latest issue of the ERJOR online.

Copyright ©The authors 2022. This version is distributed under the terms of the Creative Commons Attribution Non-Commercial Licence 4.0. For commercial reproduction rights and permissions contact permissions@ersnet.org

Title: Impact of computed tomographic patterns and extent on clinical management and outcomes of patients with organizing pneumonia

Authors' full names: Tang-Hsiu Huang[1,2]*, Sheng-Huan Wei[1]*, Li-Ting Huang[3], Hong-Ping Er[1,4], Yu-Ting Yu[5], Chung-Ta Lee[5], Yau-Lin Tseng[6], Chao-Liang Wu[2,7]

Authors' affiliation(s):

[1] Division of Chest Medicine, Department of Internal Medicine, National Cheng Kung University, College of Medicine and Hospital, Tainan, Taiwan.

[2] Institute of Clinical Medicine, College of Medicine, National Cheng Kung University, Tainan, Taiwan.

[3] Department of Diagnostic Radiology, National Cheng Kung University Hospital, College of Medicine, National Cheng Kung University, Tainan, Taiwan

[4] Department of Internal Medicine, Tainan Hospital, Ministry of Health and Welfare, Tainan, Taiwan

[5] Department of Pathology, National Cheng Kung University Hospital, College of Medicine, National Cheng Kung University, Tainan, Taiwan

[6] Division of Thoracic Surgery, Department of Surgery, National Cheng Kung University Hospital, College of Medicine, National Cheng Kung University, Tainan, Taiwan

[7] Department of Biochemistry and Molecular Biology, College of Medicine, National Cheng Kung University, Tainan, Taiwan

*** These two authors <u>contributed equally</u> to this manuscript**

Corresponding author details:

Name: Chao-Liang Wu

Department of Biochemistry and Molecular Biology, College of Medicine, National Cheng Kung University,

Tainan, Taiwan (R.O.C.)

Tel: +886-6-2353535 ext. 5536 / Fax number: +886-6-2741692

Email: wumolbio@mail.ncku.edu.tw

Word count: abstract 250 words; main text 3326 words

Take home message: Patients with organizing pneumonia whose CT images exhibit multi-lobe involvement and mixed patterns have an enhanced risk of adverse outcomes.

Abstract

Background: Organizing pneumonia (OP) has variable clinical and radiographic presentations and unstandardized treatments. Most patients with OP have favourable outcomes, but some develop respiratory insufficiency, experience recurrence, or die. In this study we investigated the impact of computed tomographic (CT) patterns and extent of OP on the diagnostic and therapeutic management that patients received, and that on the therapeutic response and prognosis (particularly the risk of respiratory insufficiency and death).

Methods: We retrospectively studied 156 patients with OP followed at our hospital between 2010 and 2021. The diagnosis was confirmed histologically and verified by multidisciplinary specialists. We performed Firth's logistic regression to determine the relationship between CT features and aetiologies, management, and outcomes including the risk of severe disease (defined as the need of supplemental oxygen or mechanical ventilation). We conducted Kaplan-Meier analyses to assess survival differences.

Results: Patients exhibiting multi-lobe involvement or mixed patterns, or both, were more likely to have secondary OP and receive immunosuppressants. Higher proportions of these patients experienced recurrence. Compared to patients with single-lobe involvement and single-pattern, they also had an enhanced risk of severe disease (the adjusted odds ratio for patients who simultaneously had multi-lobe involvement and mixed patterns was 27.64; 95% confidence interval, 8.25 – 127.44). Besides, these patients had decreased survival probabilities.

Conclusion: Different CT features of OP impact patients' management and prognosis. When treating patients with OP exhibiting multi-lobe involvement or mixed patterns, or both, it is important to identify the possible causative aetiology and follow closely for adverse outcomes.

Keywords: interstitial lung disease, immunosuppressive agents, recurrence, respiratory insufficiency

Main Text

Introduction

Organizing pneumonia (OP) is a rare type of interstitial lung disease [1-3]. It is either cryptogenic or secondary, depending on whether a causative aetiology is identified [2-5]. Common aetiologies of secondary OP include autoimmune disorder, drug reactions, inhalational injury, and post-transplantation [1,3,5]. The histology of OP has been well described and that helps to resolve diagnostic uncertainty. Typical histological features of OP include Masson bodies (type III collagen-rich granulation plugs) filling in the distal airspaces in a background of well-preserved alveolar architecture accompanied by a mild-to-moderate degree of interstitial infiltrate by chronic inflammatory cells [2-4, 6-7]. Historically OP was used interchangeably with another term “BOOP” (bronchiolitis obliterans organizing pneumonia), but these two terms now specify distinct entities based on histologic, radiographic, and spirometric differences [1-3]. The clinical presentations of OP, on the other hand, are quite nonspecific and variable. Some patients are asymptomatic or complain only of non-productive cough with or without flu-like illness, while others have manifestations that are indistinguishable from acute pyogenic pneumonia [3-8]. Still others may develop severe disease, progressively leading to hypoxemia, respiratory insufficiency, or death [3, 9-12]. Similarly, although corticosteroids are commonly

used, the treatment for OP has not been standardized, and patients may exhibit variable therapeutic responses [1-3, 13-15].

Computed tomographic (CT) features of OP also varies. Alveolar consolidation is the archetypal pattern, but other CT patterns have been subsequently reported. Different patterns of OP may appear alone or in combination, involving the lung parenchyma focally or extensively [1-3, 13-18]. Radiographic differential diagnosis includes infectious pneumonia or granuloma, malignancy, vasculitis, and some forms of interstitial lung diseases (ILDs) with an alveolar component (particularly acute interstitial pneumonia, nonspecific interstitial pneumonia, eosinophilic pneumonia, hypersensitivity pneumonia, and pulmonary alveolar proteinosis) [1-4]. CT findings, however, can rapidly and non-invasively provide useful information for the initial diagnosis, assessment, and subsequent follow-up of OP. Previous researchers have found that certain imaging patterns, and the extent of consolidation, on CT images are associated with residual disease and recurrence of OP [14-15, 19-20]. Nevertheless, it remains to be determined whether patients exhibiting different CT features would undergo different management and have distinct risk of other clinically important outcomes. Therefore, in this study, we aimed to investigate the impact of CT imaging patterns and extent of OP on the modalities of diagnostic and therapeutic management that patients received, and that on the

therapeutic response and prognosis, particularly the risk of respiratory insufficiency and death.

Material and Methods

Study design and population

We conducted this single-center retrospective study, analysing the clinical and CT presentations of adult patients (age ≥ 20 years) with OP longitudinally followed at National Cheng Kung University Hospital (NCKUH, a tertiary medical center in southern Taiwan) between January 1, 2010, and December 31, 2021. The study protocol has been approved by the Institutional Review Board of NCKUH (B-ER-111-038). The clinical and radiographic manifestations of OP are nonspecific. Therefore, to ensure diagnostic accuracy that was essential for all subsequent analysis, we required that all candidates for study inclusion must have previously undergone lung biopsy and histologic study to exclude masquerading conditions (Supplemental Document 1).

Review of the diagnosis and histology

For each potential candidate, the de-identified clinical and laboratory data, histologic slides and reports, serial CT images and chest radiographs, and records of

treatments and outcomes were carefully reviewed. The diagnosis of OP (originally made by treating physicians) was verified jointly by the authors consisting of three pulmonologists, a pulmonary radiologist, two pathologists, a thoracic surgeon, and a clinical biochemist (Supplemental Document 1). Consensus was reached by direct discussion. To be considered as having definite OP (either cryptogenic or secondary), a candidate must have compatible symptomology and CT images [1-4], typical histological features [1-3, 6-7], and the absence of clinical or histological findings (initially or subsequently) suggesting alternative diagnoses (particularly evidence of ongoing infection, bronchiole-centered or bronchiole-obliterative pathology, granulomas, vasculitis, neoplasm, alveolar hemorrhage or proteinosis, and dense infiltration of neutrophils, monocyte-macrophages, or eosinophils) [3].

Acquisition of CT images and the classification of CT features

Thoracic CT was acquired at NCKUH during the study period by using scanners from two different manufacturers (Siemens Healthineers and General Electric Healthcare). The patient's entire lung was scanned in the supine caudocranial direction with suspended full inspiration. The scanning parameters were 100 or 120 kVp, 1- or 0.6 mm collimation, and a pitch of 1. Volumetric CT images at 1.0 to 1.5 mm slice thickness were reconstructed into contiguous axial images at 2.0 mm and

5.0 mm slice thickness and 5mm intervals. High-spatial-frequency reconstruction images were reconstructed at 1 to 1.25 mm of slice thickness and 10 mm intervals. Contrast medium was administered based on clinical indications.

For each patient, the last CT scan that was nearest in time before the histologic diagnosis of OP was selected as the baseline. CT images were reviewed and classified independently by a pulmonary radiologist and two pulmonologists unaware of patients' aetiologies and outcomes, whereby a final consensus was reached by direct discussion. Radiopacity of OP was classified as alveolar consolidation, ground-glass opacity (GGO), bronchocentric opacity, nodular, mass-like, band-like, reticulo-infiltrative, crazy paving, or reverse halo sign, according to previously published descriptions [1-3, 16-18, 21-22]. Patients whose images exhibited only one of these nine patterns were considered as having "single-pattern", whereas those exhibiting multiple patterns simultaneously, "mixed-pattern". Patients were also classified according to the extent of involvement by OP as "single-lobe" or "multi-lobe". Based on the combined assessment of patterns and extent, we further stratified the patients into three subgroups: Group 1 included patients exhibiting single-pattern and single-lobe involvement, Groups 2, single-lobe and mixed-pattern or multi-lobe and single-pattern, and Group 3, multi-lobe and mixed-pattern.

Definition of outcomes

Outcomes of all included patients were determined jointly by the authors (Supplemental Document 1). Briefly, “improvement” indicates the radiographic resolution of OP by more than fifty percent (with or without decrement in radiodensity) during follow-ups without re-emergence, plus symptomatic alleviation with or without de-escalation in relevant pharmacological (for example, decrement in the number and dosage of immunosuppressive and/or symptom-relieving agents) and non-pharmacological management (for example, decrement or discontinue ation in oxygen supplementation or mechanical ventilatory support). “Persistent disease” indicates no subsequent radiographic change or a diminishment of less than fifty percent, with the associated persistence (or limited change) in clinical symptoms and management. “Recurrence” refers to the radiographic re-emergence or enlargement of pneumonic lesions following an initial “improvement” with the associated escalation in symptoms and management, but without any alternative explanation. The radiographic opacities of OP may fluctuate and migrate with time. Depending on the timing and extent of new migratory opacities in relation to serial changes of the initial lesions and symptoms, patients can be classified has having “persistent disease” or “recurrence” based on the above definitions. “Death” specifies only those mortality events that were causally OP-related. Patients were considered to have the “need of

supplemental oxygen" if they had ever breathed supplemental oxygen via any mode to correct hypoxemia during the follow-up; by this definition elective peri-biopsy oxygen supplement was excluded. "Use of mechanical ventilation" refers specifically to the application of either non-invasive or invasive positive-pressure mechanical ventilation to treat OP-related respiratory failure, but excluding mechanical ventilation during general anesthesia for surgical biopsy. Changes in pulmonary function tests were not included as essential criteria for the determination of outcomes because only 27 (17%) patients in our cohort had a follow-up pulmonary spirometry (at the discretion of the treating physicians). However, for those patients having follow-up tests, serial changes in forced vital capacity (FVC) were calculated and used as supporting data for outcome assignment.

Statistical analysis

Categorical data are presented as counts and percentages, and continuous data are presented as means and standard deviation if normally distributed, or as medians and interquartile ranges (IQR) if otherwise. No imputation was made for missing data. Variables were analyzed for between-group non-random differences using the Mann-Whitney U test or Fischer's exact test, whichever was more appropriate. Fleiss' kappa values were calculated to assess the initial (before the final consensus)

inter-observer agreement among the three independent reviewers of CT features. Univariate and multivariable Firth's logistic regression models were constructed to analyze the relationship between CT features and outcomes. For multivariable analyses, we incorporated sex, age, body heights and weights, smoking status, Charlson comorbidity indices, and aetiology as covariables; no multicollinearity was found among these variables. Survival difference was assessed by Kaplan-Meier methods. Sensitivity analysis was performed to determine the potential effect from unidentified confounders. A P value < 0.05 was considered to indicate statistical significance, and all tests were two-tailed. Statistical analysis was performed using the statistical packages SPSS (Version 26) and R (Version 3.6.3). Graphs were plotted using MedCal (Version 20.109).

Results

Patient characteristics, treatments, and outcomes

In total 156 patients were included in this study (Figure 1); Table 1 displays their characteristics and outcomes. Overall, the cohort was relatively male-predominant, with a median age of 61.5 (IQR, 54.4 to 71.1) years. More than two thirds of the patients never smoked. Ninety-one (58%) patients underwent video-assisted thoracoscopic biopsy, fifteen (10%) received transbronchial forceps

biopsy, while forty-nine (31%) and one (1%) received percutaneous needle biopsy via CT-guidance and sonography-guidance, respectively. Regarding aetiology, 130 (83%) patients were classified as having cryptogenic OP. Of those twenty-six (17%) with secondary OP, fourteen were connective tissue diseases (CTD)-related, ten were drug-related (most frequently amiodarone), and two were post-transplantation (of peripheral-blood stem cells). Patients were followed for a median of 120.6 (IQR, 31.1 to 269.4) weeks. Ninety-three (60%) patients received non-pharmacological treatments, either close observation or resection (as during the initial biopsy). The remaining sixty-three (40%) received immunosuppressive therapies that involved corticosteroid in most cases. During the follow-ups, forty-one (26%) patients developed hypoxemia requiring supplemental oxygen, of whom seventeen (11%) deteriorated to respiratory failure mandating mechanical ventilation, while the others were successfully weaned off supplemental oxygen. All patients had at least one follow-up radiographic study for comparison, wherein 101 (65%) had at least one follow-up CT scan. The median duration of radiographic follow-up was 27.5 (IQR, 14.2 to 88.0) weeks. Overall, 129 (82%) patients exhibited improvement of the OP, eleven (7%) had persistent disease, five (3%) experienced recurrence, and eleven (8%) died from OP. Follow-up pulmonary spirometry was available in 27 patients,

which showed changes that were consistent with the outcome assignment (Supplemental Table S1).

CT features of the cohort

The median time between the baseline CT scan and the histologic establishment of the OP diagnosis was 13 (IQR, 7 to 30) days. Table 2 summarizes the various CT features of OP observed in our cohort. The initial pre-consensus inter-observer agreement was good (Supplemental Table S2). Comparable proportions of the cohort had single- and multi-lobe involvement. Regarding imaging patterns, two thirds of the patients exhibited a single pattern, while the other third had mixed patterns. The most common pattern (either as single- or mixed-pattern) in the cohort was alveolar consolidation (45%), which was followed in decreasing frequencies by nodular (34%), GGO (31%), mass-like (14%), and bronchocentric opacity (13%). Less common patterns included reticulo-infiltrative (4%), reverse halo sign (4%), and crazy paving (3%). The band-like pattern was not observed. Examples of the various CT features are presented in Figure 2 and Supplemental Figure S1.

CT features and outcomes

No significant difference was found in methods of biopsy and seasons of diagnosis among patients with different CT features. However, higher proportions of patients with multi-lobe involvement, and of patients with mixed patterns, had secondary OP and received immunosuppressive therapies. Compared to those with single-lobe and single-pattern OP, higher proportions of patients with multi-lobe involvement and mixed patterns developed hypoxemia and respiratory failure. All five patients with recurrence had multi-lobe involvement and mixed patterns. Of those eleven patients who died, ten exhibited multi-lobe and mixed-pattern OP, and one had single-pattern but multi-lobe involvement (Supplemental Table S3). When the cohort was stratified into Groups 1 to 3 as described above (Supplemental Table S4 shows characteristics of the 3 subgroups), we obtained concordant findings such that with increasing complexity and extent of pneumonic involvement from Group 1 to Group 3, we observed incremental proportions of patients who had secondary OP, received immunosuppressive therapies, and developed adverse outcomes (Figure 3 and Supplemental Table S3). Moreover, baseline pulmonary function measurements were available from 86 patients. When we further stratified these patients according to CT features and baseline FVC values using the cutoff levels of 50% and 80% of prediction, similar trends were observed such that Group 3 patients consistently had

the highest frequencies of adverse outcome events regardless of what the baseline FVC strata was (Supplemental Table S5).

Because the frequencies of some adverse outcomes are very low in certain subgroups (Figure 3), for subsequent analyses, “need of supplemental oxygen” and “use of mechanical ventilation” were combined into one composite outcome as “severe disease”. Univariate and multivariable Firth’s logistic regression analysis showed that “multi-lobe” and “mixed-pattern”, when analysed separately, were each associated with secondary OP and subsequent immunosuppressive treatments: the adjusted odds ratio (aOR) of secondary OP and the aOR of immunosuppressive treatments were 6.99 (95% confidence interval or 95% CI, 2.35–27.76) and 12.45 (95% CI, 5.20–33.70) for “multi-lobe”, and 6.38 (95% CI, 2.51–18.14) and 7.97 (95% CI, 3.55–18.94) for “mixed-pattern”, respectively. “Multi-lobe” and “mixed-pattern” were also each associated with an enhanced risk of severe disease: the aOR was 17.84 (95% CI, 5.55–79.66) for “multi-lobe” and 12.87 (95% CI, 5.12 – 36.50) for “mixed-pattern”. When “multi-lobe” and “mixed-pattern” were analysed simultaneously within the same model, we obtained similar findings. The analysis was then performed among the three subgroups. Relative to Group 1, patients in Group 2 had significantly increased odds of secondary OP (aOR, 11.77; 95% CI, 2.36–115.80) and immunosuppressive treatments (aOR, 3.39; 95% CI, 1.11 – 10.67),

and the odds ratios rose further in Group 3 (aORs were 19.08, 95% CI, 4.46–177.80, and 19.58, 95% CI, 7.28–59.81, respectively). Moreover, while patients in Group 2 exhibited a trend of increasing odds (aOR, 4.24, 95% CI, 0.89–22.84), patients in Group 3 had a significantly enhanced risk of severe disease (aOR, 27.64, 95% CI, 8.25 – 127.44; Supplemental Table S6–S8 and Figure 4). Results from sensitivity analyses showed that, even in the presence of an unidentified confounder, findings derived from the above analyses remained consistent (Supplemental Figure S2).

CT features and survival difference

The overall prognosis of OP was good, but Kaplan-Meier analyses detected significant differences in survival probabilities among patients with different CT features. Compared to “single-lobe” and “single-pattern”, patients having multi-lobe involvement and those exhibiting mixed patterns had decreased survival probabilities. Similarly, the survival probabilities differed among the three subgroups, with Group 3 exhibiting the worst survival (Figure 5).

Discussion

In this study, we found that CT features of OP had impact on important clinical aspects. Specifically, patients whose OP exhibited multi-lobe involvement, or

mixed CT patterns, or both, were more likely to have an identifiable causative aetiology and receive immunosuppressive therapies. These patients also had an enhanced risk of severe disease and lower probabilities of survival. Higher proportions of these patients also experienced recurrence. Pathophysiologically our findings appear reasonable. Aetiologies of secondary OP are generally systemic processes and would therefore affect the lungs extensively. This explains for the higher odds of secondary OP in patients with multi-focal and mixed-pattern lesions. Moreover, increasing extent and complexity of the parenchymal involvement by OP is likely to increasingly impair the pulmonary function (this was supported by the significant decrement in FVC and TLC from Group 1 to Group 3; Supplemental Table S4). This subsequently leads to an enhanced disease severity and thereby the escalation of therapeutic actions. Furthermore, CT features provides prognostic prediction beyond the revelation of structural and physiological impairment.

Previous researchers have investigated potential predictors of treatment response and recurrence of OP [14-15, 19-20, 25-28]. The study by Barroso *et al.* found that higher proportions of patients with recurrence had multi-focal opacities on chest radiographs [19]. Saito *et al.* also identified certain CT features as possible predictors of recurrence in univariate analyses [20]. By analysing serial CT images in a cohort of Korean patient with cryptogenic OP, Chung *et al*. reported that the extent

of consolidation on CT images is associated with residual disease [14]. Recently, Cho *et al*. also found that the presence of bronchiectasis and >10% of consolidation on CT images were associated with recurrence [15]. Our study is consistent with these previous works in demonstrating a significantly higher frequency of recurrence among patients with multi-lobe (more extensive) OP. On the other hand, we identified "mixed-pattern" as still another feature associated with recurrence. In addition to recurrence, we further addressed the risk prediction of other clinically important outcomes. The methods by which we stratified CT features and grouped the patients are straightforward, avoiding the complexity of radiopacity quantification and allowing for convenient application in real-world clinical settings.

The heterogeneity between cryptogenic and secondary OP (particularly CTD-related) might be a confounding factor [5, 15, 23-24]. Cho *et al.* reported that CTD-related OP was also associated with a higher risk of residual disease and recurrence [15]. In our cohort, patients with secondary OP indeed had a lower median body weight, lower spirometric volumes, a higher median Charlson comorbidity index, and higher frequencies of adverse outcomes (Supplemental Table 9). However, when analyses were performed solely in patients with cryptogenic OP, we obtained consistent findings (Supplemental Table S10 and Supplemental Figure S3a). Lower survival probabilities were also observed in patients with cryptogenic OP exhibiting

multi-lobe involvement and mixed patterns (Supplemental Figure S3b-S3d). Therefore, the findings of our study were not biased toward the contribution from patients with secondary OP.

There are possible limitations to our study. We included only patients whose OP had been confirmed histologically, though OP can also be diagnosed clinically. Nevertheless, the clinical and radiographic characteristics of OP are nonspecific and even indistinguishable from bacterial pneumonia and some ILDs. Had we included patients based on clinical diagnoses only, we might have included other mimicking conditions than true OP. We might have also missed out those patients exhibiting unusual radiographic features (such as mass-like and reticulo-infiltrative patterns) whereby histology would be necessary for the definite diagnosis. Histological confirmation, in our opinion, was important to ensure diagnostic accuracy and the validity of our conclusions. Besides, the retrospective design was inherently susceptible to potentially unidentified confounders, despite that great effort has been made for the comprehensiveness of data collection and statistical control of confounders, and that the findings were supported by results of sensitivity analyses. A prospective cohort is preferable, but patient recruitment would be practically difficult due to the rarity of OP. Thirdly, not all patients had follow-up CT scans; for those 55 (35%) patients without subsequent CT scans, assessment of radiographic changes in

outcome determination was performed using serial plain chest radiographs. In our opinion, this should not have compromised the accuracy of our assignment of patient outcomes. The definitions for the radiographic domain of different outcomes were also applicable to the assessment using plain radiographs. In addition to the radiographic domain, when determining outcomes we also considered the clinical domain, incorporating changes in patients' symptoms, treatments, demand of supplemental oxygen, and need of mechanical ventilation over time. Furthermore, we included only patients from a tertiary medical center in Taiwan. We also did not include cases of post-COVID-19 OP, because it was not until late 2021 that SARS-CoV-2 became pandemic in Taiwan [29-30]. Future studies involving patients with OP of more diverse ethnicity and aetiologies would be helpful to broaden the generalization of our findings.

Conclusions

In this study involving patients with histologically confirmed OP, we found that patterns and extent of OP on CT images had impact on patients' management and outcomes. Patients with multi-lobe mixed-pattern CT features were more likely to have secondary OP, receive immunosuppressive treatments, and experience a recurrence. These patients also had an enhanced risk of severe disease and a worse survival. Therefore, when treating patients exhibiting these CT imaging features,

clinicians need to be vigilant to identify any underlying aetiology, and closely follow for the timely detection and management of clinical deterioration.

List of Abbreviations:

aOR, adjusted odds ratio

CT, computed tomographic / computed tomography

CTD, connective tissue disease

D_{LCO}, diffusion capacity of the lung for carbon monoxide

FVC, forced vital capacity

GGO, ground-glass opacity

ILDs, interstitial lung diseases

IQR, interquartile range

OP, organizing pneumonia

OR, odds ratio

TLC, total lung capacity

95% CI, 95% confidence interval

Declarations

Ethics Approval: The study protocol has been approved by the Institutional Review Board of National Cheng Kung University Hospital (B-ER-111-038).

Consent to participate and consent for publication: Not applicable.

Availability of data and materials: The data that support the findings of this study are available from the corresponding author upon reasonable request.

Conflict of Interest Statement: The authors have nothing to disclose.

Funding: The authors received no specific funding for this work.

Authors' contributions: HTH and WSH contributed equally to this manuscript; HTH and WCL contributed to the conception and design; HTH, WSH, EHP contributed to the data collection and curation; HTH, WSH, EHP, YLT, WCL contributed to the review of medical records and clinical data; HLT, HTH, WSH, EHP contributed to the review of radiographic images and reports; HTH, YYT, LCT, TYL contributed to the review of surgical records and histological reports and slides; HTH, WSH, WCL contributed to the statistical analysis; HTH, WSH, EHP, HLT, YYT contributed to the drafting of the manuscript; HTH, WSH, WCL, TYL contributed to the critical review of the manuscript.

Acknowledgements: We thank all the patients enrolled in this study for their contribution. We are thankful to rheumatologists from the Department of Internal Medicine of National Cheng Kung University Hospital for providing professional consultation and assistance on the diagnosis and verification of connective tissue disease-related organizing pneumonia. We are thankful to Wan-Ni Chen (M.S.), a statistician from the Biostatistics Consulting Center of National Cheng Kung University Hospital, for providing statistical consultation and assistance.

This article has online supplemental material.

REFERENCES

1. Roberton BJ, Hansell DM. Organizing pneumonia: a kaleidoscope of concepts and morphologies. *Eur Radiol* 2011; 21: 2244 - 2254.
2. Travis WD, Costabel U, Hansell DM, King TE Jr, Lynch DA, Nicholson AG, et al. ATS/ERS Committee on Idiopathic Interstitial Pneumonias. An official American Thoracic Society/European Respiratory Society statement: update of the international multidisciplinary classification of the idiopathic interstitial pneumonias. *Am J Respir Crit Care Med* 2013; 188: 733-748.
3. Raghu G, Meyer KC. Cryptogenic organising pneumonia: current understanding of an enigmatic lung disease. *Eur Respir Rev* 2021; 30(161): 210094.

4. Cordier JF. Cryptogenic organising pneumonia. *Eur Respir J* 2006; 28: 422-446.
5. Drakopanagiotakis F, Paschalaki K, Abu-Hijleh M, Aswad B, Karagianidis N, Kastanakis E, et al. Cryptogenic and secondary organizing pneumonia: clinical presentation, radiographic findings, treatment response, and prognosis. *Chest* 2011; 139(4): 893-900.
6. Davison AG, Heard BE, McAllister WA, Turner-Warwick ME. Cryptogenic organizing pneumonitis. *Q J Med* 1983; 52: 382-394.
7. Miao L, Wang Y, Li Y, Ding J, Chen L, Dai J, et al. Lesion with morphologic feature of organizing pneumonia (OP) in CT-guided lung biopsy samples for diagnosis of bronchiolitis obliterans organizing pneumonia (BOOP): a retrospective study of 134 cases in a single center. *J Thorac Dis* 2014; 6(9): 1251-1260.
8. Lohr RH, Boland BJ, Douglas WW, Dockrell DH, Colby TV, Swensen SJ, et al. Organizing pneumonia. Features and prognosis of cryptogenic, secondary, and focal variants. *Arch Intern Med* 1997; 157(12): 1323-1329.
9. King TE Jr, Mortenson RL. Cryptogenic organizing pneumonitis. The North American experience. *Chest* 1992; 102(1 Suppl): 8S-13S.
10. Nizami IY, Kissner DG, Visscher DW, Dubaybo BA. Idiopathic bronchiolitis obliterans with organizing pneumonia. An acute and life-threatening syndrome.

Chest 1995; 108: 271-277.

11. Chang J, Han J, Kim DW, Lee I, Lee KY, Jung S, et al. Bronchiolitis obliterans organizing pneumonia: clinicopathologic review of a series of 45 Korean patients including rapidly progressive form. *J Korean Med Sci* 2002; 17: 179-186.
12. V Vasu TS, Cavallazzi R, Hirani A, Sharma D, Weibel SB, Kane GC. Clinical and radiologic distinctions between secondary bronchiolitis obliterans organizing pneumonia and cryptogenic organizing pneumonia. *Respir Care* 2009; 54(8): 1028-1032.
13. Lazor R, Vandevenne A, Pelletier A, Leclerc P, Court-Fortune I, Cordier JF. Characteristics of relapses in a series of 48 patients. *Am J Respir Crit Care Med* 2000; 162: 571-577.
14. Chung MP, Nam BD, Lee KS, Han J, Park JS, Hwang JH, Cha MJ, Kim TJ. Serial chest CT in cryptogenic organizing pneumonia: Evolutional changes and prognostic determinants. *Respirology* 2018; 23(3): 325-330.
15. Cho YH, Chae EJ, Song JW, Do KH, Jang SJ. Chest CT imaging features for prediction of treatment response in cryptogenic and connective tissue disease-related organizing pneumonia. *Eur Radiol* 2020; 30(5): 2722-2730.
16. Polverosi R, Maffesanti M, Dalpiaz G. Organizing pneumonia: typical and atypical HRCT patterns. *Radiol Med* 2006; 111(2): 202-212.

17. Faria IM, Zanetti G, Barreto MM, Rodrigues RS, Araujo-Neto CA, Silva JL, et al. Organizing pneumonia: chest HRCT findings. *J Bras Pneumol* 2015; 41(3): 231-237.

18. Torrealba JR, Fisher S, Kanne JP, Butt YM, Glazer C, Kershaw C, Burguete D, Gokaslan T, Batra K. Pathology-radiology correlation of common and uncommon computed tomographic patterns of organizing pneumonia. *Hum Pathol* 2018; 71: 30-40.

19. Barroso E, Hernandez L, Gil J, Garcia R, Aranda I, Romero S. Idiopathic organizing pneumonia: a relapsing disease. 19 years of experience in a hospital setting. *Respiration* 2007; 74(6): 624-631.

20. Saito Z, Kaneko Y, Hasegawa T, Yoshida M, Odashima K, Horikiri T, et al. Predictive factors for relapse of cryptogenic organizing pneumonia. BMC Pulm Med 2019; 19: 10.

21. Raju S, Ghosh S, Mehta AC. Chest CT Signs in Pulmonary Disease: A Pictorial Review. *Chest* 2017; 151(6): 1356-1374.

22. Tiralongo F, Palermo M, Distefano G, Vancheri A, Sambataro G, Torrisi SE, et al. Cryptogenic organizing pneumonia: evolution of morphological patterns assessed by HRCT. *Diagnostics (Basel)* 2020; 10(5): 262.

23. Basarakodu KR, Aronow WS, Nair CK, Lakkireddy D, Kondur A, Korlakunta H,

et al. Differences in treatment and in outcomes between idiopathic and secondary forms of organizing pneumonia. *Am J Ther* 2007; 14(5): 422-426.

24. Yoo JW, Song JW, Jang SJ, Lee CK, Kim MY, Lee HK, et al. Comparison between cryptogenic organizing pneumonia and connective tissue disease-related organizing pneumonia. *Rheumatology (Oxford)* 2011; 50(5): 932-938.
25. Yousem SA, Lohr RH, Colby TV. Idiopathic bronchiolitis obliterans organizing pneumonia/cryptogenic organizing pneumonia with unfavorable outcome: pathologic predictors. *Mod Pathol* 1997; 10: 864-871.
26. Nishino M, Mathai SK, Schoenfeld D, Digumarthy SR, Kradin RL. Clinicopathologic features associated with relapse in cryptogenic organizing pneumonia. *Hum Pathol* 2014; 45: 342-351.
27. Onishi Y, Kawamura T, Nakahara Y, Kagami R, Sasaki S, Takahashi S, et al. Factors associated with the relapse of cryptogenic and secondary organizing pneumonia. *Respir Investig* 2017; 55(1): 10-15.
28. Zhou Y, Wang L, Huang M, Ding J, Jiang H, Zhou K, et al. A long-term retrospective study of patients with biopsy-proven cryptogenic organizing pneumonia. *Chron Respir Dis* 2019; 16: 1479973119853829.
29. Myall KJ, Mukherjee B, Castanheira AM, Lam JL, Benedetti G, Mak SM, et al. Persistent Post-COVID-19 Interstitial Lung Disease. An Observational Study of

Corticosteroid Treatment. *Ann Am Thorac Soc.* 2021; 18(5): 799-806.

30. Tsai CS, Huang TH, Su PL, Chen CZ, Chen CW, Ko WC, Lee NY. The occurrence of and risk factors for developing acute critical illness during quarantine as a response to the COVID-19 pandemic. J Formos Med Assoc. 2022; 121: 81-88.

Figure Legends

Figure 1 Flow chart of inclusion and exclusion for this study.

Figure 2 Representative images of the various computed tomographic patterns observed in patients of our study cohort: a) alveolar consolidation; b) nodular; c) multi-lobar ground-glass opacity (GGO); d) mass-like; e) bronchocentric; f) a combination of GGO and reticulo-infiltrative opacity; g) reverse halo sign in a background of mixed GGO and alveolar consolidation; h) crazy paving pattern mixed with GGO.

Figure 3 Distribution of frequencies of: a) aetiologies; b) methods of tissue sampling; c) treatments; d) need of supplemental oxygen; e) use of mechanical ventilation; f) different outcomes; among patients of the three subgroups based on the combined assessment of the extent and patterns of involvement on computed tomographic images (Group 1, single-lobe and single-pattern; Group 2, single-lobe and mixed-pattern or multi-lobe and single-pattern; Group 3, multi-lobe and mixed-pattern).

Abbreviation: CT, computed tomographic.

Figure 4 Forest plots showing: a) crude and adjusted odds ratios of secondary organizing pneumonia; b) crude and adjusted odds ratios of immunosuppressive treatments; c) crude and adjusted odds ratios of severe disease, for patients with different radiographic features.

Note: Groups are based on the combined assessment of the extent and patterns of involvement on computed tomographic images: Group 1, single-lobe and single-pattern; Group 2, single-lobe and mixed-pattern or multi-lobe and single-pattern; Group 3, multi-lobe and mixed-pattern. Abbreviation: OR, odds ratio.

Figure 5 Kaplan-Meier survival analyses: a) between “single-lobe” and “multi-lobe” groups; b) between “single-pattern” and “mixed-pattern” groups; c) among Groups 1, 2, and 3.

Note: Groups are based on the combined assessment of the extent and patterns of involvement on computed tomographic images: Group 1, single-lobe and single-pattern; Group 2, single-lobe and mixed-pattern or multi-lobe and single-pattern; Group 3, multi-lobe and mixed-pattern.

Table 1 Baseline characteristics, management, and outcomes of the study cohort

Age, years	61.5 (54.4 – 71.1)
Sex	
Female, n (%)	66 (42)
Male, n (%)	90 (58)
Body height, cm	160.9 (± 9.3)
Body weight, kg	60.3 (53.7 – 66.6)
Charlson comorbidity index	3 (2 – 5)
Cigarette smoking status:	
Never smoker, n (%)	105 (67)
Current smoker, n (%)	29 (19)
Former smoker, n (%)	22 (14)
Time between CT and histologic diagnosis of OP, days	13 (7 – 30)
Methods of biopsy:	
Surgical, n (%)	91 (58)
CT-guided percutaneous, n (%)	49 (31)
Transbronchial forceps, n (%)	15 (10)
Sonography-guided percutaneous, n (%)	1 (1)
Season of diagnosis:	
Spring (March - May), n (%)	40 (26)
Summer (June – August), n (%)	50 (32)
Fall (September – November), n (%)	37 (24)
Winter (December – February), n (%)	29 (18)
Aetiology:	
Cryptogenic, n (%)	130 (83)
Secondary, n (%)	26 (17)
CTD-related, n (%)	14 (9)
Rheumatoid arthritis, n (%)	6 (4)
Dermatomyositis / polymyositis, n (%)	3 (2)
Primary Sjögren's syndrome, n (%)	3 (2)
Anti-synthetase syndrome, n (%)	1 (1)
Systemic lupus erythematosus, n (%)	1 (1)
Drug-related, n (%)	10 (6)

Amiodarone, n (%)	5 (3)
Pembrolizumab, n (%)	2 (2)
Agent(s) in cancer chemotherapeutic regimens, n (%)	2 (2)
Crizotinib, n (%)	1 (1)
Post-transplantation, n (%)	2 (2)
Duration of follow-up, weeks	120.6 (31.1 – 269.4)
Treatments:	
Observation only, n (%)	45 (29)
Surgical resection, n (%)	48 (31)
Corticosteroid alone, n (%)	55 (35)
Combined corticosteroid and another immunosuppressant, n (%)	7 (4)
Non-steroid immunosuppressant, n (%)	1 (1)
Needed supplementary oxygen during the course, n (%)	40 (26)
Needed mechanical ventilatory support during the course, n (%)	17 (11)
Outcomes:	
Improved without recurrence, n (%)	129 (82)
Persistent disease, n (%)	11 (7)
Improved but then recurred, n (%)	5 (3)
Death, n (%)	11 (8)

CT, computed tomography; CTD, connective tissue disease; D_{LCO}, diffusion capacity of the lung for carbon monoxide; OP, organizing pneumonia. Discrete variables are presented as counts (% of the total 156 patients). Continuous variables are presented as means (± standard deviation) if normally distributed, and medians (interquartile ranges) if not normally distributed.

Table 2 Computed tomographic (CT) features of organizing pneumonia

	N (%)	Age, years	Male / Female
Extent of parenchymal involvement on CT images			
Single lobe	74 (47)	61 (53 – 70)	47 (30) / 27 (17)
Multiple lobes	82 (53)	63 (57 – 74)	43 (28) / 39 (25)
Ipsilateral	9 (6)	75 (53 – 81)	6 (4) / 3 (2)
Bilateral	73 (47)	62 (57 – 70)	37 (24) / 36 (23)
CT imaging patterns			
Single pattern	100 (64)	61 (53 – 69)	58 (37) / 42 (27)
Nodular	42 (27)	63 (54 – 70)	21 (13) / 21 (13)
Alveolar consolidation	32 (21)	61 (53 – 69)	20 (13) / 12 (8)
Mass-like	18 (11)	56 (51 – 67)	13 (8) / 5 (3)
GGO	8 (5)	61 (47 – 67)	4 (3) / 4 (3)
Mixed patterns	56 (36)	65 (57 – 76)	32 (20) / 24 (16)
Alveolar consolidation + GGO	13 (7)	69 (58 – 79)	10 (6) / 3 (2)
Alveolar consolidation + bronchocentric	6 (4)	64 (41 – 73)	3 (2) / 3 (2)
Alveolar consolidation + nodular	4 (3)	65 (51 – 75)	2 (1) / 2 (1)
GGO + bronchocentric	7 (4)	58 (56 – 75)	3 (2) / 4 (3)
GGO + reticulo-infiltrative	3 (2)	66 (41 – 70)	1 (1) / 2 (1)
GGO + nodular	2 (1)	61 (58 – 63)	0 (0) / 2 (1)
GGO + crazy paving	2 (1)	79 (74 – 84)	2 (1) / 0 (0)
Mass + nodular	3 (2)	65 (62 – 71)	2 (1) / 1 (1)
Mass + reverse halo	1 (1)	45 (NA)	1 (1) / 0 (0)
Alveolar consolidation + GGO + bronchocentric	6 (4)	68 (53 – 81)	3 (2) / 3 (2)
Alveolar consolidation + GGO + reverse halo	3 (2)	57 (54 – 60)	2 (1) / 1 (1)
Alveolar consolidation + GGO + reticulo-infiltrative	1 (1)	69 (NA)	0 (0) / 1 (1)
Alveolar consolidation + GGO + crazy paving	1 (1)	58 (NA)	0 (0) / 1 (1)
Alveolar consolidation + GGO + nodular	1 (1)	87 (NA)	1 (1) / 0 (0)
GGO + reverse halo + reticulo-infiltrative	1 (1)	61 (NA)	0 (0) / 1 (1)
Alveolar consolidation + GGO + bronchocentric + crazy paving	2 (1)	62 (58 – 66)	2 (1) / 0 (0)
Combined extent and patterns on CT images			
Single lobe and single pattern	71 (46)	61 (53-70)	46 (29) / 25 (16)
Multiple lobes and single pattern	29 (18)	61 (52-66)	12 (8) / 17 (11)
Single lobe and mixed patterns	3 (2)	57 (50-64)	1 (1) / 2 (1)
Multiple lobes and mixed patterns	53 (34)	65 (57-76)	31 (20) / 22 (14)

Values are presented in counts (% of total 156 patients) or medians (inter-quartile range or range, as appropriate). CT, computed tomographic; GGO, ground-glass opacity; NA, not available. Examples of the

various radiographic features are presented in Figure 2 and Supplemental Figure S1a – S1q.

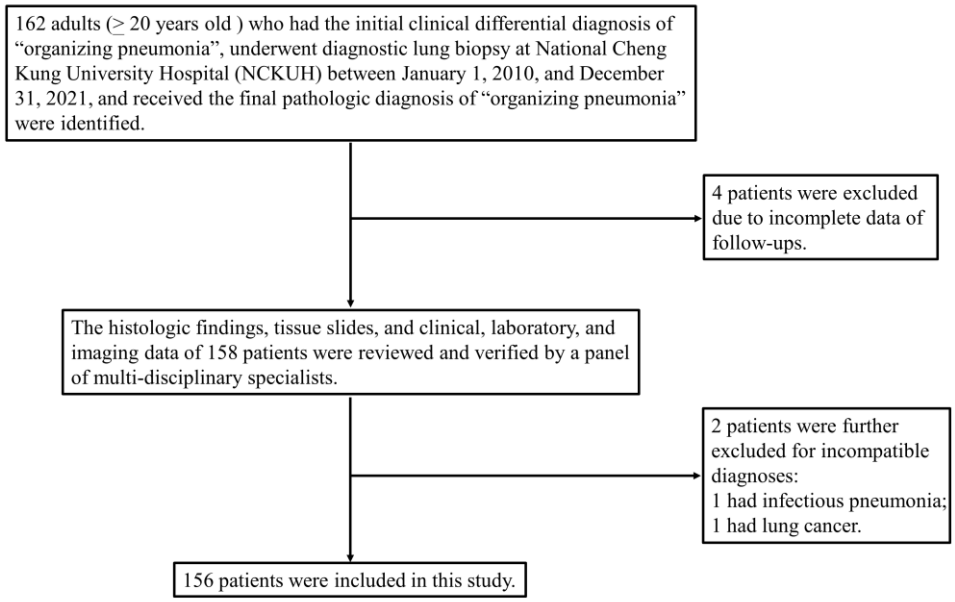
162 adults (≥ 20 years old) who had the initial clinical differential diagnosis of "organizing pneumonia", underwent diagnostic lung biopsy at National Cheng Kung University Hospital (NCKUH) between January 1, 2010, and December 31, 2021, and received the final pathologic diagnosis of "organizing pneumonia" were identified.
4 patients were excluded due to incomplete data of follow-ups.
The histologic findings, tissue slides, and clinical, laboratory, and imaging data of 158 patients were reviewed and verified by a panel of multi-disciplinary specialists.
2 patients were further excluded for incompatible diagnoses:
1 had infectious pneumonia;
1 had lung cancer.
156 patients were included in this study.

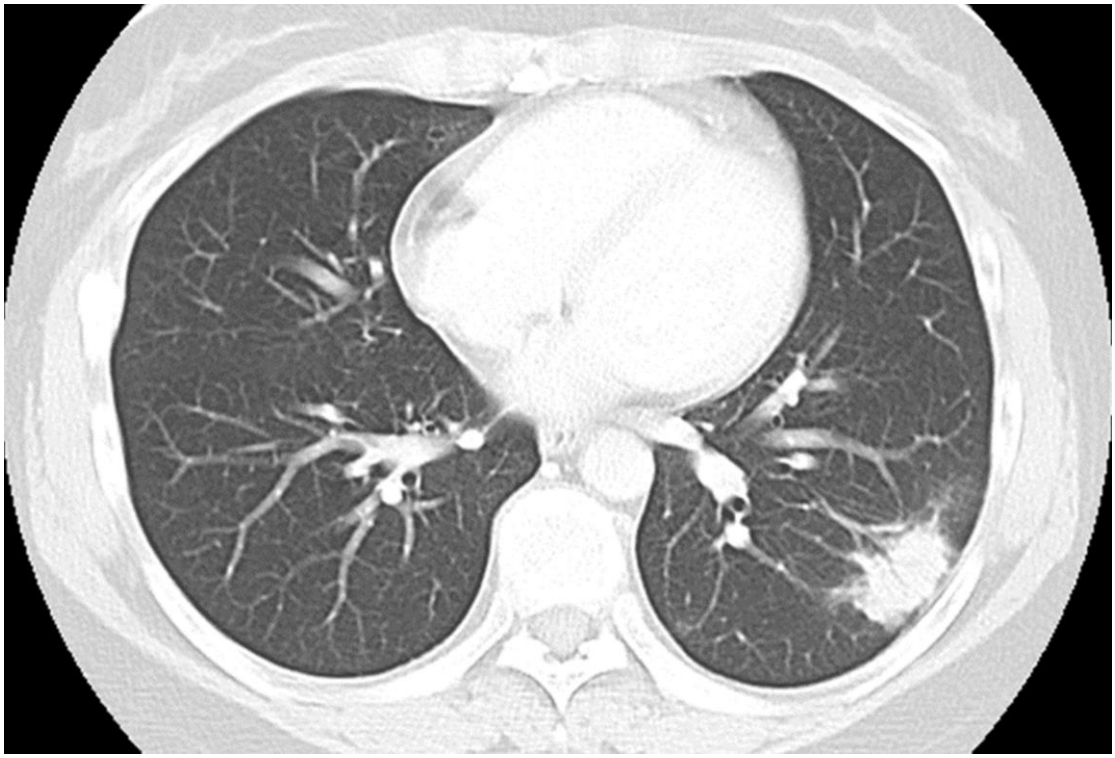

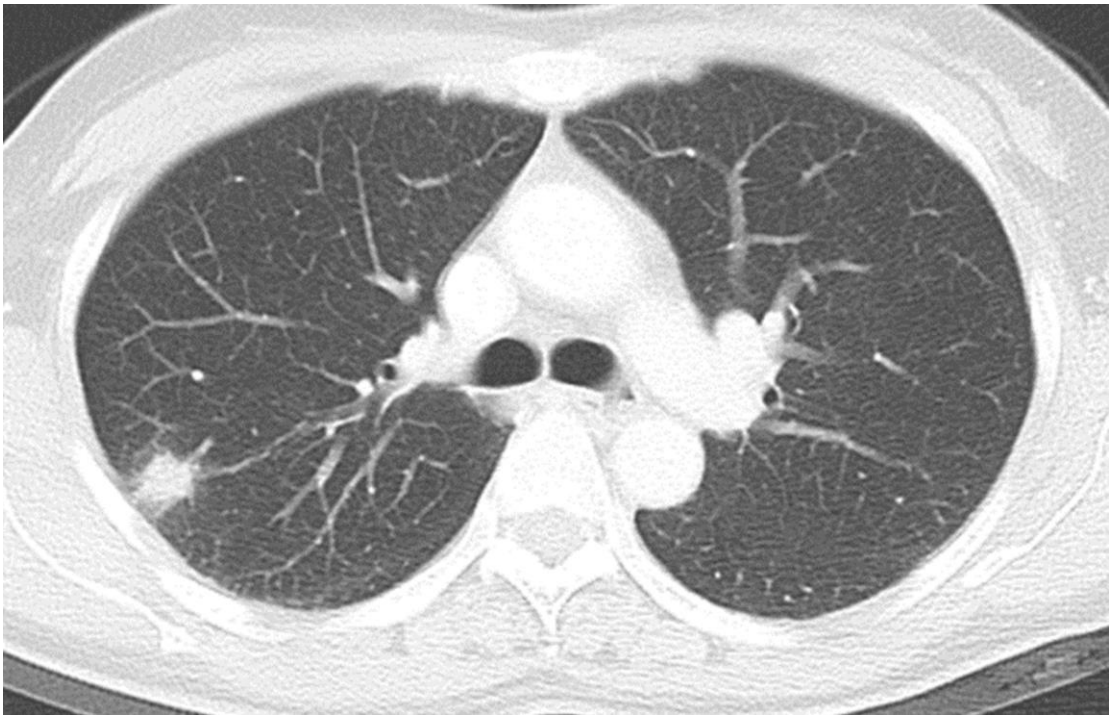

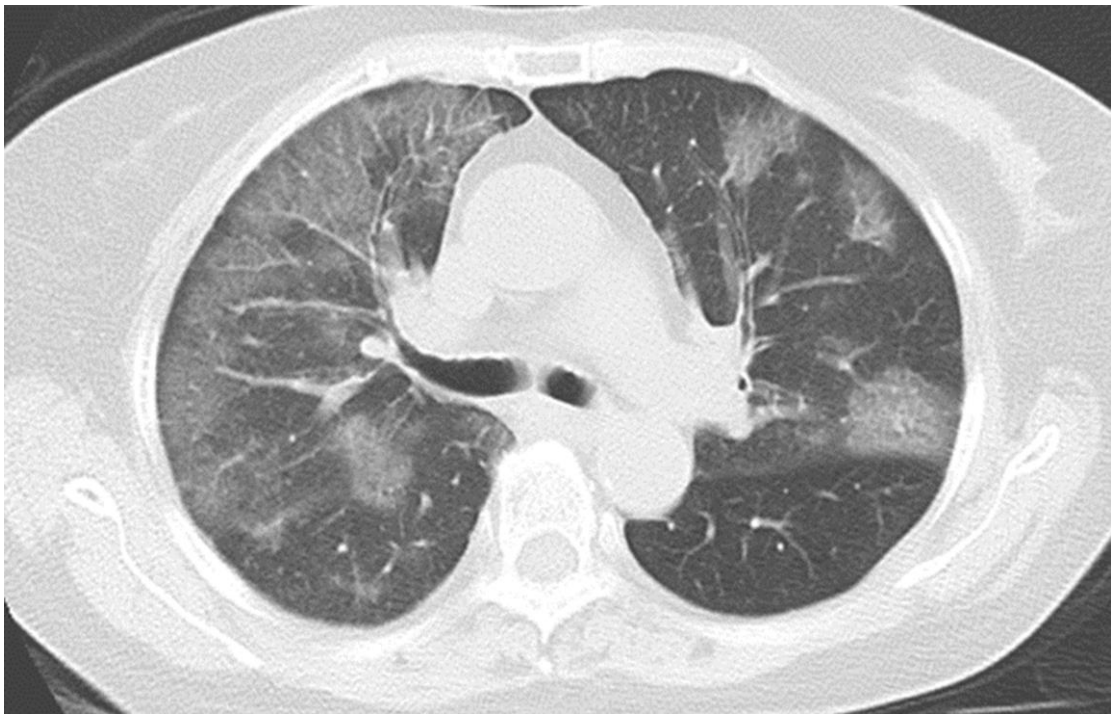

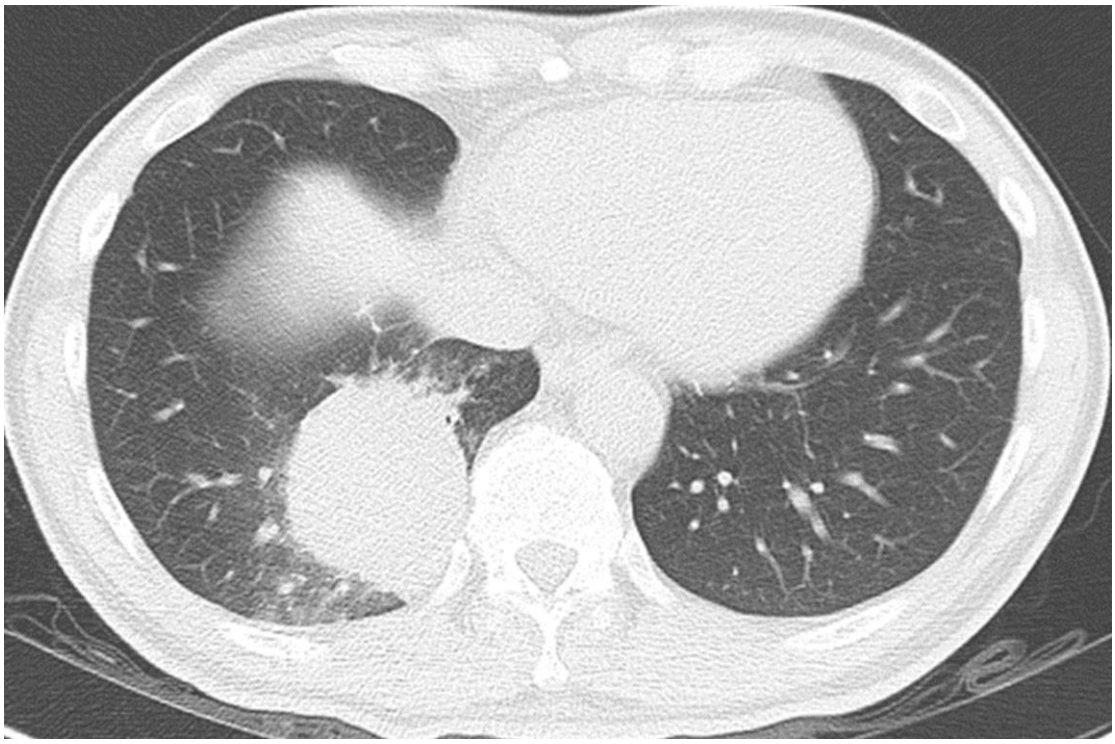

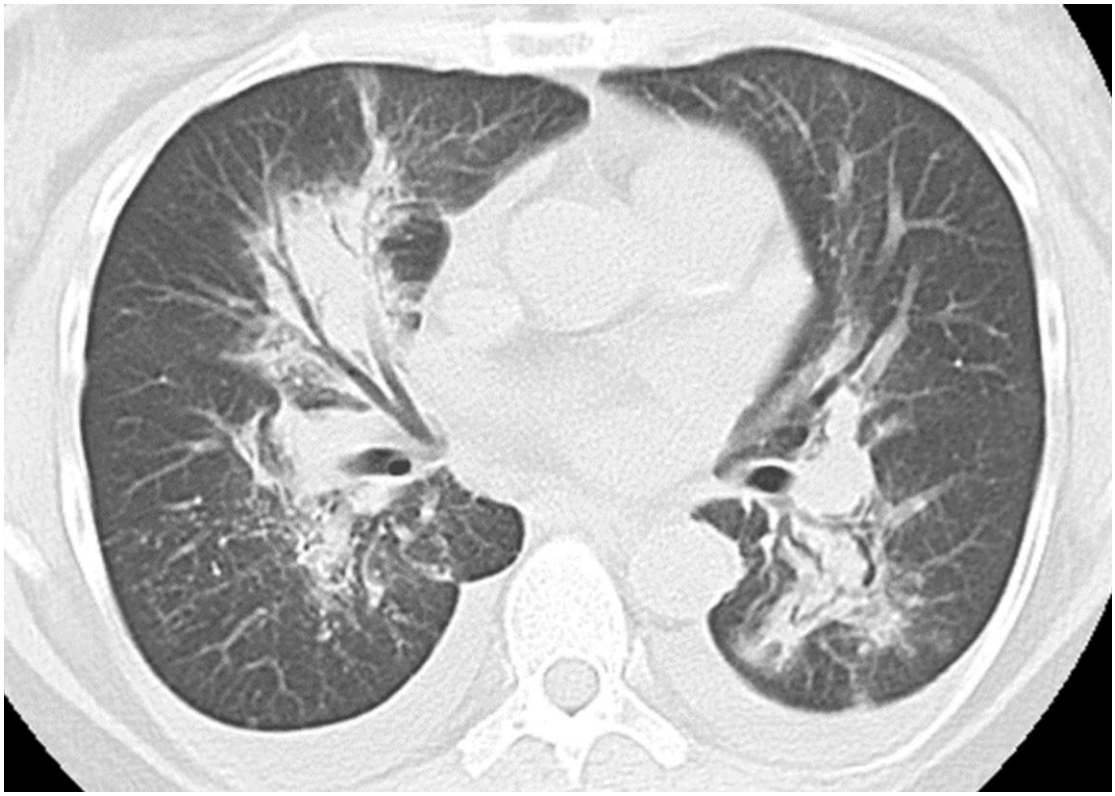

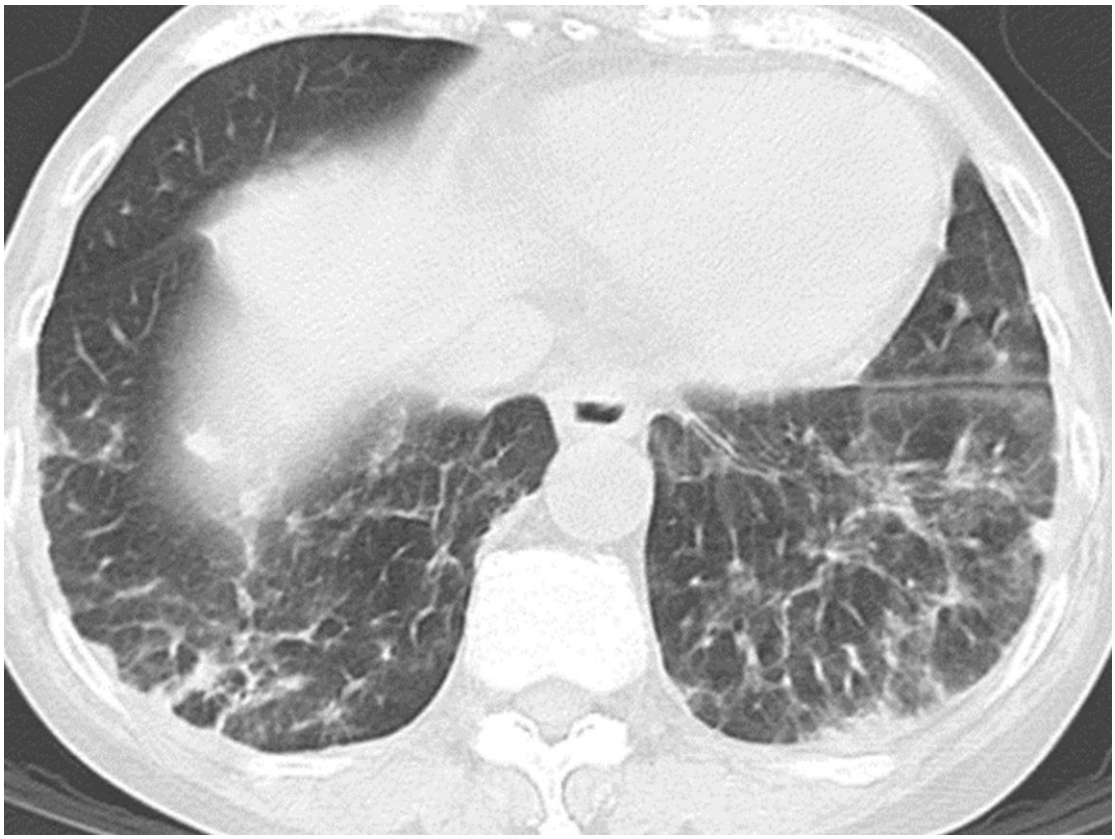

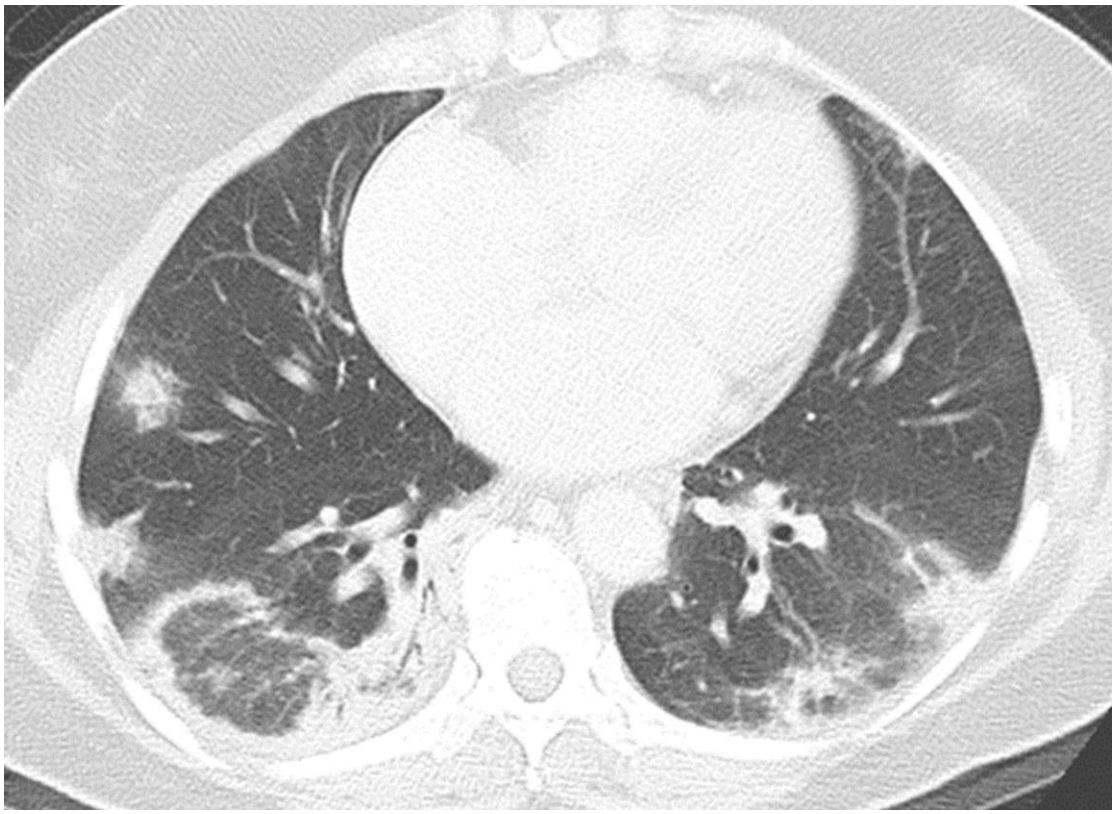

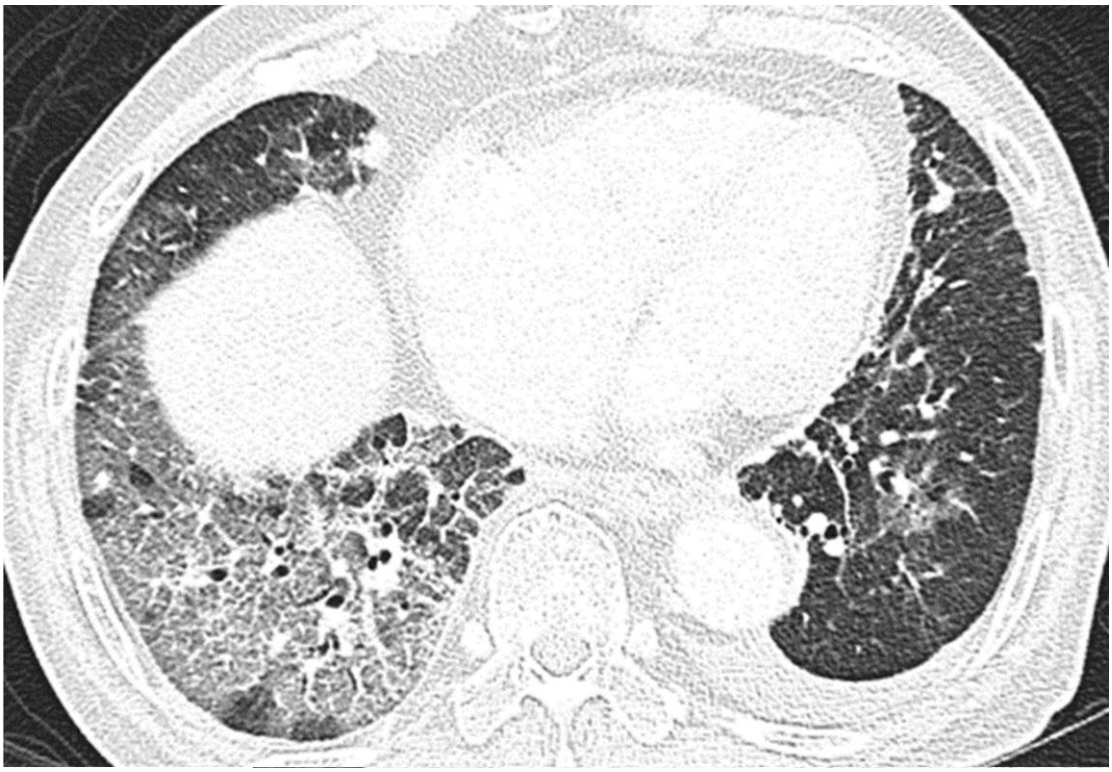

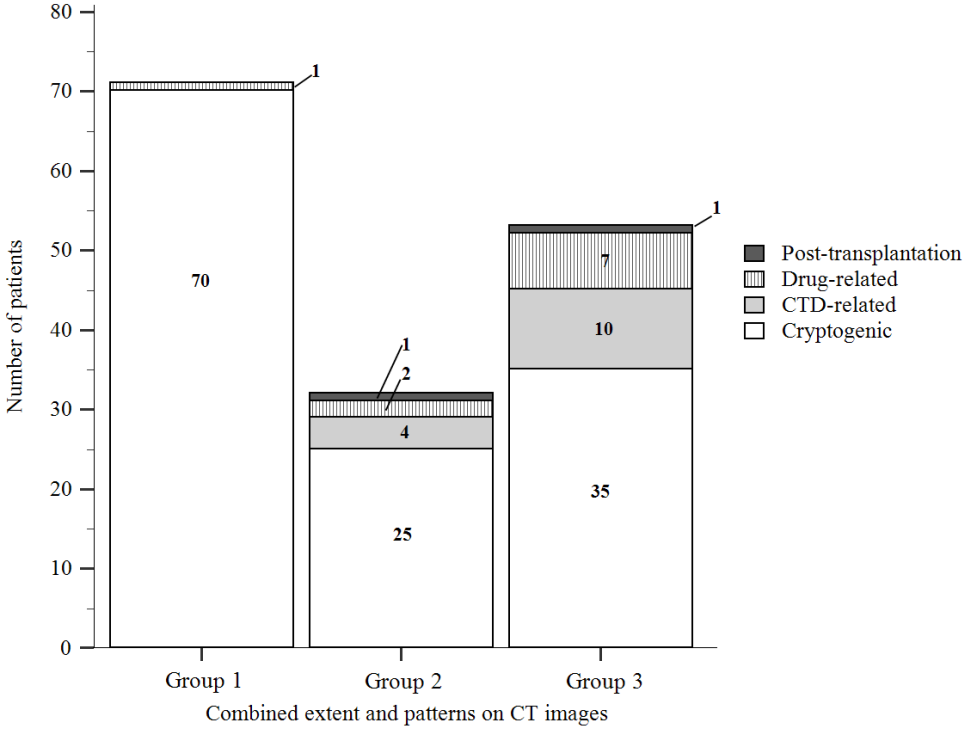
80
70
60
50
40
30
20
10
0
Number of patients
1
70
1
2
4
25
1
7
10
35
Post-transplantation
Drug-related
CTD-related
Cryptogenic
Group 1
Group 2
Group 3
Combined extent and patterns on CT images

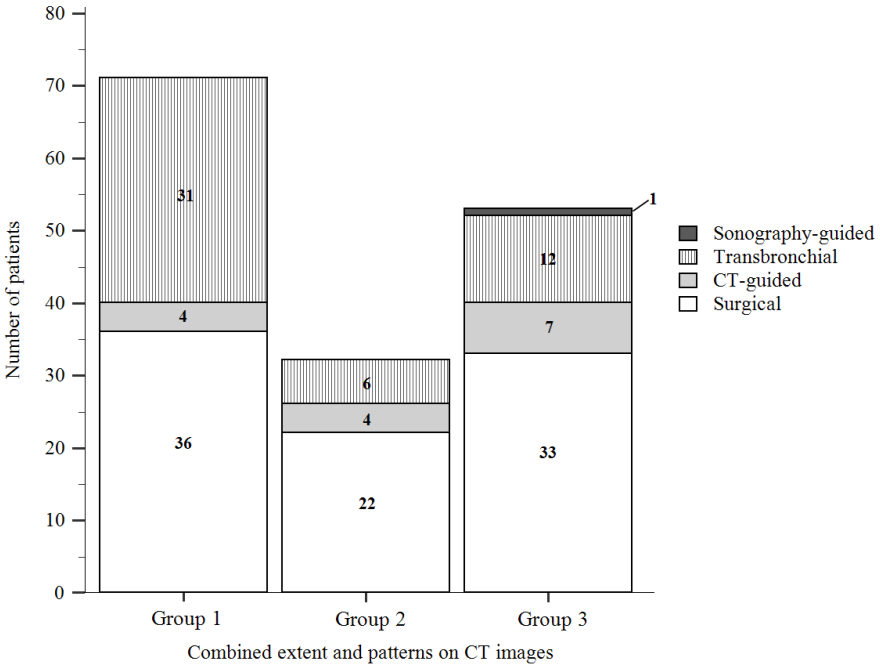
80
70
60
50
40
30
20
10
0
Number of patients
31
4
36
6
4
22
12
7
33
1
Sonography-guided
Transbronchial
CT-guided
Surgical
Group 1
Group 2
Group 3
Combined extent and patterns on CT images

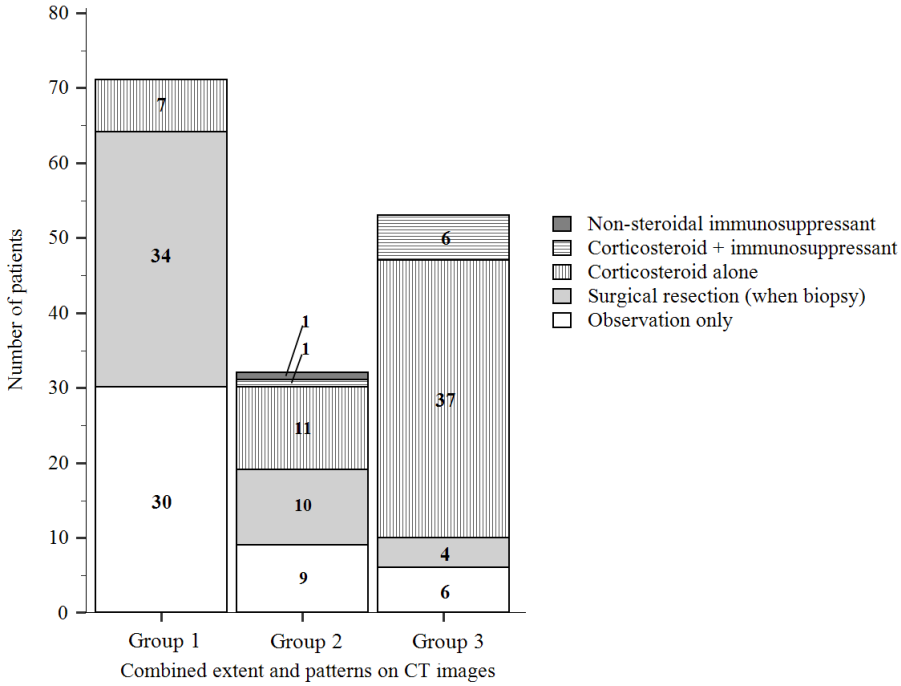
80
70
60
50
40
30
20
10
0
Number of patients
7
34
30
1
1
11
10
9
6
37
4
6
Group 1
Group 2
Group 3
Combined extent and patterns on CT images
Non-steroidal immunosuppressant
Corticosteroid + immunosuppressant
Corticosteroid alone
Surgical resection (when biopsy)
Observation only

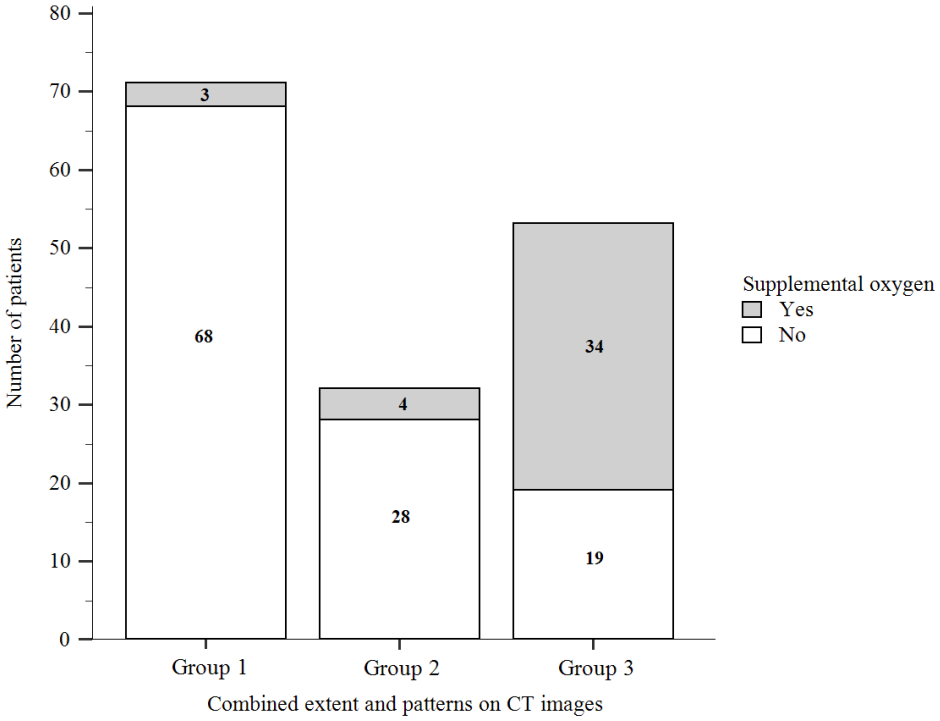
80
70
60
50
40
30
20
10
0
Number of patients
3
68
4
28
34
19
Group 1
Group 2
Group 3
Combined extent and patterns on CT images
Supplemental oxygen
Yes
No

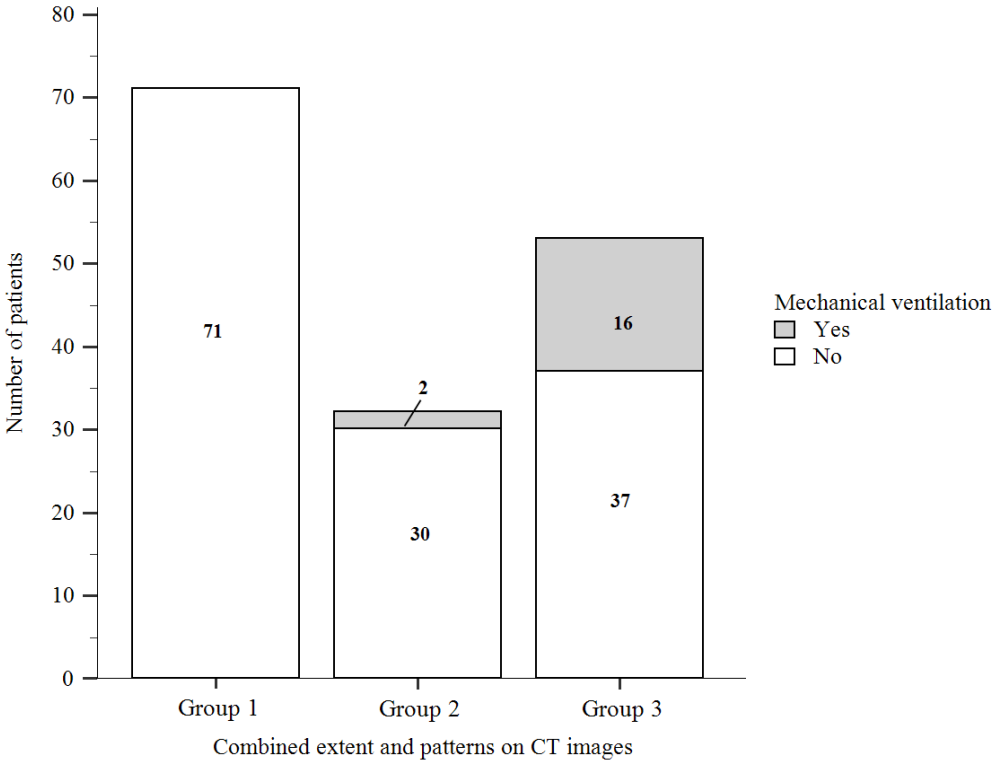
80
70
60
50
40
30
20
10
0
Number of patients
71
2
30
16
37
Group 1
Group 2
Group 3
Combined extent and patterns on CT images
Mechanical ventilation
Yes
No

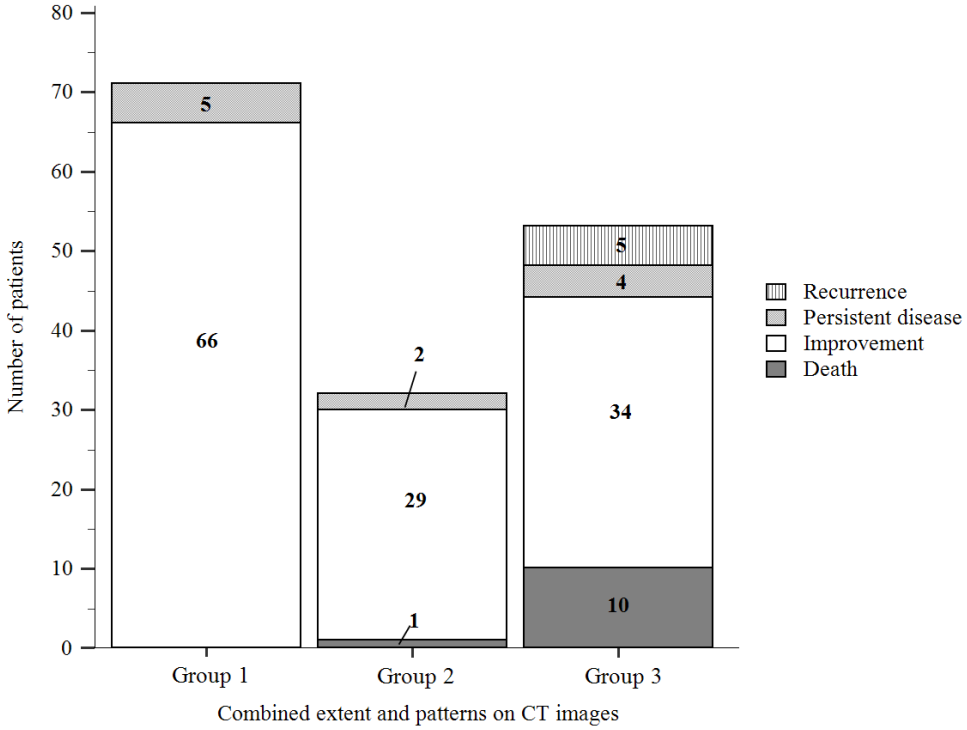
80
70
60
50
40
30
20
10
0
Number of patients
5
66
2
29
1
5
4
34
10
Recurrence
Persistent disease
Improvement
Death
Group 1
Group 2
Group 3
Combined extent and patterns on CT images

Crude OR

Multi-lobe (versus single-lobe): 8.07 (2.79 – 31.31)

Mixed-patterns (versus single-pattern): 8.17 (3.27 – 22.97)

Combined extent and patterns (with Group 1 as reference):
Group 2: 13.82 (2.82 – 135.76)
Group 3: 24.49 (5.83 – 227.54)

Adjusted OR

Multi-lobe (versus single-lobe):
Model 1: 6.99 (2.35 – 27.76)
Model 2: 3.44 (0.88 – 15.71)

Mixed-patterns (versus single-pattern):
Model 1: 6.38 (2.51 – 18.14)
Model 2: 3.32 (1.13 – 10.96)

Combined extent and patterns (with Group 1 as reference):
Group 2: 11.77 (2.36 – 115.80)
Group 3: 19.08 (4.46 – 177.80)

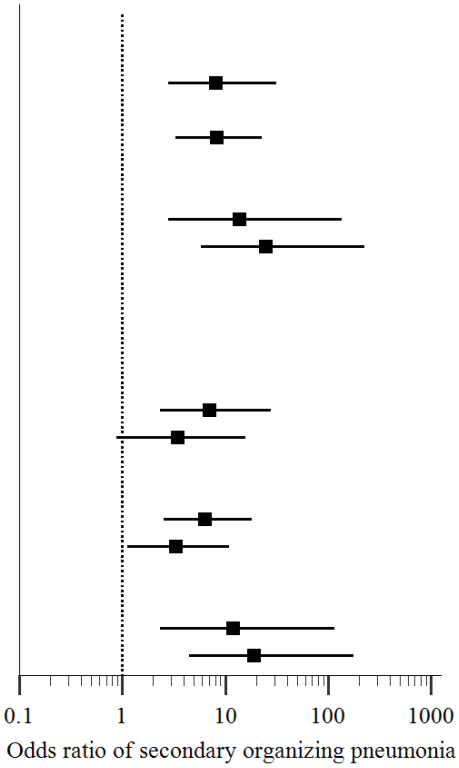

Crude OR

Multi-lobe (versus single-lobe): 19.19 (8.34 – 49.77)

Mixed-patterns (versus single-pattern): 12.65 (5.95 – 28.50)

Combined extent and patterns (with Group 1 as reference):
Group 2: 5.95 (2.19 – 17.39)
Group 3: 35.63 (13.68 – 105.24)

Adjusted OR

Multi-lobe (versus single-lobe):
Model 1: 12.45 (5.20 – 33.70)
Model 2: 7.39 (2.70 – 22.00)

Mixed-patterns (versus single-pattern):
Model 1: 7.97 (3.55 – 18.94)
Model 2: 2.80 (1.06 – 7.47)

Combined extent and patterns (with Group 1 as reference):
Group 2: 3.39 (1.11 – 10.67)
Group 3: 19.58 (7.28 – 59.81)

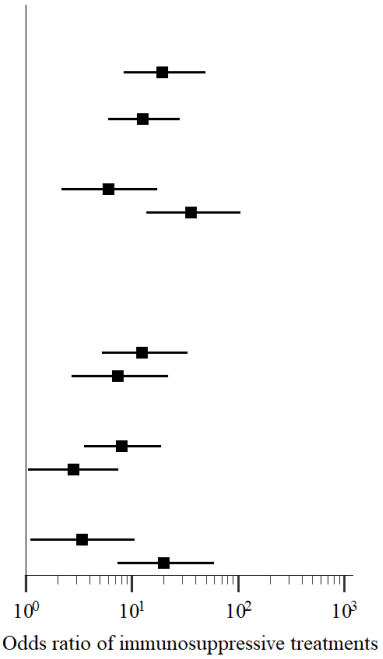

Crude OR

Multi-lobe (versus single-lobe): 17.67 (6.28 – 67.78)

Mixed-patterns (versus single-pattern): 19.12 (8.04 – 50.89)

Combined extent and patterns (with Group 1 as reference):
Group 2: 3.09 (0.71 – 14.63)
Group 3: 34.63 (11.59 – 138.37)

Adjusted OR

Multi-lobe (versus single-lobe):
Model 1: 17.84 (5.55 – 79.66)
Model 2: 6.20 (1.59 – 30.29)

Mixed-patterns (versus single-pattern):
Model 1: 12.87 (5.12 – 36.50)
Model 2: 5.11 (1.80 – 16.07)

Combined extent and patterns (with Group 1 as reference):
Group 2: 4.24 (0.89 – 22.84)
Group 3: 27.64 (8.25 – 127.44)

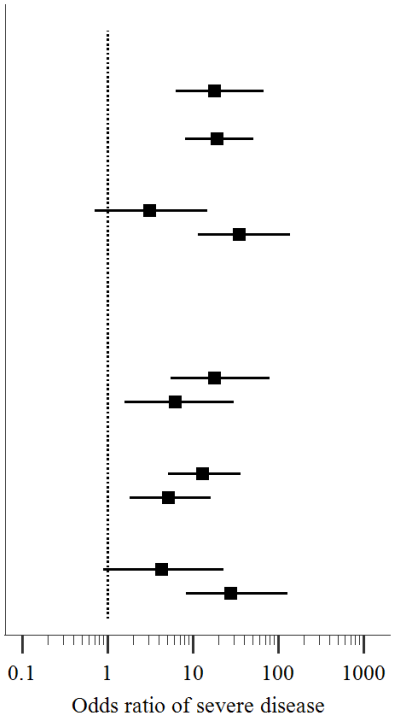

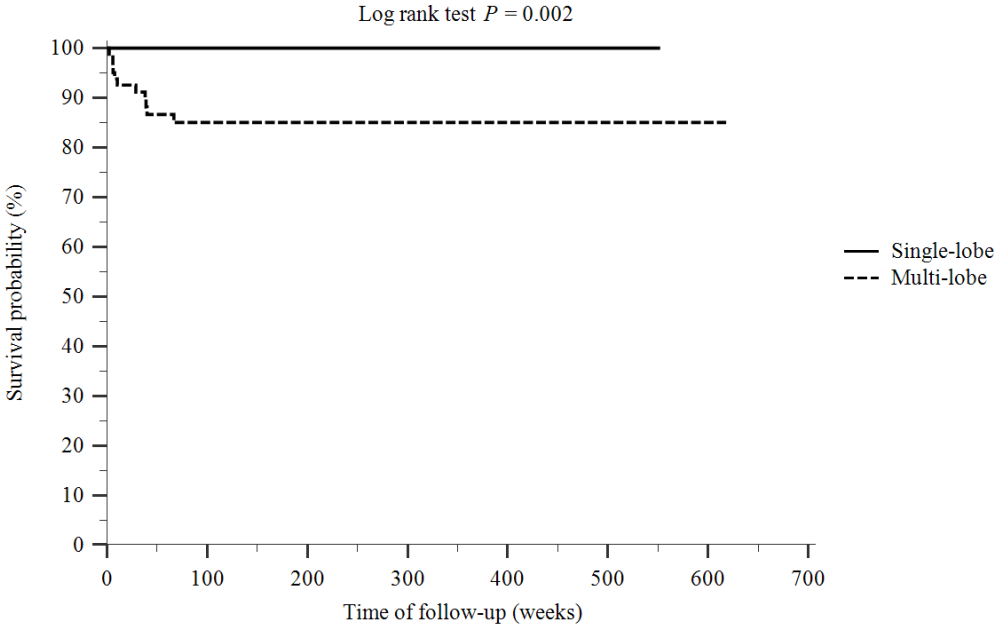

Number at risk							
Single-lobe							
74	45	27	16	8	3	0	0
Multi-lobe							
82	44	27	14	5	2	1	0

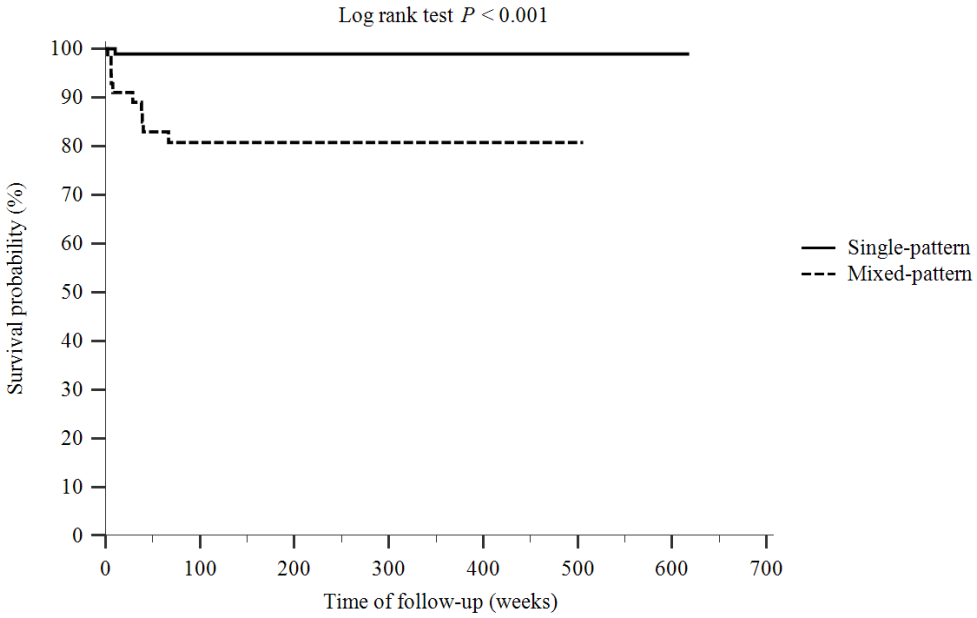

Number at risk							
Single-pattern							
100	58	34	18	8	4	1	0
Mixed-pattern							
56	31	20	12	5	1	0	0

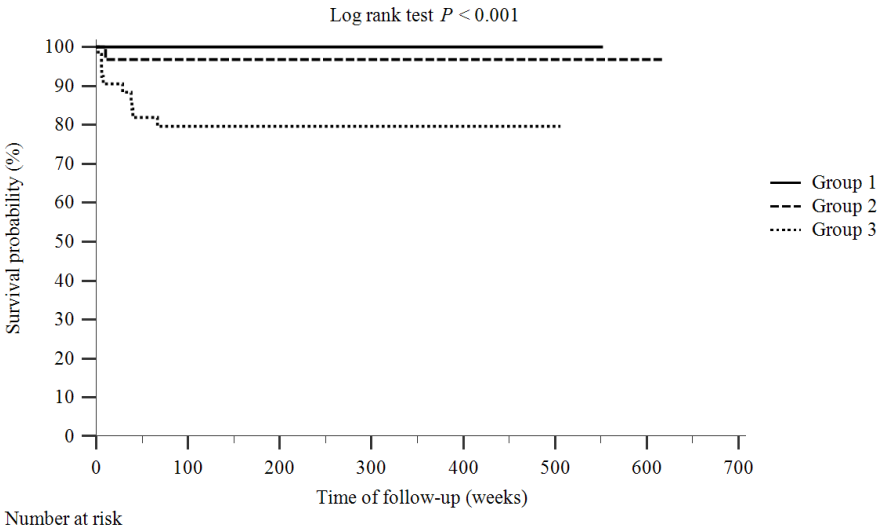

Number at risk							
Group Group 1							
71	43	25	15	7	3	0	0
Group Group 2							
32	17	11	4	2	1	1	0
Group Group 3							
53	29	18	11	4	1	0	0

Impact of computed tomographic patterns and extent on clinical management and outcomes of patients with organizing pneumonia

Tang-Hsiu Huang*, Sheng-Huan Wei*, Li-Ting Huang, Hong-Ping Er, Yu-Ting Yu, Chung-Ta Lee, Yau-Lin Tseng, Chao-Liang Wu

* These two authors contributed equally to this manuscript

Online Supplemental Material

Corresponding Author:
Chao-Liang Wu, PhD, Professor Emeritus
Address: Department of Biochemistry and Molecular Biology, College of Medicine, National Cheng Kung University,
Cheng-Hsing Campus, No.1, Dasyue Road, East District,
Tainan City 701, Taiwan (R.O.C.)
Telephone number: +886-6-2353535 ext. 5536 / Fax number: +886-6-2741692
E-mail: wumolbio@mail.ncku.edu.tw

Table of Content

Supplementary Material	Page
Supplemental Table S1 Outcomes and changes in forced vital capacity of the 27 patients with serial spirometric measurements	3
Supplemental Table S2 Fleiss' kappa for the inter-observer agreement among the three interpreters of computed tomographic features	4
Supplemental Table S3 Distribution of different aetiologies, clinical managements, and outcomes among patients with different computed tomographic features	5 - 6
Supplemental Table S4 Baseline characteristics of the three groups based on the combined assessment of the extents and patterns of organizing pneumonia	7
Supplemental Table S5 Distribution of different aetiologies, clinical managements, and outcomes among 86 patients having baseline pulmonary function tests available and different computed tomographic features	8
Supplemental Table S6 Univariate and multivariable logistic regression analysis on the association between computed tomographic features and ***secondary*** organizing pneumonia	9
Supplemental Table S7 Univariate and multivariable logistic regression analysis on the association between computed tomographic features and subsequent immunosuppressive treatments	10
Supplemental Table S8 Univariate and multivariable logistic regression analysis on the association between computed tomographic features and the risk of severe disease	11
Supplemental Table S9 Baseline characteristics and outcomes of patients with cryptogenic and secondary organizing pneumonia	12 - 13
Supplemental Table S10 Univariate and multivariable logistic regression analysis on the association between computed tomographic features and the risk of severe disease, involving **only** patients with ***cryptogenic*** organizing pneumonia (N = 130)	14
Supplemental Figure S1a – S1q Example images of the various computed tomographic features observed in patients of our study cohort	15 - 31
Supplemental Figure S2a – S2i Results of the sensitivity analysis	32 - 40
Supplemental Figure S3a – S3d Results from the analyses involving **only** patients with ***cryptogenic*** organizing pneumonia (N = 130)	40 - 43
Supplemental Document 1: The protocols on patient inclusion / exclusion, diagnostic verification and classification, and outcome determination	44 - 49

Supplemental Table S1 Outcomes and changes in forced vital capacity of the 27 patients with serial spirometric measurements

Final outcomes	FVC increased < 10%	FVC increased ≥ 10%	FVC decreased < 10%	FVC decreased ≥ 10%
Improvement	9	10	2*	1**
Persistent disease				2
Recurrence	1		1	
Death			1	

Numbers indicate patient counts. 27 patients had follow-up pulmonary spirometric measurements in the stable state for serial comparison; the median interval between tests was 376 (inter-quartile range, 136 – 651) days. FVC, forced vital capacity.

* One of the patients received right-upper lobectomy for the mass-like organizing pneumonia. ** This patient also had asthma.

Supplemental Table S2 Fleiss' kappa for the inter-observer agreement among the three interpreters of computed tomographic features

Computed tomographic features	Fleiss' kappa (95% CI)
Single-lobe or multi-lobe	0.914 (0.911 – 0.917)
Single-pattern or mixed-pattern	0.811 (0.808 – 0.814)
Alveolar consolidation	0.746 (0.744 – 0.749)
Ground glass opacity	0.705 (0.702 – 0.708)
Nodular opacity	0.751 (0.748 – 0.753)
Mass-like opacity	0.751 (0.748 – 0.754)
Bronchocentric opacity	0.770 (0.767 – 0.773)
Reverse halo sign	0.751 (0.748 – 0.754)
Crazy paving opacity	1.000 (0.997 – 1.003)
Reticulo-infiltrative opacity	0.704 (0.701 – 0.707)
Band-like opacity	0.756 (0.753 – 0.759)

95% CI, 95% confidence interval.

The three independent interpreters: Li-Ting Huang is a pulmonary radiologist; Hong-Ping Er and Sheng-Huan Wei are pulmonologists.

Supplementa1 Table S3 Distribution of different aetiologies, clinical managements, and outcomes among patients with different computed tomographic features

	Extent of parenchymal involvement			CT imaging patterns			Combined assessment of extent and patterns[1]			
	Single lobe N = 74	Multi-lobes N = 82	*P*-value	Single N = 100	Mixed N = 56	*P*-value	Group 1 N = 71	Group 2 N = 32	Group 3 N = 53	*P*-value
Aetiology			0.001			< 0.001				< 0.001
Cryptogenic	71 (96)	59 (72)		94 (94)	36 (64)		70 (99)	25 (78)	35 (66)	
Secondary	3 (4)	23 (28)		6 (6)	20 (36)		1 (1)	7 (22)	18 (34)	
CTD-related	1 (1)	13 (16)		3 (3)	11 (20)		0 (0)	4 (13)	10 (19)	
Drug-related	2 (3)	8 (10)		2 (2)	8 (14)		1 (1)	2 (6)	7 (13)	
Post-transplant	0 (0)	2 (2)		1 (1)	1 (2)		0 (0)	1 (3)	1 (2)	
Methods of biopsy			0.042			0.079				0.065
Surgical	38 (51)	53 (65)		56 (56)	35 (63)		36 (51)	22 (69)	33 (62)	
CT-guided percutaneous	5 (7)	10 (12)		7 (7)	8 (14)		4 (5)	4 (12)	7 (13)	
Transbronchial forceps	31 (42)	18 (22)		37 (37)	12 (21)		31 (44)	6 (19)	12 (23)	
Sonar-guided percutaneous	0 (0)	1 (1)		0 (0)	1 (2)		0 (0)	0 (0)	1 (2)	
Season of diagnosis			0.811			0.117				0.181
Spring (Mar. - May)	18 (24)	22 (27)		26 (26)	14 (25)		17 (24)	10 (31)	13 (25)	
Summer (Jun. – Aug.)	26 (35)	24 (29)		38 (38)	12 (21)		25 (35)	14 (44)	11 (21)	
Fall (Sep. – Nov.)	18 (24)	19 (23)		21 (21)	16 (29)		17 (24)	5 (16)	15 (28)	
Winter (Dec. – Feb.)	12 (17)	17 (21)		15 (15)	14 (25)		12 (17)	3 (9)	14 (26)	
Treatments			< 0.001			< 0.001				< 0.001
Non-pharmacological	67 (91)	26 (32)		80 (80)	13 (23)		64 (90)	19 (59)	10 (19)	
Observation alone	31 (42)	14 (17)		38 (38)	7 (12)		30 (42)	9 (28)	6 (11)	
Surgical resection	36 (49)	12 (14)		42 (42)	6 (11)		34 (48)	10 (31)	4 (8)	
Immunosuppressive	7 (9)	56 (68)		20 (20)	43 (77)		7 (10)	13 (41)	43 (81)	

Corticosteroid alone	7 (9)	48 (59)		18 (18)	37 (66)		7 (10)	11 (35)	37 (70)	
Corticosteroid and another immunosuppressant	0 (0)	7 (9)		1 (1)	6 (11)		0 (0)	1 (3)	6 (11)	
Other immunosuppressant	0 (0)	1 (1)		1 (1)	0 (0)		0 (0)	1 (3)	0 (0)	
Needed supplemental oxygen	3 (4)	38 (46)	< 0.001	7 (7)	34 (61)	< 0.001	3 (4)	4 (13)	34 (64)	< 0.001
Needed mechanical ventilation	0 (0)	18 (22)	< 0.001	2 (2)	16 (29)	< 0.001	0 (0)	2 (6)	16 (30)	< 0.001
Outcomes			0.001			< 0.001				< 0.001
Improved	69 (93)	60 (73)		92 (92)	37 (66)		66 (93)	29 (91)	34 (64)	
Persistent disease	5 (7)	6 (7)		7 (7)	4 (7)		5 (7)	2 (6)	4 (8)	
Recurrence	0 (0)	5 (6)	0.031	0 (0)	5 (9)	0.002	0 (0)	0 (0)	5 (9)	0.007
Death	0 (0)	11 (14)	0.001	1 (1)	10 (18)	< 0.001	0 (0)	1 (3)	10 (19)	< 0.001

Values are presented as counts and percentages of the group N. CT, computed tomography; CTD, connective tissue diseases.

[1] Group 1, single-lobe and single-pattern; Group 2, single-lobe and mixed-pattern or multi-lobe and single-pattern; Group 3, multi-lobe and mixed-pattern.

Supplemental Table S4 Distribution of different aetiologies, clinical managements, and outcomes among 86 patients having baseline pulmonary function tests available and different computed tomographic features

	Patients with FVC ≥ 80% of prediction			
	Group 1[1] N = 36	Group 2[1] N = 16	Group 3[1] N = 10	*P*-value
Needed supplemental oxygen	0 (0)	1 (6)	6 (60)	< 0.001
Needed mechanical ventilation	0 (0)	0 (0)	3 (30)	< 0.001
Outcomes				0.001
Improved	34 (94)	15 (94)	6 (60)	
Persistent disease	2 (6)	1 (6)	0 (0)	
Recurrence	0 (0)	0 (0)	2 (20)	0.005
Death	0 (0)	0 (0)	2 (20)	0.005
	Patients with 50% ≤ FVC < 80% of prediction			
	Group 1[1] N = 2	Group 2[1] N = 4	Group 3[1] N = 13	*P*-value
Needed supplemental oxygen	0 (0)	0 (0)	9 (69)	0.019
Needed mechanical ventilation	0 (0)	0 (0)	2 (15)	0.597
Outcomes				0.905
Improved	2 (100)	4 (100)	11 (84)	
Persistent disease	0 (0)	0 (0)	1 (8)	
Recurrence	0 (0)	0 (0)	0 (0)	-
Death	0 (0)	0 (0)	1 (8)	0.784
	Patients with FVC < 50% of prediction			
	Group 1[1] N = 2	Group 2[1] N = 0	Group 3[1] N = 3	*P*-value
Needed supplemental oxygen	0 (0)	0 (0)	1 (33)	0.361
Needed mechanical ventilation	0 (0)	0 (0)	1 (33)	0.361
Outcomes				0.659
Improved	1 (50)	0 (0)	1 (33)	
Persistent disease	1 (50)	0 (0)	1 (33)	
Recurrence	0 (0)	0 (0)	1 (33)	0.361
Death	0 (0)	0 (0)	0 (0)	-

Baseline pulmonary function data was available in 86 patients. Values are presented as counts and percentages of the group N. FVC, forced vital capacity.

[1] Groups are based on the combined assessment of the extent and patterns of involvement on computed tomographic images: Group 1, single-lobe and single-pattern; Group 2, single-lobe and mixed-pattern or multi-lobe and single-pattern; Group 3, multi-lobe and mixed-pattern.

Supplemental Table S5 Baseline characteristics of the three groups based on the combined assessment of the extents and patterns of organizing pneumonia

	Group 1[1] N = 71	Group 2[1] N = 32	Group 3[1] N = 53	*P* - value
Age, years	61.0 (52.8 - 70.1)	60.4 (51.7 - 66.8)	65.2 (57.4 - 76.2)	0.093
Sex				0.071
Female, n (%)	25 (35)	19 (59)	22 (42)	
Male, n (%)	46 (65)	13 (41)	31 (58)	
Body height, cm	162.3 (± 10.0)	159.7 (± 8.6)	159.9 (± 8.7)	0.351
Body weight, kg	62.4 (54.5 – 71.0)	60.1 (55.5 – 66.3)	59.2 (51.4 – 65.3)	0.356
Charlson comorbidity index	3 (1 – 5)	2 (2 – 6)	4 (3 – 6)	0.047
Cigarette smoking status:				0.053
Never smoker, n (%)	43 (61)	23 (72)	39 (74)	
Current smoker, n (%)	20 (28)	5 (16)	4 (8)	
Former smoker, n (%)	8 (11)	4 (12)	10 (18)	
Baseline pulmonary function				
FVC, % of prediction [1]	107 (90 - 120)	94 (86 – 105)	67 (60 – 87)	< 0.001
TLC, % of prediction [2]	109 (95 – 117)	94 (87 – 106)	71 (63 – 84)	< 0.001
D_{LCO}, % [3]	NA	62 (51 – 71)	52 (46 – 73)	0.896
Aetiology				< 0.001
Cryptogenic, n (%)	70 (99)	25 (78)	35 (66)	
CTD-related, n (%)	0 (0)	4 (13)	10 (19)	
Drug-related, n (%)	1 (1)	2 (6)	7 (13)	
Post-transplant, n (%)	0 (0)	1 (3)	1 (2)	
Duration of follow-up, weeks	123.6 (30.3 – 250.1)	107.0 (30.9 – 247.5)	125.9 (38.4 – 292.4)	0.940

CTD, connective tissue disease; D_{LCO}, diffusion capacity of the lung for carbon monoxide; FVC, forced vital capacity; NA, not available; TLC, total lung capacity. Discrete variables are presented as counts (% of the group N). Continuous variables are presented as means (± standard deviation) if normally distributed, and medians (interquartile ranges) if not normally distributed. [1] Groups are based on the combined assessment of the extent and patterns of involvement on computed tomographic images: Group 1, single-lobe and single-pattern; Group 2, single-lobe and mixed-pattern or multi-lobe and single-pattern; Group 3, multi-lobe and mixed-pattern.

[1] Data available for 86 patients.

[2] Data available for 71 patients.

[3] Data available for 20 patients; data not available for Group 1.

Supplemental Table S6 Univariate and multivariable logistic regression analysis on the association between computed tomographic features and ***secondary*** organizing pneumonia

	Crude odds ratio[2] of secondary OP (95% CI)	Adjusted odds ratio[3] of secondary OP (95% CI)
Extent of involvement on CT images		
Single lobe	Reference	Reference
Multiple lobes	8.07 (2.79 – 31.31)**	Model 1[4]: 6.99 (2.35 – 27.76)**
		Model 2[5]: 3.44 (0.88 – 15.71)
Patterns on CT images		
Single pattern	Reference	Reference
Mixed patterns	8.17 (3.27 – 22.97)**	Model 1[4]: 6.38 (2.51 – 18.14)**
		Model 2[5]: 3.32 (1.13 – 10.96)*
Groups based on the combined assessment of extent and patterns on CT images[1]		
Group 1	Reference	Reference
Group 2	13.82 (2.82 – 135.76)**	11.77 (2.36 – 115.80)*
Group 3	24.49 (5.83 – 227.54)**	19.08 (4.46 – 177.80)**

CT, computed tomography; OP, organizing pneumonia; 95% CI, 95% confidence interval. [1] Groups are based on the combined assessment of the extent and patterns of involvement on CT images: Group 1, single-lobe and single-pattern; Group 2, single-lobe and mixed-pattern or multi-lobe and single-pattern; Group 3, multi-lobe and mixed-pattern. [2] Derived from the univariate Firth's logistic regression analysis. [3] Derived from the multivariable Firth's logistic regression models, incorporating sex, age, body height, body weight, Charlson comorbidity index, and smoking status as covariables. [4] In Model 1, either extent of involvement or patterns on CT was separately included (together with other covariables) in the multivariable Firth's logistic regression analysis. [5] In Model 2, *both* extent of involvement and patterns on CT were simultaneously included (together with other covariables) in the multivariable Firth's logistic regression analysis. * P <0.05. ** P < 0.001.

Supplemental Table S7 Univariate and multivariable logistic regression analysis on the association between computed tomographic features and subsequent immunosuppressive treatments

	Crude odds ratio[2] of immunosuppressive treatments (95% CI)	Adjusted odds ratio[3] of immunosuppressive treatments (95% CI)
Extent of involvement on CT images		
Single lobe	Reference	Reference
Multiple lobes	19.19 (8.34 – 49.77)**	Model 1[4]: 12.45 (5.20 – 33.70)**
		Model 2[5]: 7.39 (2.70 – 22.00)**
Patterns on CT images		
Single pattern	Reference	Reference
Mixed patterns	12.65 (5.95 – 28.50)**	Model 1[4]: 7.97 (3.55 – 18.94)**
		Model 2[5]: 2.80 (1.06 – 7.47)*
Groups based on the combined assessment of extent and patterns on CT images[1]		
Group 1	Reference	Reference
Group 2	5.95 (2.19 – 17.39)**	3.39 (1.11 – 10.67)*
Group 3	35.63 (13.68 – 105.24)**	19.58 (7.28 – 59.81)**

CT, computed tomography; 95% CI, 95% confidence interval. [1] Groups are based on the combined assessment of the extent and patterns of involvement on CT images: Group 1, single-lobe and single-pattern; Group 2, single-lobe and mixed-pattern or multi-lobe and single-pattern; Group 3, multi-lobe and mixed-pattern. [2] Derived from the univariate Firth's logistic regression analysis. [3] Derived from the multivariable Firth's logistic regression models, incorporating sex, age, body height, body weight, Charlson comorbidity index, smoking status, and aetiology as covariables. [4] In Model 1, either extent of involvement or patterns on CT was separately included (together with other covariables) in the multivariable Firth's logistic regression analysis. [5] In Model 2, *both* extent of involvement and patterns on CT were simultaneously included (together with other covariables) in the multivariable Firth's logistic regression analysis. * P <0.05. ** P < 0.001.

Supplemental Table S8 Univariate and multivariable logistic regression analysis on the association between computed tomographic features and the risk of severe disease

	Crude odds ratio[2] of severe disease (95% CI)	Adjusted odds ratio[3] of severe disease (95% CI)
Extent of involvement on CT images		
Single lobe	Reference	Reference
Multiple lobes	17.67 (6.28 – 67.78)**	Model 1[4]: 17.84 (5.55 – 79.66)**
		Model 2[5]: 6.20 (1.59 – 30.29)*
Patterns on CT images		
Single pattern	Reference	Reference
Mixed patterns	19.12 (8.04 – 50.89)**	Model 1[4]: 12.87 (5.12 – 36.50)**
		Model 2[5]: 5.11 (1.80 – 16.07)*
Groups based on the combined assessment of extent and patterns on CT images[1]		
Group 1	Reference	Reference
Group 2	3.09 (0.71 – 14.63)	4.24 (0.89 – 22.84)
Group 3	34.63 (11.59 – 138.37)**	27.64 (8.25 – 127.44)**

CT, computed tomography; 95% CI, 95% confidence interval. Please refer to the main text for the definition of severe disease. [1] Groups are based on the combined assessment of the extent and patterns of involvement on CT images: Group 1, single-lobe and single-pattern; Group 2, single-lobe and mixed-pattern or multi-lobe and single-pattern; Group 3, multi-lobe and mixed-pattern. [2] Derived from the univariate Firth's logistic regression analysis. [3] Derived from the multivariable Firth's logistic regression models, incorporating sex, age, body height, body weight, Charlson comorbidity index, smoking status, and aetiology as covariables. [4] In Model 1, either extent of involvement or patterns on CT was separately included (together with other covariables) in the multivariable Firth's logistic regression analysis. [5] In Model 2, *both* extent of involvement and patterns on CT were simultaneously included (together with other covariables) in the multivariable Firth's logistic regression analysis. * P <0.05. ** P < 0.001.

Supplemental Table S9 Baseline characteristics and outcomes of patients with cryptogenic and secondary organizing pneumonia

	Cryptogenic (N = 130)	Secondary (N = 26)	*P* - value
Age, years	61.5 (54.0 – 71.0)	62.6 (55.8 – 73.7)	0.913
Sex			0.192
Female, n (%)	52 (40)	14 (54)	
Male, n (%)	78 (60)	12 (46)	
Body height, cm	161.5 (± 9.6)	158.2 (± 7.0)	0.078
Body weight, kg	62.3 (54.0 – 67.5)	56.9 (49.2 – 61.8)	0.042
Charlson comorbidity index	3 (2 – 5)	5 (3 – 6)	0.024
Cigarette smoking status:			0.226
Never smoker, n (%)	84 (65)	21 (81)	
Current smoker, n (%)	27 (21)	2 (8)	
Former smoker, n (%)	19 (14)	3 (11)	
Baseline pulmonary function tests			
Forced vital capacity, % of prediction [1]	98 (83 – 113)	75 (60 – 91)	0.005
Total lung capacity, % of prediction [2]	97 (89 – 114)	77 (62 – 86)	0.001
D_{LCO}, % [3]	66 (52 – 75)	51 (45 – 71)	0.280
Radiographic features			
Multi-lobe involvement, n (%)	59 (45)	23 (88)	< 0.001
Mixed-patterns, n (%)	36 (28)	20 (77)	< 0.001
Alveolar consolidation, n (%)	53 (41)	16 (62)	0.052
Ground-glass opacity, n (%)	32 (25)	16 (62)	< 0.001
Bronchocentric opacity, n (%)	15 (12)	7 (27)	0.040
Mass-like, n (%)	20 (15)	2 (8)	0.304
Nodule-like, n (%)	50 (38)	2 (8)	0.002
Infiltrative, n (%)	1 (1)	5 (19)	< 0.001
Reverse halo sign, n (%)	1 (1)	4 (15)	< 0.001
Crazy paving, n (%)	3 (2)	2 (8)	0.155
Aetiology			-
Cryptogenic, n (%)	130 (100)	-	
CTD-related, n (%)	-	14 (54)	
Drug-related, n (%)	-	10 (38)	
Post-transplant, n (%)	-	2 (8)	
Duration of follow-up, weeks	120.6 (31.0 – 274.6)	114.1 (34.0 – 255.7)	0.571
Treatments:			< 0.001
Observation only, n (%)	43 (33)	2 (8)	
Surgical resection, n (%)	47 (36)	1 (4)	

Corticosteroid alone, n (%)	38 (29)	17 (65)	
Combined corticosteroid and another immunosuppressant, n (%)	1 (1)	6 (23)	
Non-steroid immunosuppressant, n (%)	1 (1)	0 (0)	
Needed supplementary oxygen, n (%)	28 (22)	12 (46)	0.009
Needed mechanical ventilatory support, n (%)	10 (8)	7 (27)	0.004
Outcomes:			0.001
Improved without recurrence, n (%)	114 (87)	15 (57)	
Persistent disease, n (%)	8 (6)	3 (12)	
Improved but then recurred, n (%)	2 (2)	3 (12)	0.008
Death, n (%)	6 (5)	5 (19)	0.008

CTD, connective tissue disease; D_{LCO}, diffusion capacity of the lung for carbon monoxide. Discrete variables are presented as counts (% of the group N). Continuous variables are presented as means (± standard deviation) if normally distributed, and medians (interquartile ranges) if not normally distributed.

[1] Data available for 86 patients.

[2] Data available for 71 patients.

[3] Data available for 20 patients.

Supplemental Table S10 Univariate and multivariable logistic regression analysis on the association between computed tomographic features and the risk of severe disease, involving **only** patients with ***cryptogenic*** organizing pneumonia (N = 130)

	Crude odds ratio[2] for severe disease (95% CI)	Adjusted odds ratio[3] for severe disease (95% CI)
Extent of involvement on CT images		
Single lobe	Reference	Reference
Multiple lobes	21.99 (6.66 – 113.06)**	Model 1[4]: 21.25 (6.03 – 118.55)**
		Model 2[5]: 7.58 (1.59 – 48.55)*
Patterns on CT images		
Single pattern	Reference	Reference
Mixed patterns	21.13 (7.90 – 63.88)**	Model 1[4]: 13.55 (5.15 – 39.69)**
		Model 2[5]: 4.13 (1.26 – 15.01)*
Groups based on the combined assessment of extent and patterns on CT images[1]		
Group 1	Reference	Reference
Group 2	5.73 (1.18 – 34.86)*	7.06 (1.38 – 46.38)*
Group 3	45.67 (12.75 – 247.24)**	30.69 (8.59 – 167.10)**

CT, computed tomography; GGO, ground-glass opacity; 95% CI, 95% confidence interval. The analyses were performed involving **only** patients with ***cryptogenic*** organizing pneumonia (N = 130). Please refer to the main text for the definition of severe disease. [1] Groups are based on the combined assessment of the extent and patterns of involvement on CT images: Group 1, single-lobe and single-pattern; Group 2, single-lobe and mixed-pattern or multi-lobe and single-pattern; Group 3, multi-lobe and mixed-pattern. [2] Derived from the univariate Firth's logistic regression analysis, setting patients in Group 1 as the reference group. [3] Derived from the multivariable Firth's logistic regression models, incorporating sex, age, body height, body weight, Charlson comorbidity index, and smoking status as covariables. [4] In Model 1, either extent of involvement or patterns on CT was separately included (together with other covariables) in the multivariable Firth's logistic regression analysis. [5] In Model 2, *both* extent of involvement and patterns on CT were simultaneously included (together with other covariables) in the multivariable Firth's logistic regression analysis. * P <0.05. ** P < 0.001.* P <0.05. ** P < 0.001.

Supplemental Figure S1 Example images of the various computed tomographic features observed in patients of our study cohort

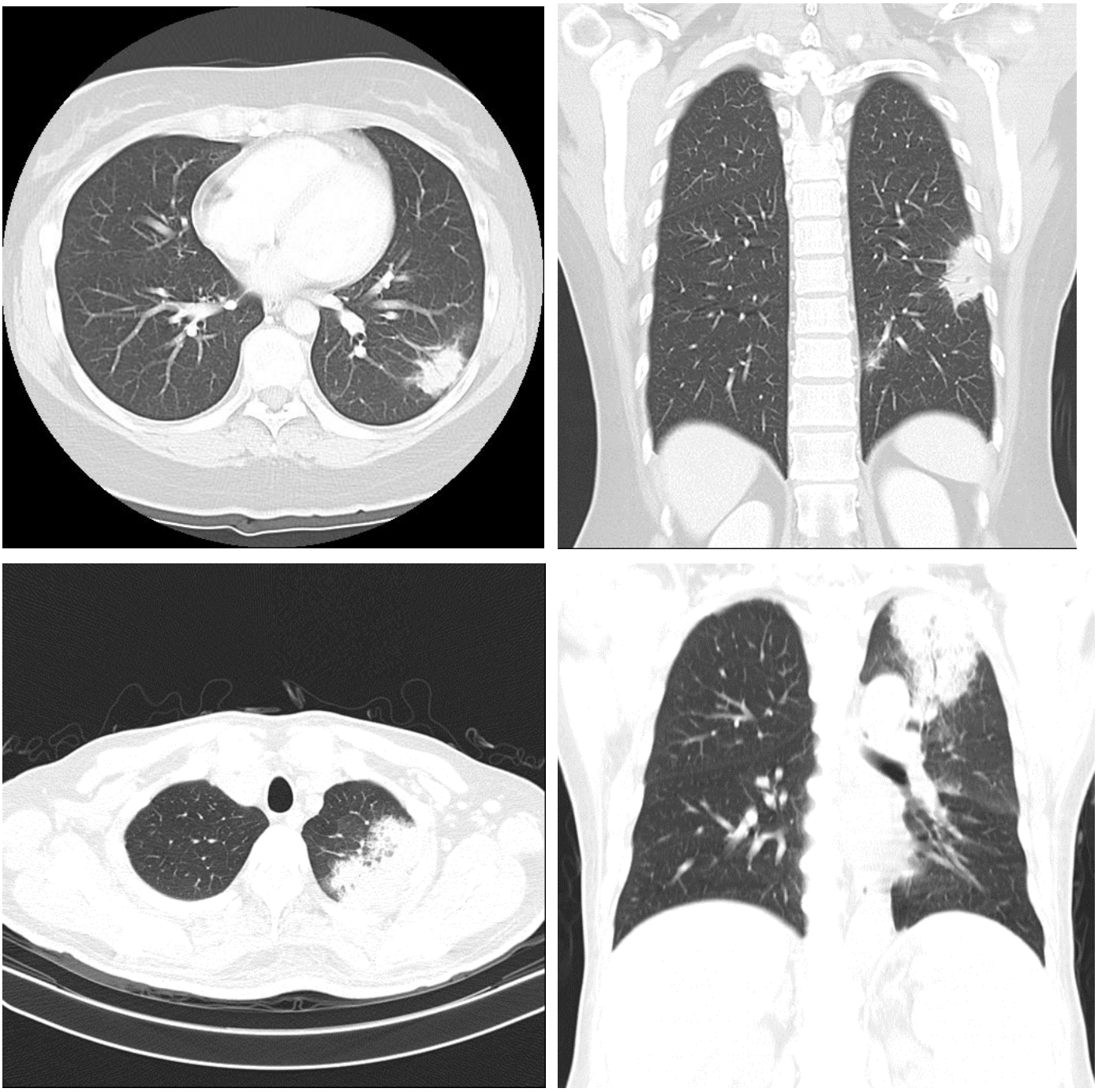

(S1a) Single-lobe focal alveolar consolidation of two different patients; upper left and right: transverse and coronal views (5-mm-slice) from a 41-year-old female; lower left and right: transverse and coronal views (2-mm-slice) from a 61-year-old male (**single-lobe and single-pattern**).

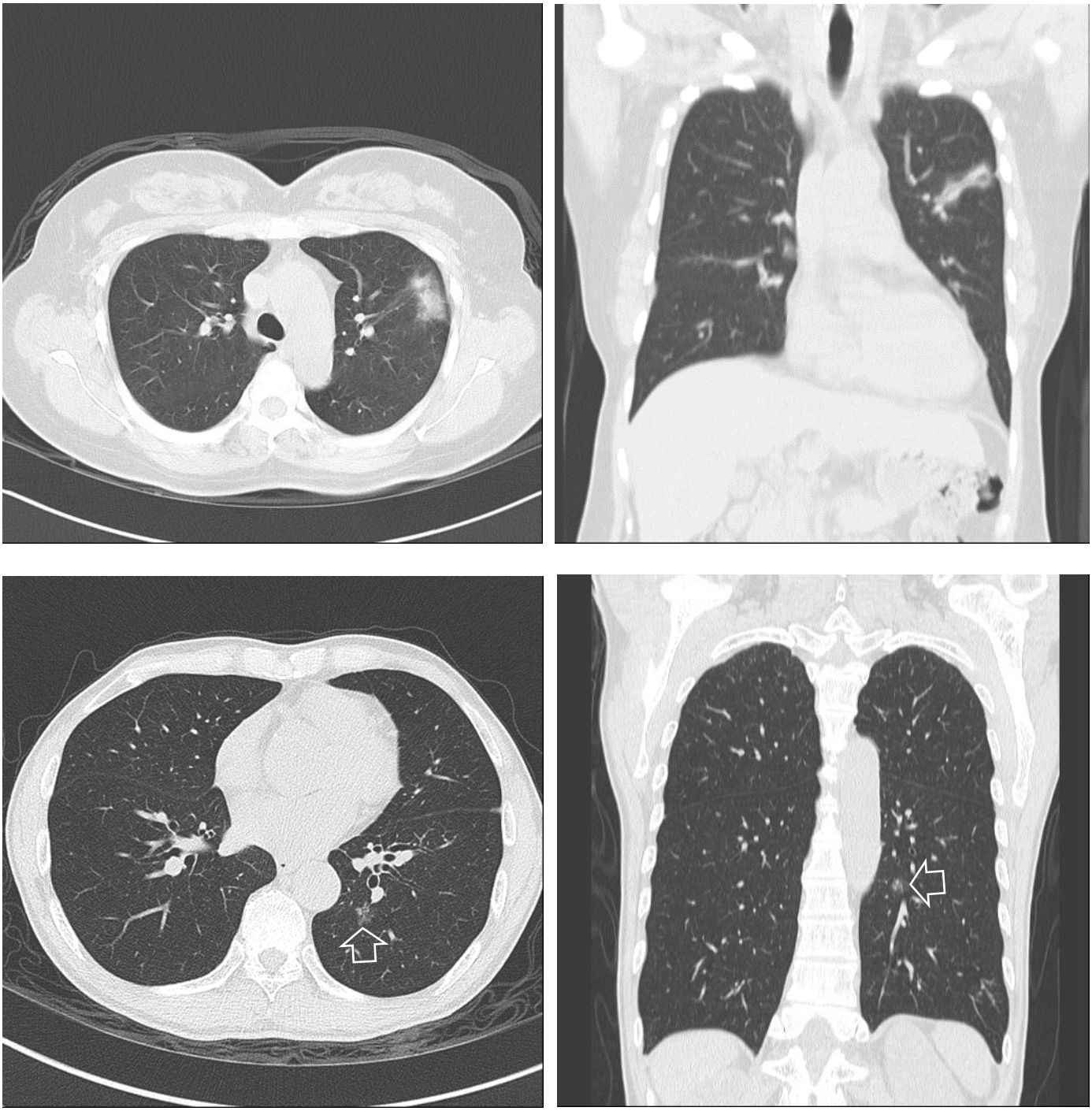

(S1b) Single-lobe focal ground-glass opacity of two different patients; upper left and right: transverse and coronal views (5-mm-slice) from a 49-year-old female; lower left and right: transverse and coronal views (2-mm-slice) from a 68-year-old male, with the lesion arrowed (**single-lobe and single-pattern**).

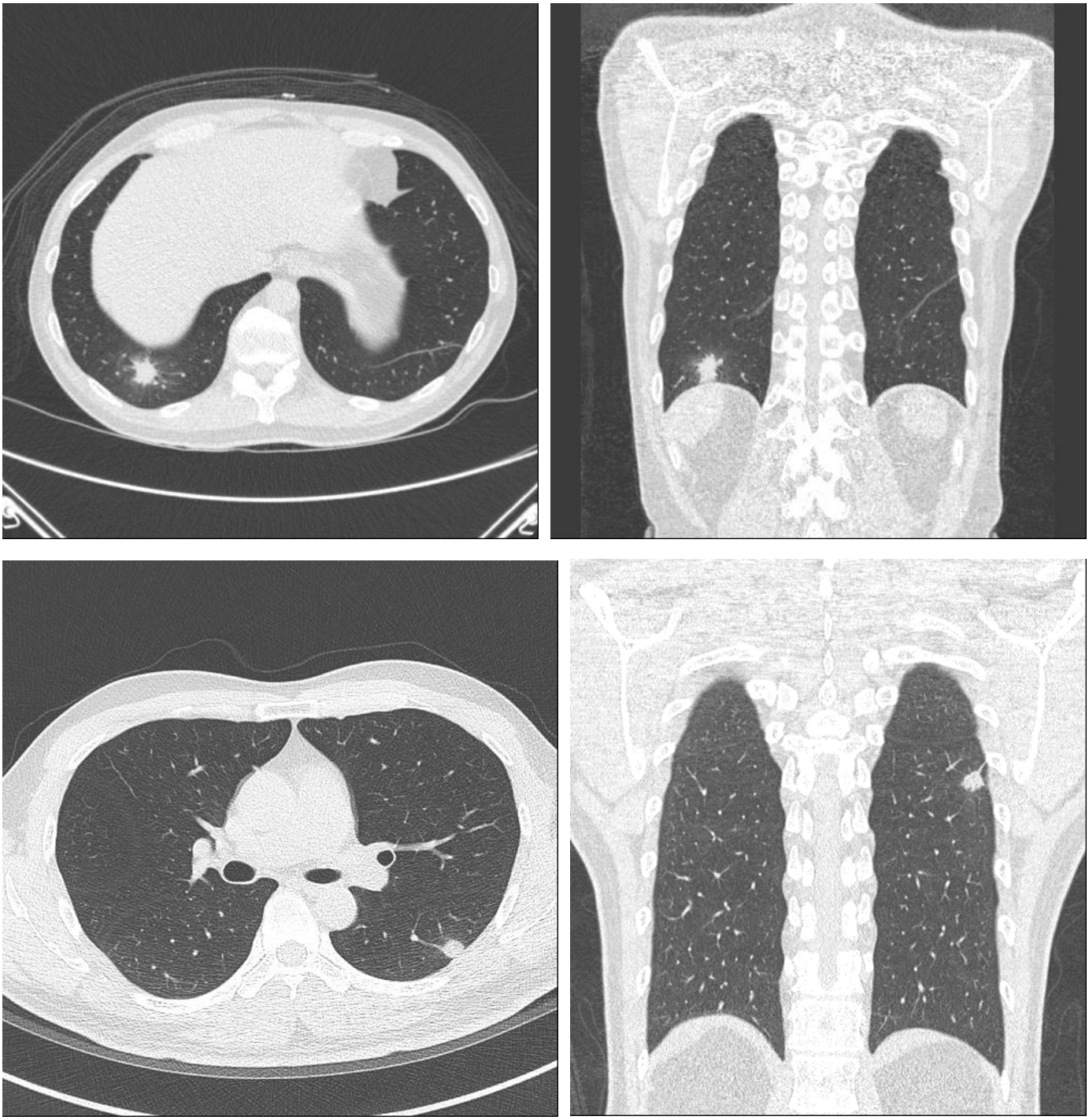

(S1c) Single-lobe nodular opacity of two different patients; upper left and right: transverse and coronal views (1-mm-slice) from a 57-year-old male; lower left and right: transverse and coronal views (2-mm-slice) from a 53-year-old male (**single-lobe and single-pattern**).

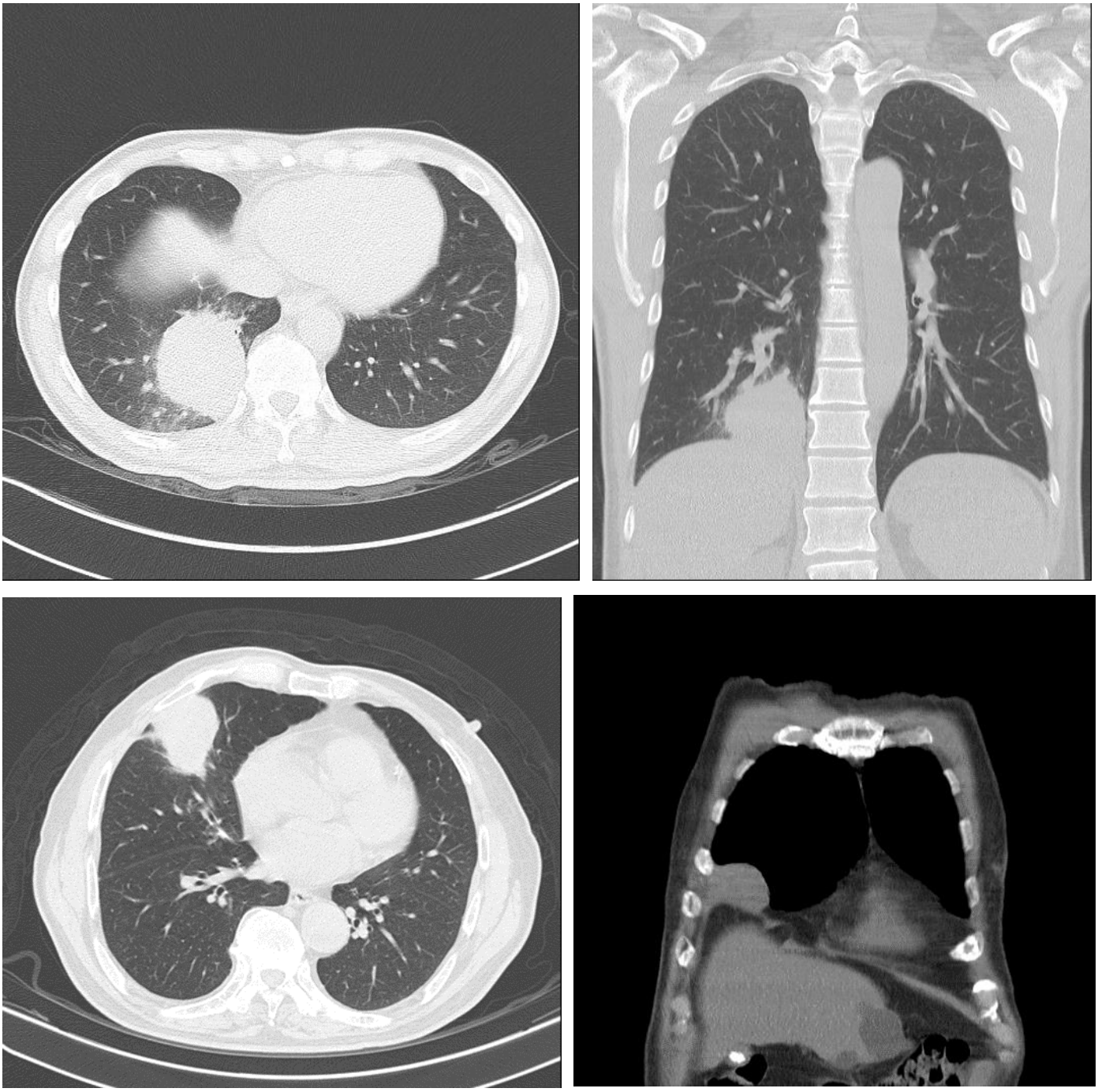

(S1d) Single-lobe mass-like opacity of two different patients; upper left and right: transverse and coronal views (5-mm-slice) from a 52-year-old male; lower left and right: transverse and coronal views (2-mm-slice) from an 82-year-old male (**single-lobe and single-pattern**).

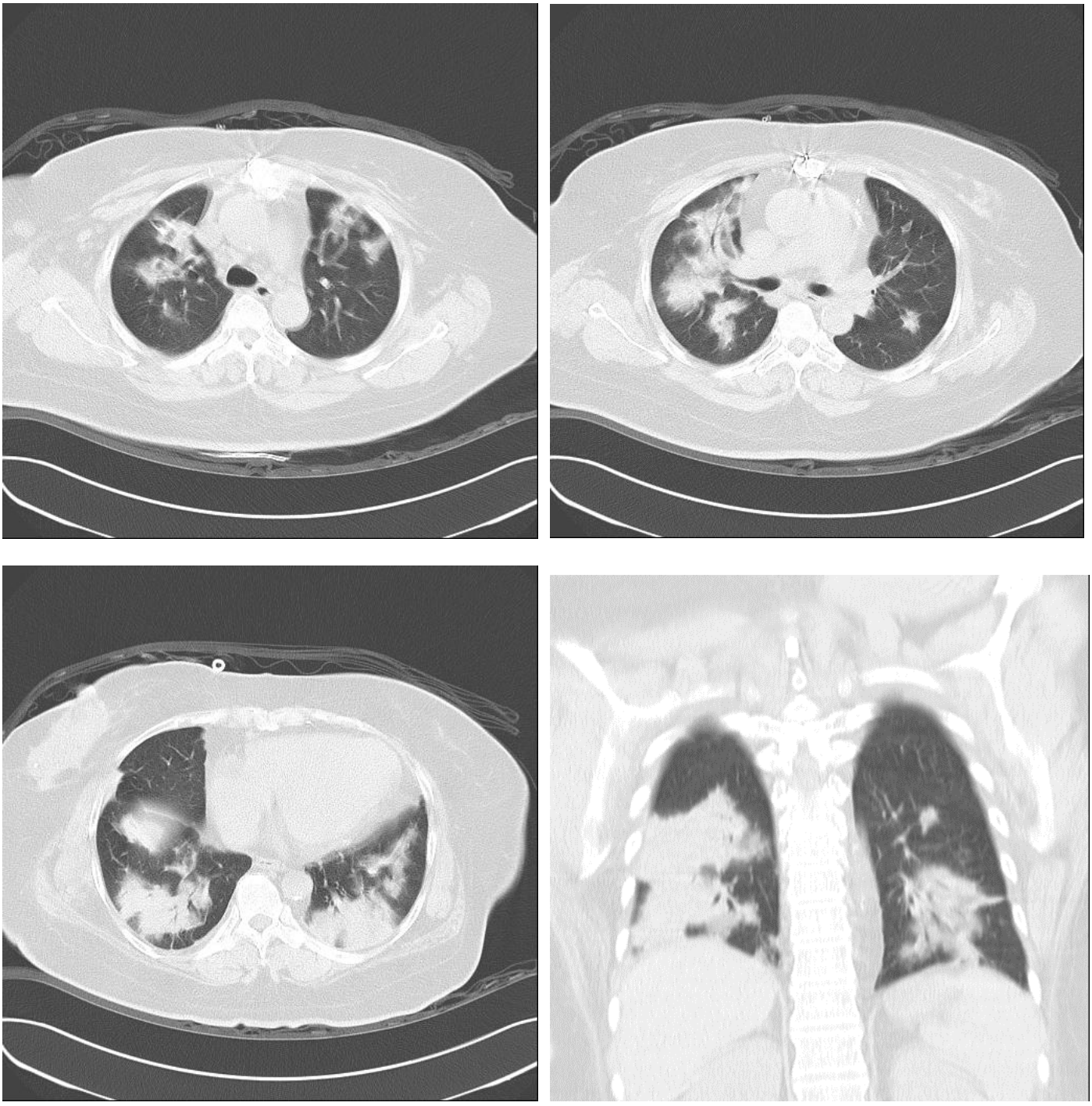

(S1e) Bilateral multi-lobe alveolar consolidations: transverse and coronal views (5-mm-slice) from a 58-year-old female with systemic lupus erythematosus (**multi-lobe and single-pattern**).

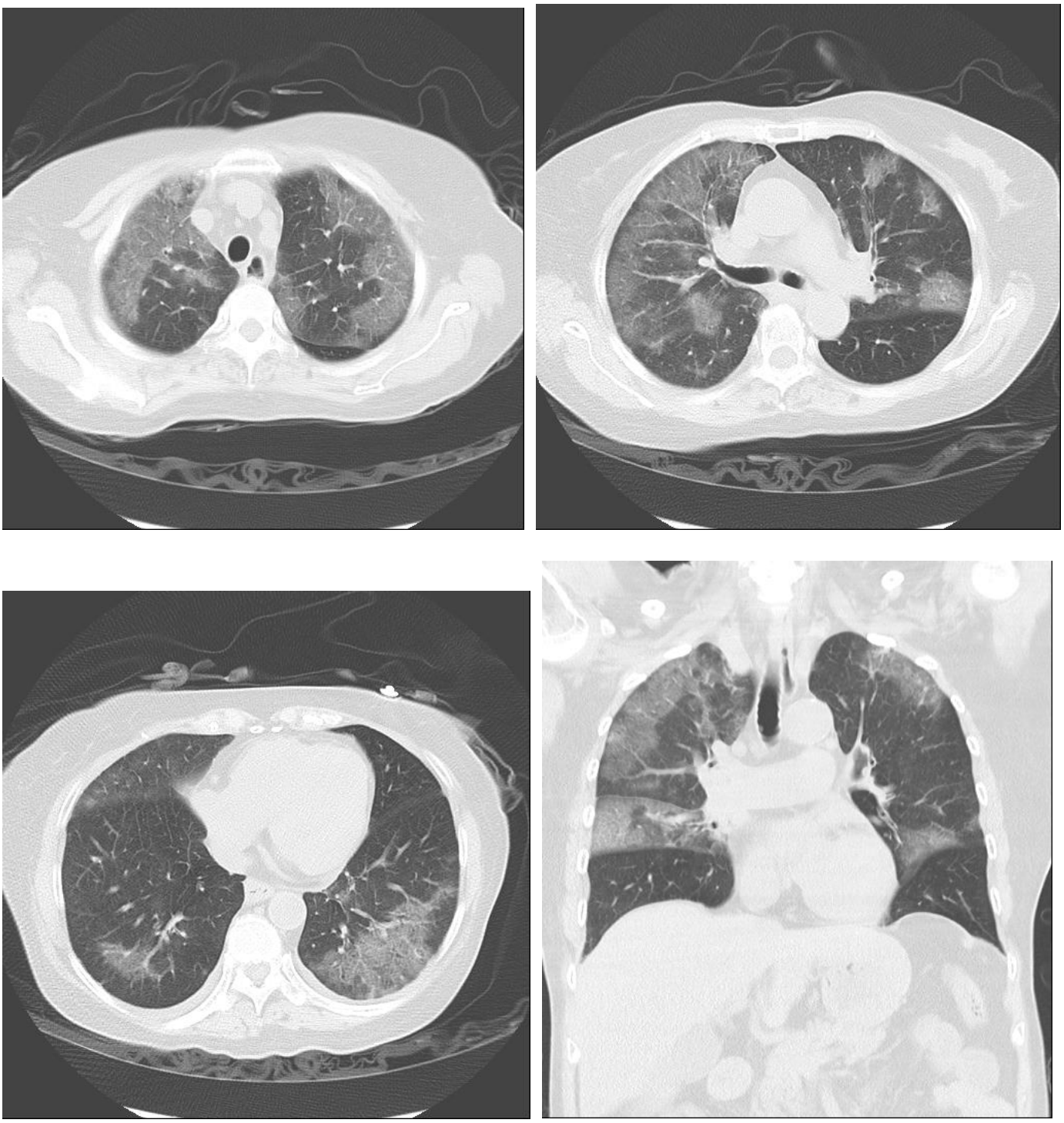

(S1f) Bilateral multi-lobe ground-glass opacities: transverse and coronal views (5-mm-slice) from a 67-year-old female (**multi-lobe and single-pattern**).

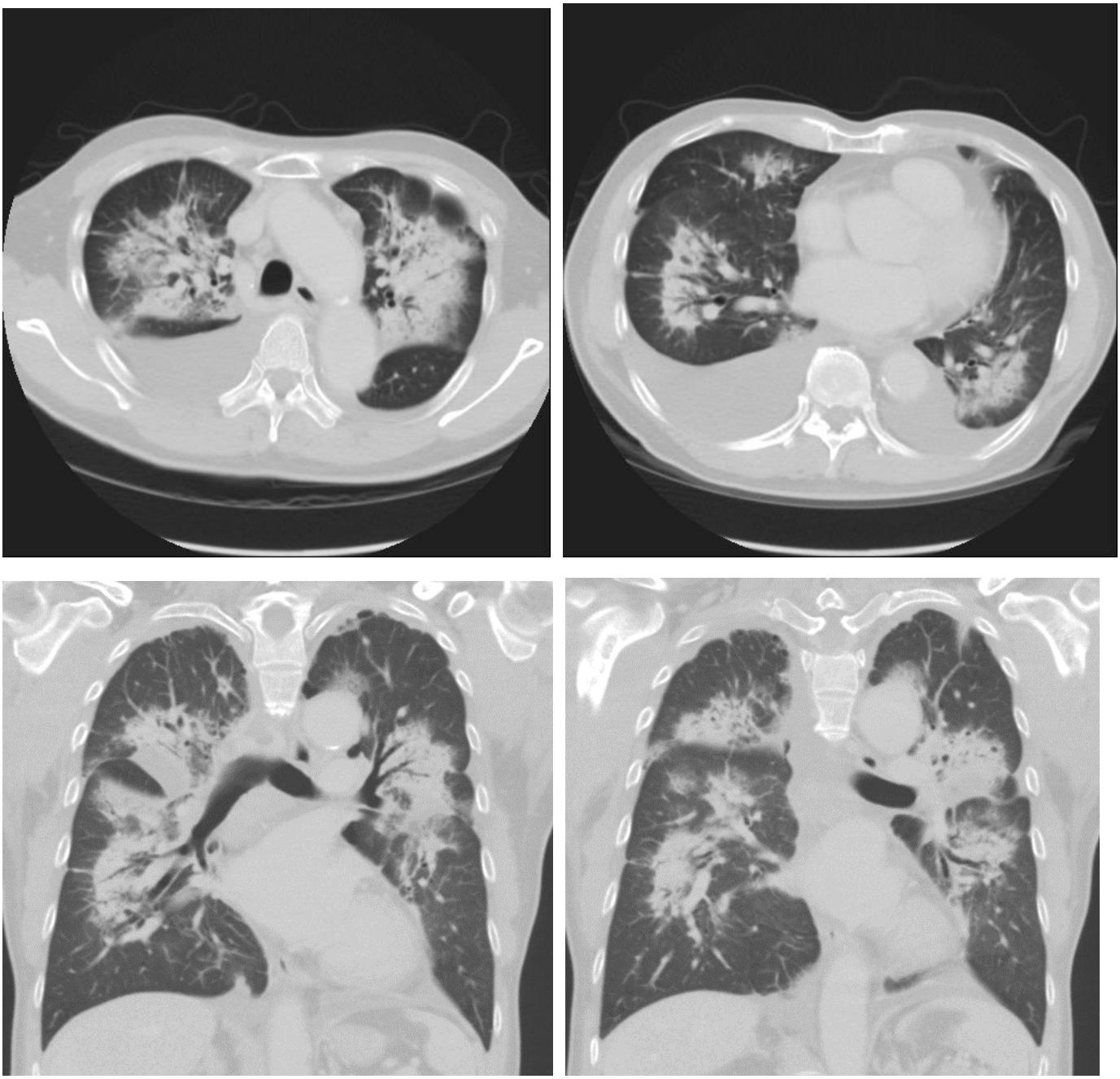

(S1g) Bilateral multi-lobe bronchocentric opacities: transverse and coronal views (5-mm-slice) from a 60-year-old male (**multi-lobe and single-pattern**).

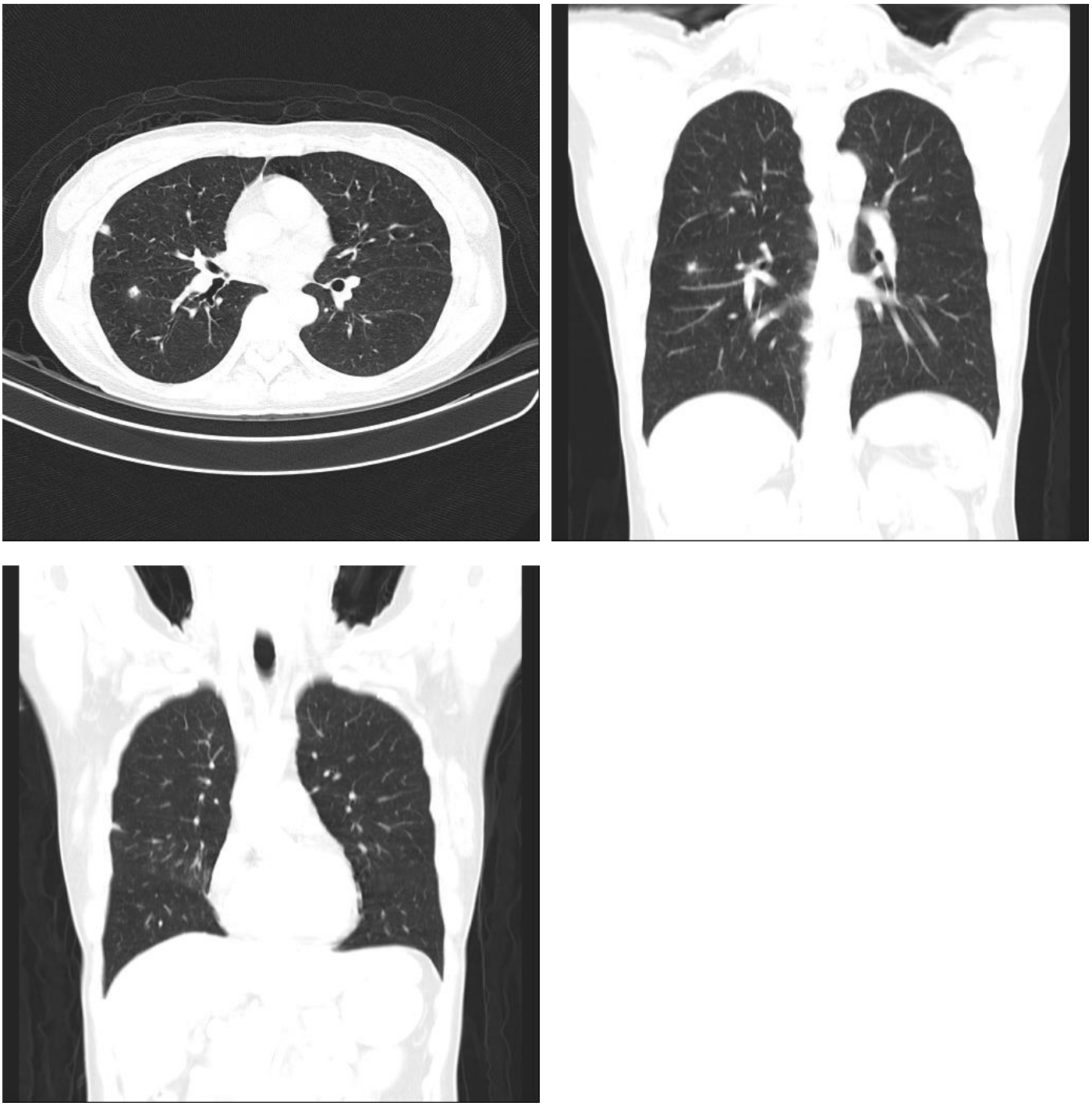

(S1h) ***Ipsilateral*** multi-lobe nodular opacities: transverse (2-mm-slice) and coronal (5-mm-slice) views from a 50-year-old female (**multi-lobe and single-pattern**).

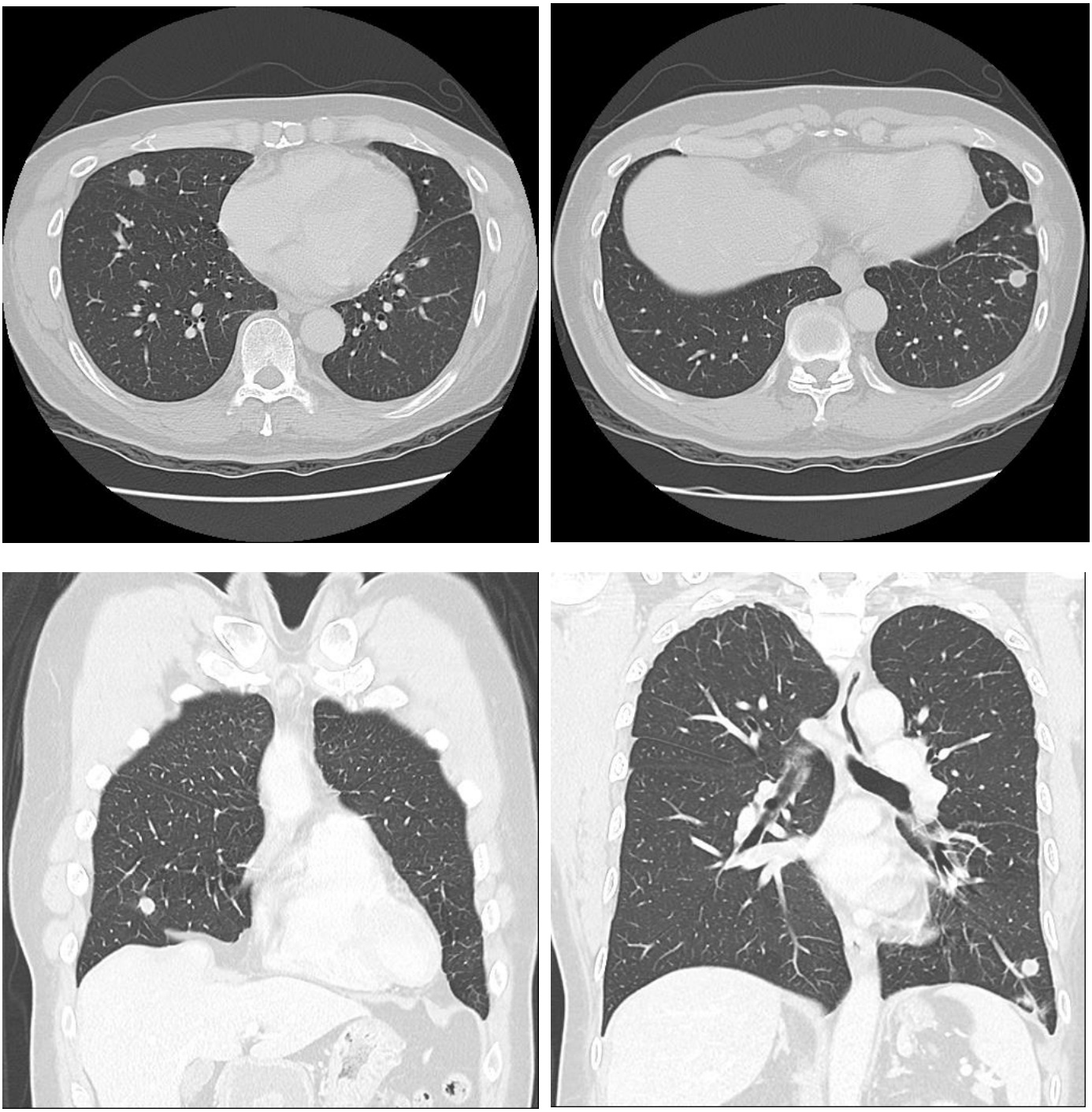

(S1i) ***Bilateral*** multi-lobe nodular opacities: transverse (2-mm-slice) and coronal (2-mm-slice) views from a 58-year-old male; both lesions were wedge-resected via video-assisted thoracoscopy (**multi-lobe and single-pattern**).

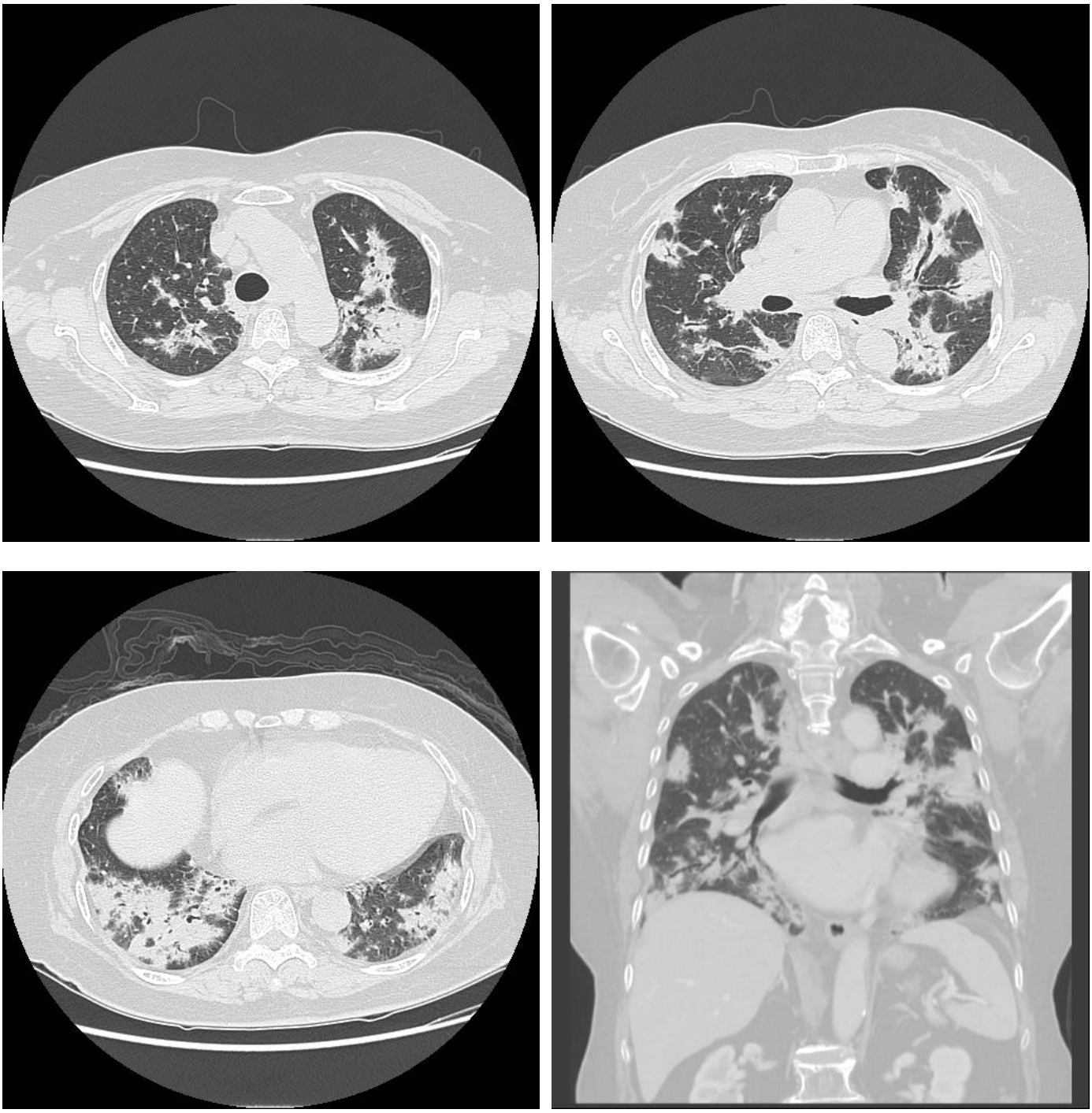

(S1j) Bilateral multi-lobe alveolar consolidations plus bronchocentric opacities: transverse and coronal views (1.25-mm-slice) from a 72-year-old female (**multi-lobe and mixed-pattern**).

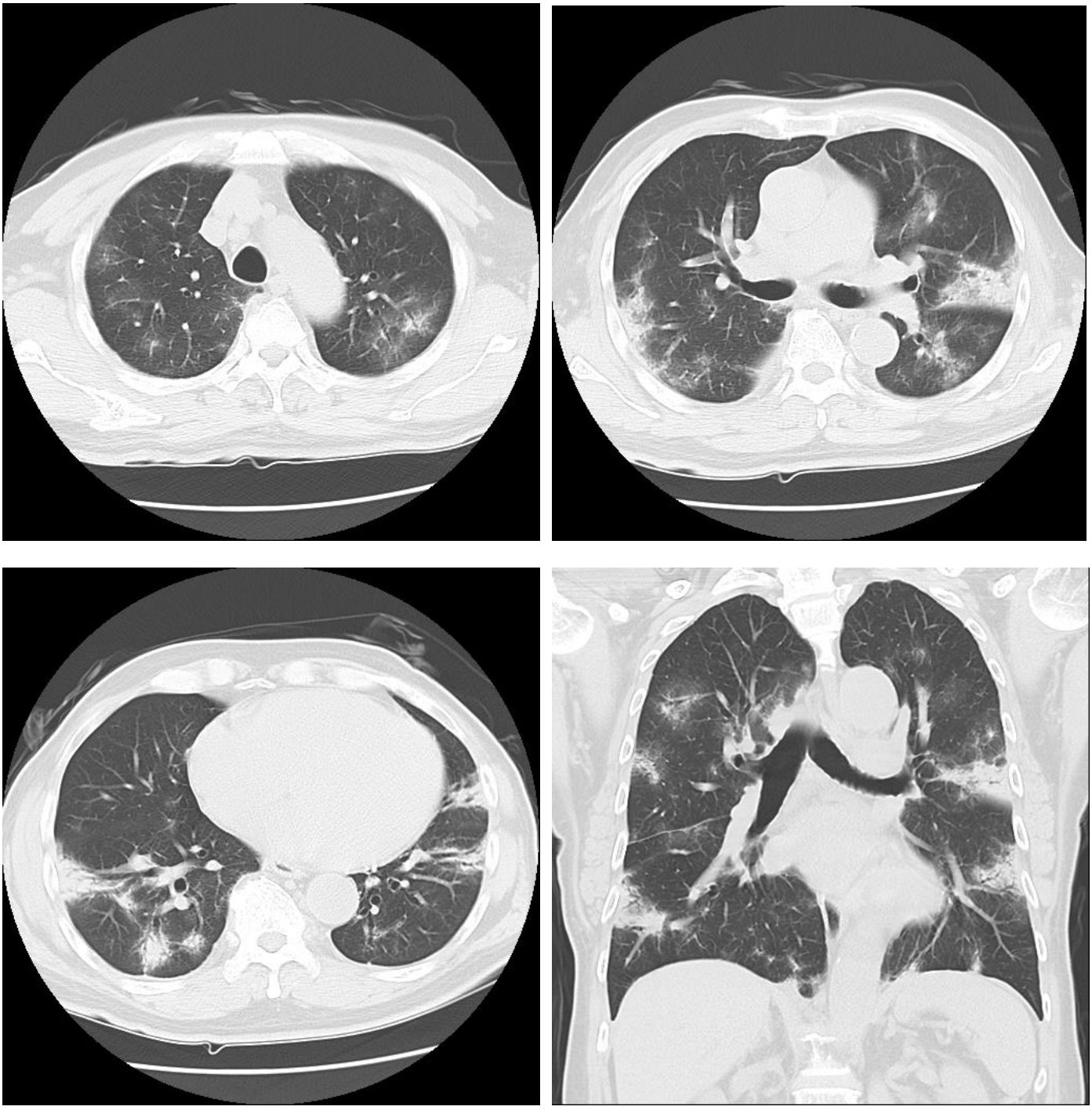

(S1k) Bilateral multi-lobe alveolar consolidations and ground-glass opacities: transverse and coronal views (5-mm-slice) from a 75-year-old male who was receiving amiodarone treatment at that time (**multi-lobe and mixed-pattern**).

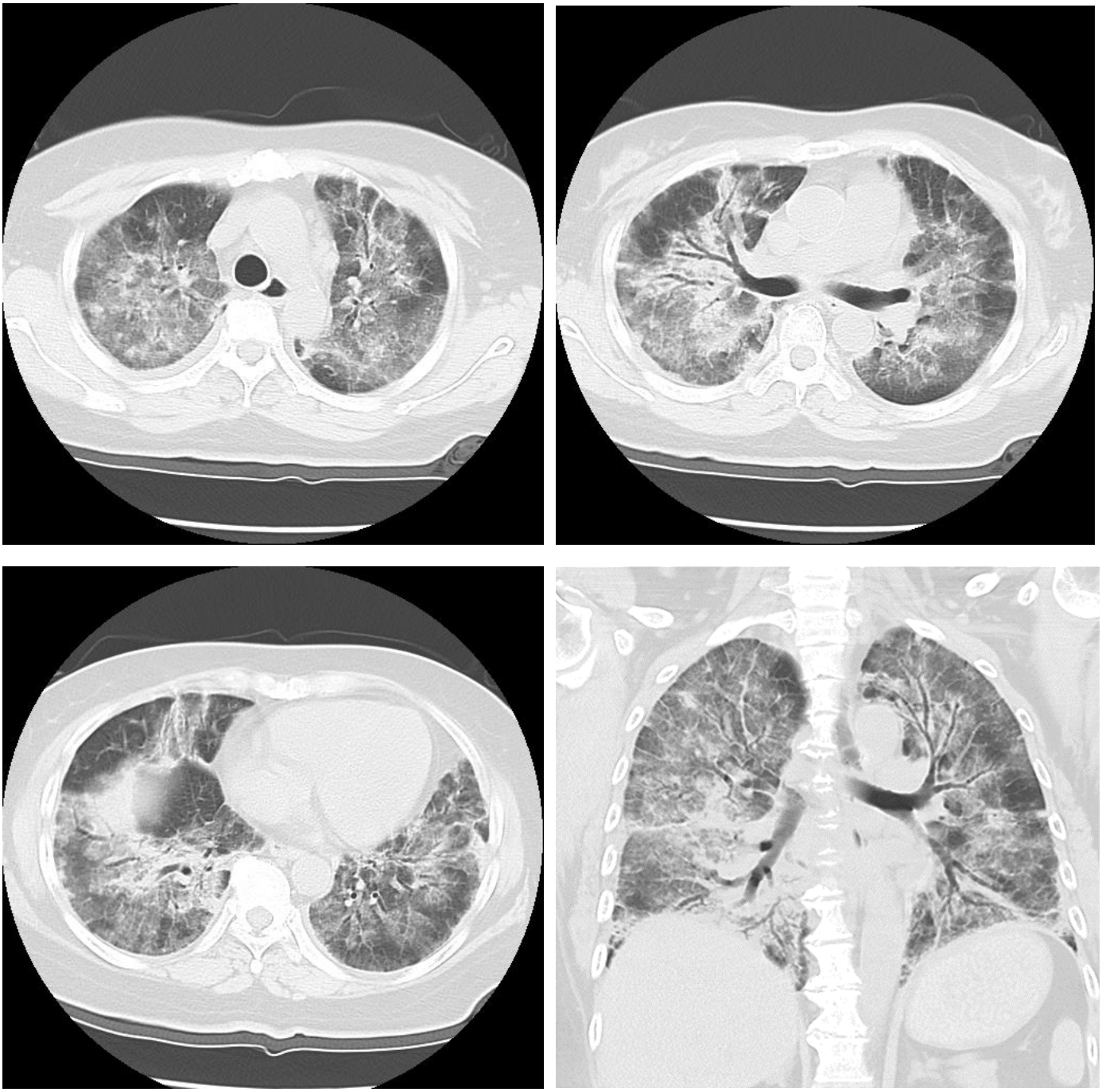

(S1l) Bilateral multi-lobe ground-glass and bronchocentric opacities: transverse and coronal views (5-mm-slice) from a 58-year-old female (**multi-lobe and mixed-pattern**).

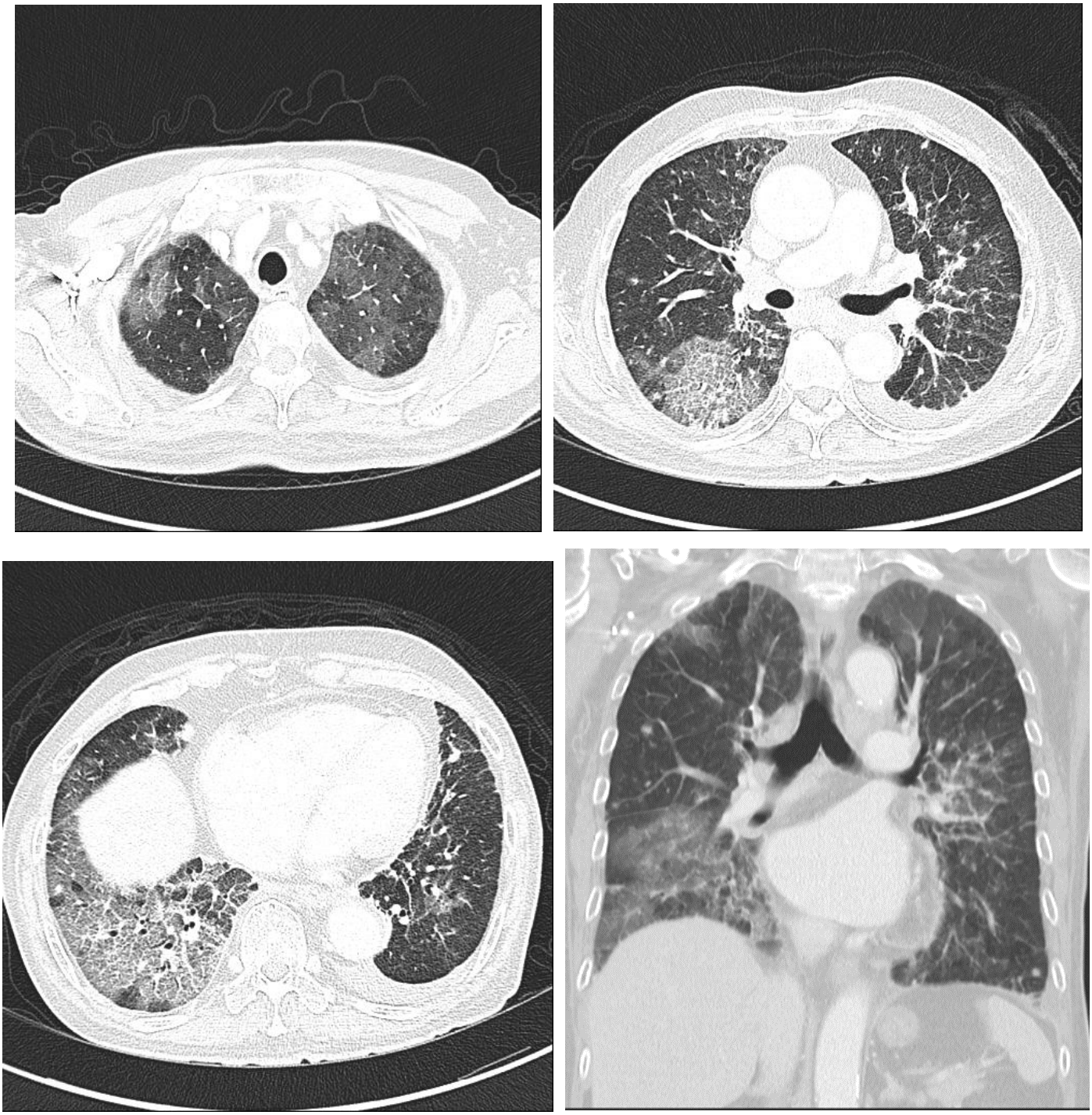

(S1m) Bilateral multi-lobe ground-glass opacities combined with a crazy paving pattern: transverse (2-mm-slice) and coronal (5-mm-slice) views from a 74-year-old male who was receiving amiodarone treatment at that time (**multi-lobe and mixed-pattern**).

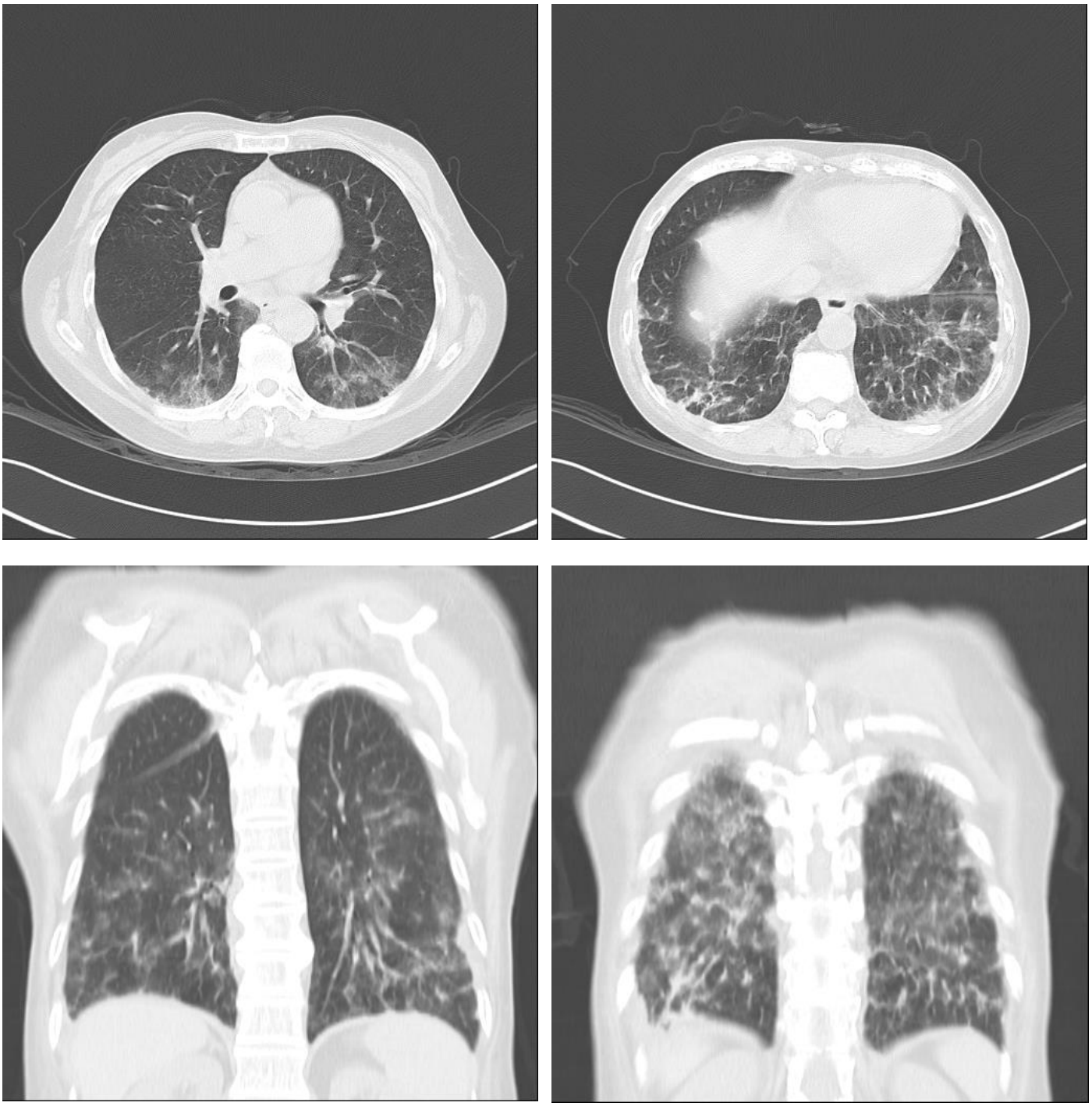

(S1n) Bilateral multi-lobe ground-glass opacities combined with a reticulo-infiltrative pattern: transverse and coronal (5-mm-slice) views from a 61-year-old female with rheumatoid arthritis (**multi-lobe and mixed-pattern**).

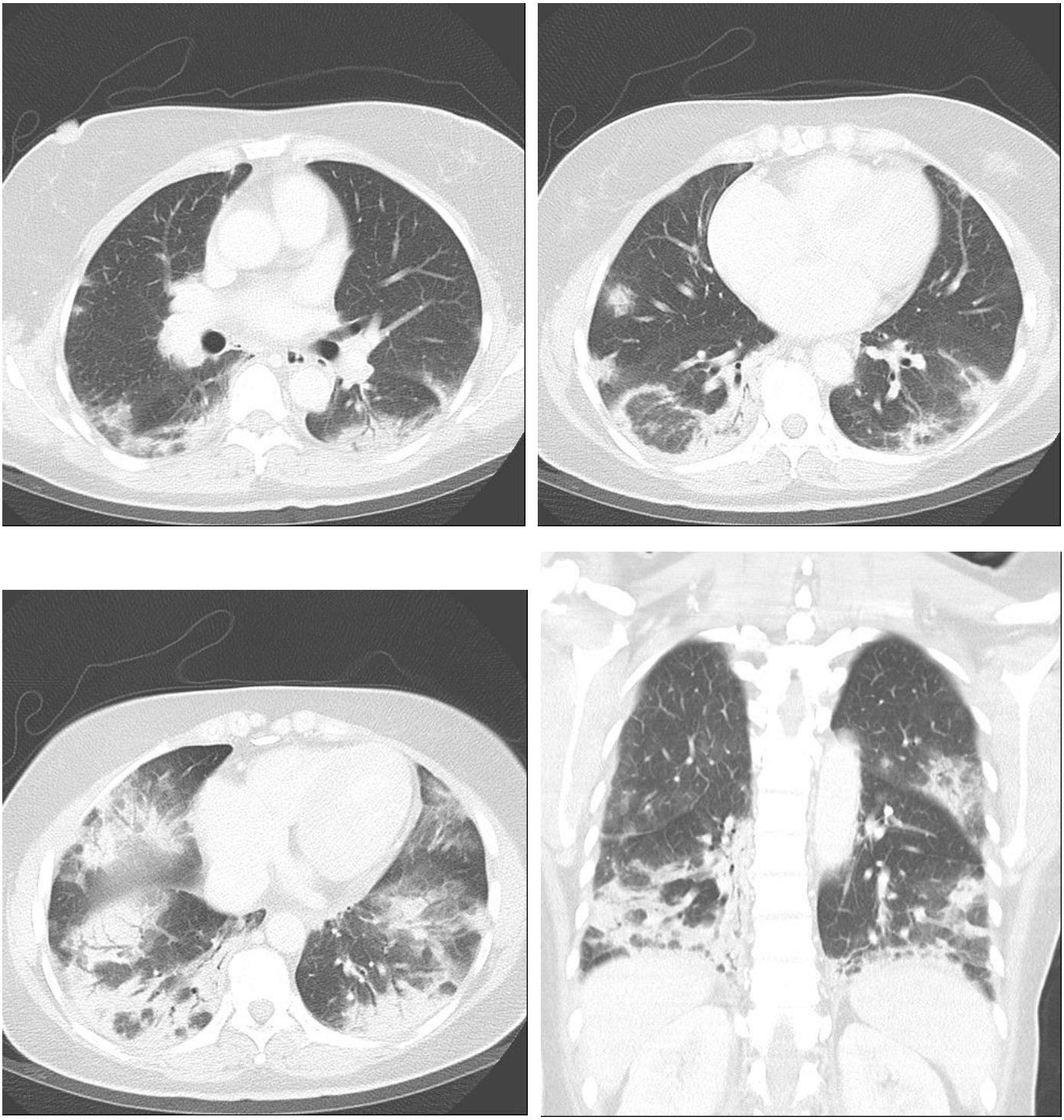

(S1o) Bilateral multi-lobe alveolar consolidations, ground-glass opacities, and reverse halo signs: transverse and coronal (5-mm-slice) views from a 50-year-old female with dermatomyositis (**multi-lobe and mixed-pattern**).

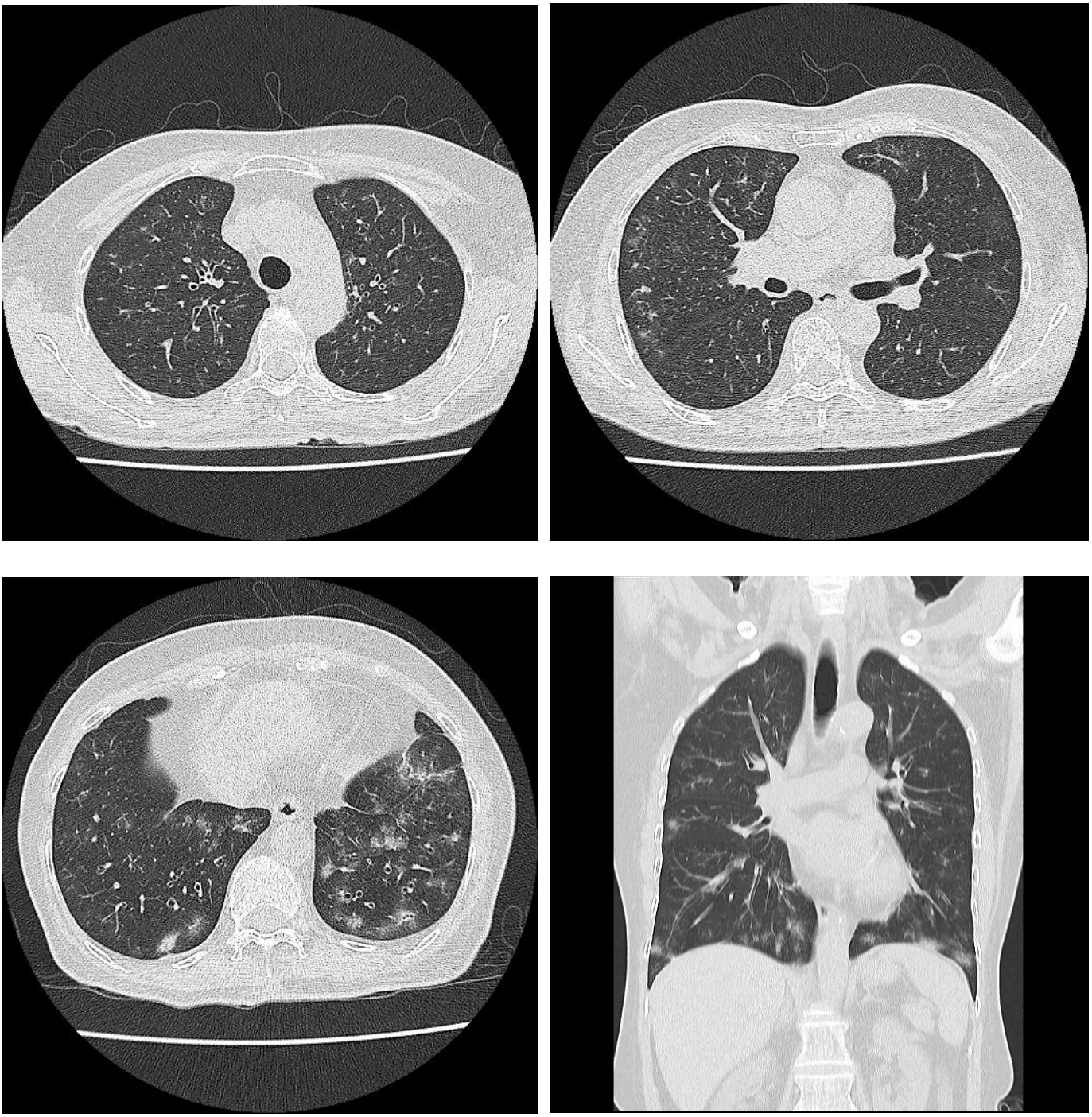

(S1p) Bilateral multi-lobe ground-glass and nodular opacities: transverse (2-mm-slice) and coronal (5-mm-slice) views from a 63-year-old female (**multi-lobe and mixed-pattern**).

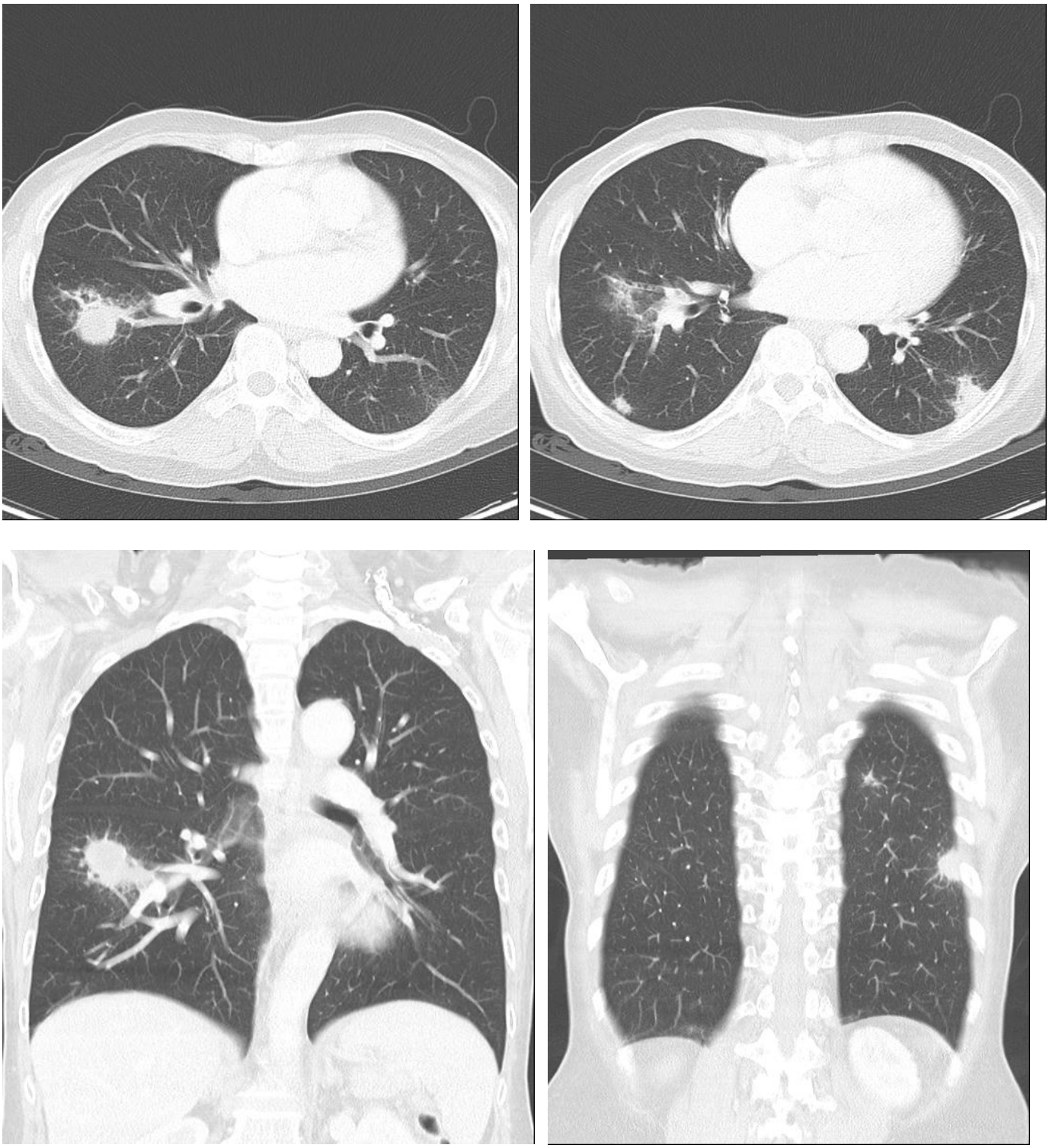

(S1q) Mass-like and multi-lobe nodular opacities: transverse and coronal views (5-mm-slice) from a 65-year-old female (**multi-lobe and mixed-pattern**).

Supplemental Figure S2 Results of the sensitivity analysis

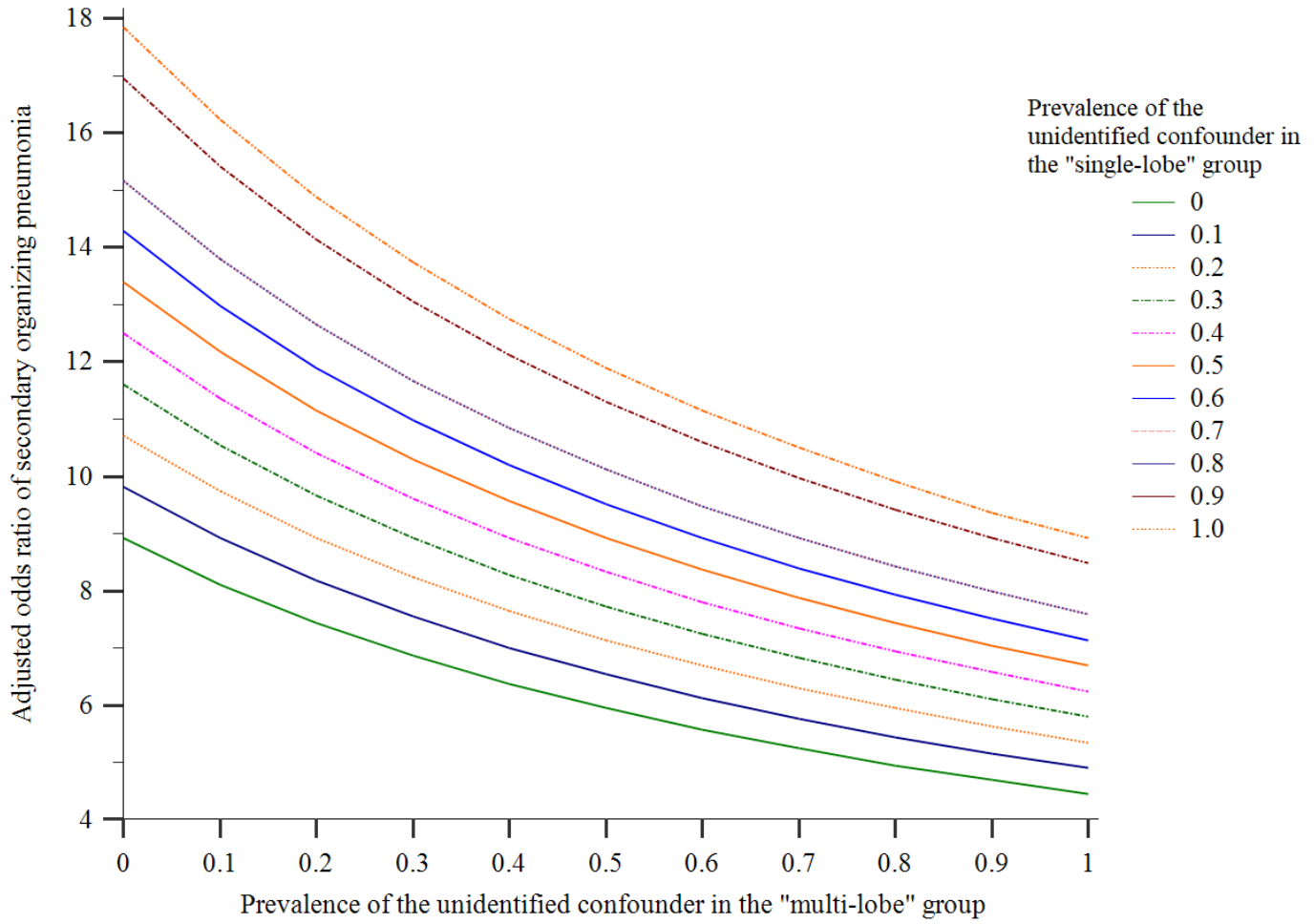

(S2a) Sensitivity analysis shows that, regardless of the various ratios of prevalence of the potentially unidentified confounder among the patient groups, the multivariable logistic regression model remained valid such that having multi-lobe involvement on the computed tomographic images persisted as a predictor of secondary organizing pneumonia.

Note: For sensitivity analysis, the adjusted odds ratios were derived from ordinary logistic regression analysis, using the R function “glm’ and controlling for such covariables as sex, age, body heights and weights, smoking status, and Charlson comorbidity indices. The sensitivity analysis was performed using the R package “obsSens”. The multiple line graph was plotted using MedCal.

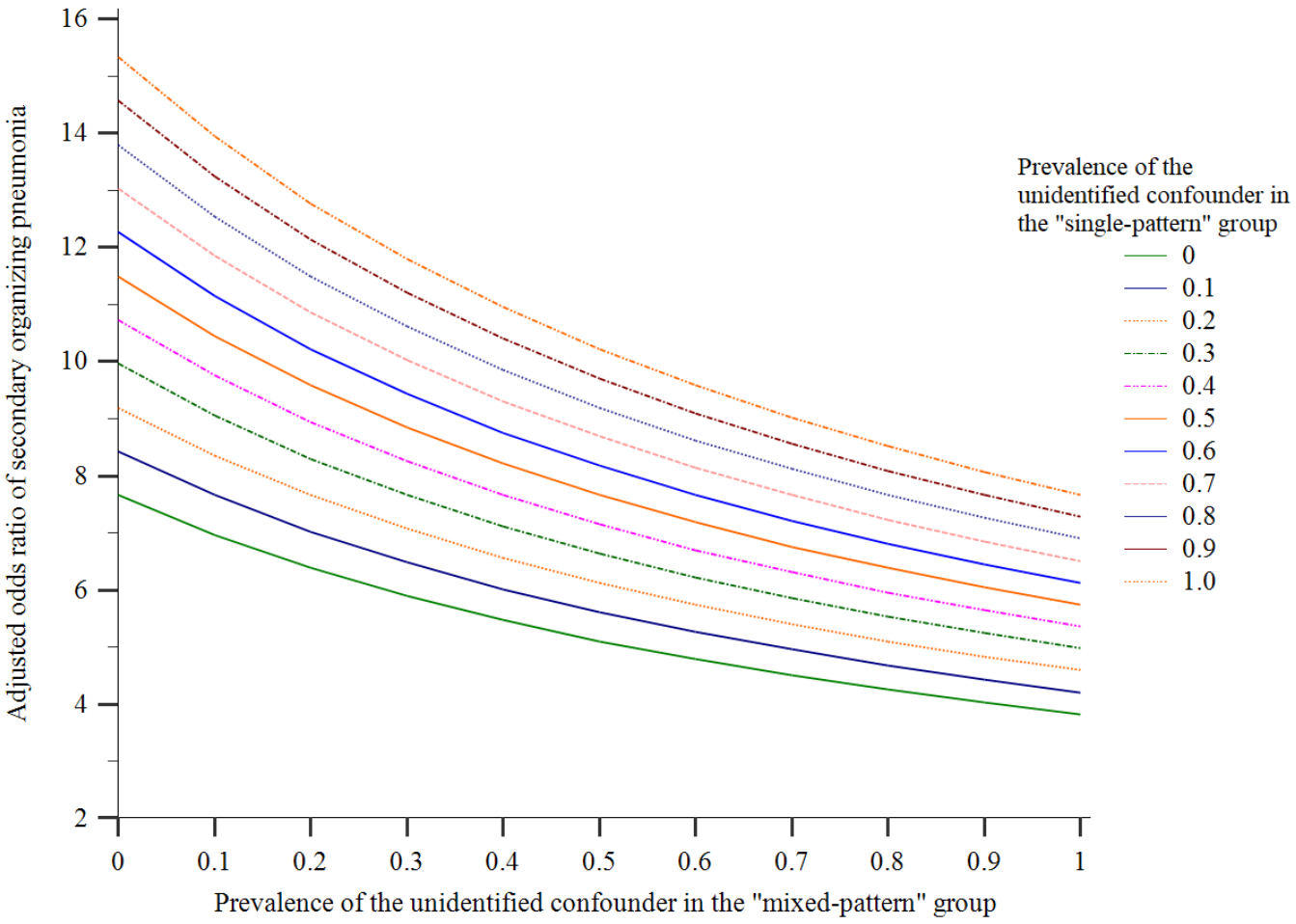

(S2b) Sensitivity analysis shows that, regardless of the various ratios of prevalence of the potentially unidentified confounder among the patient groups, the multivariable logistic regression model remained valid such that having mixed radiographic patterns on the computed tomographic images persisted as a predictor of secondary organizing pneumonia.

Note: For sensitivity analysis, the adjusted odds ratios were derived from ordinary logistic regression analysis, using the R function “glm’ and controlling for such covariables as sex, age, body heights and weights, smoking status, and Charlson comorbidity indices. The sensitivity analysis was performed using the R package “obsSens”. The multiple line graph was plotted using MedCal.

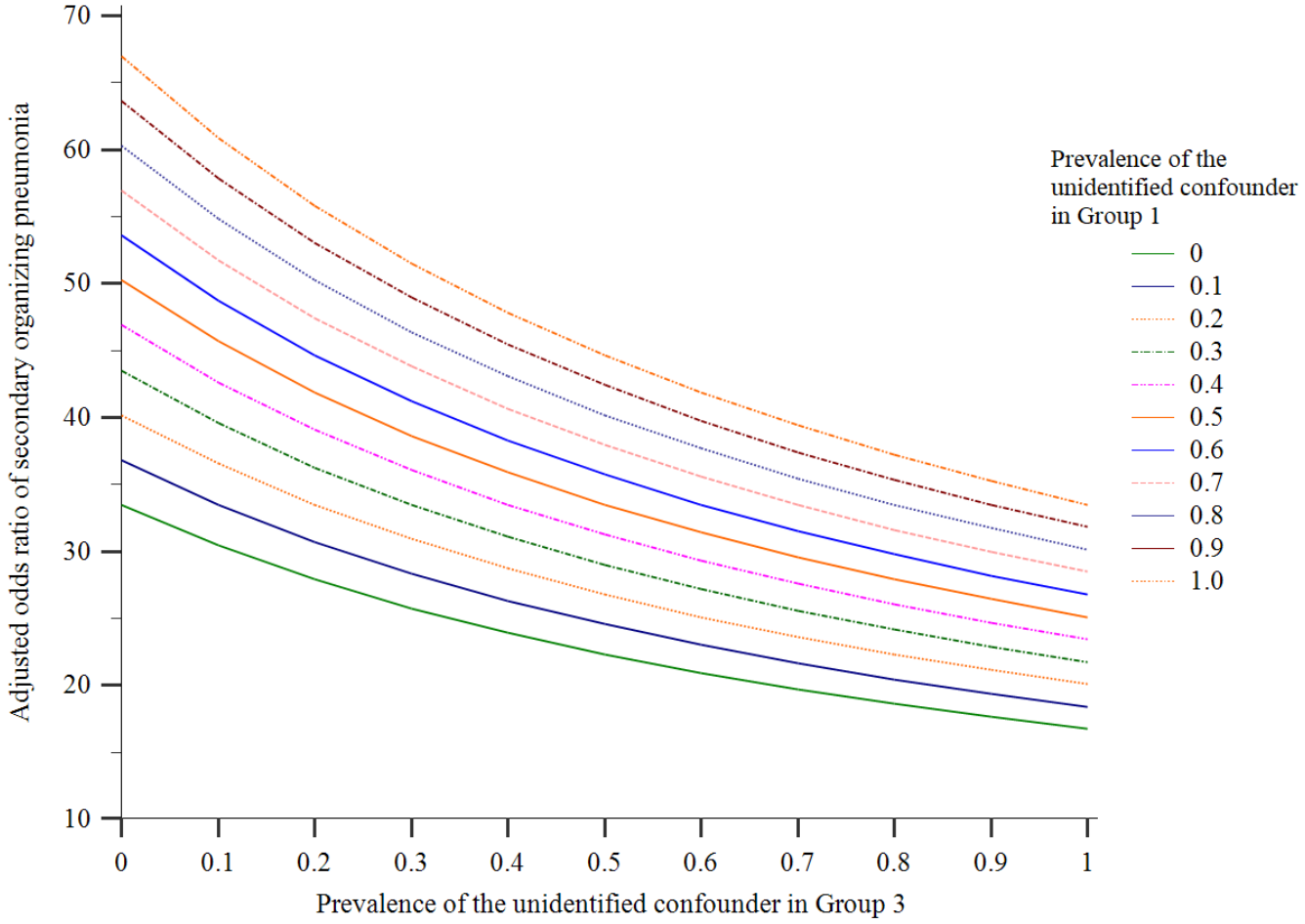

(S2c) Sensitivity analysis shows that, regardless of the various ratios of prevalence of the potentially unidentified confounder among the patient groups, the multivariable logistic regression model remained valid such that patients classified as Group 3 still had an increased odds (relative to Group 1) of secondary organizing pneumonia.

Note 1: Groups are based on the combined assessment of the extent and patterns of involvement on CT images: Group 1, single-lobe and single-pattern; Group 2, single-lobe and mixed-pattern or multi-lobe and single-pattern; Group 3, multi-lobe and mixed-pattern.

Note 2: For sensitivity analysis, the adjusted odds ratios were derived from ordinary logistic regression analysis, using the R function “glm’ and controlling for such covariables as sex, age, body heights and weights, smoking status, and Charlson comorbidity indices. The sensitivity analysis was performed using the R package “obsSens”. The multiple line graph was plotted using MedCal

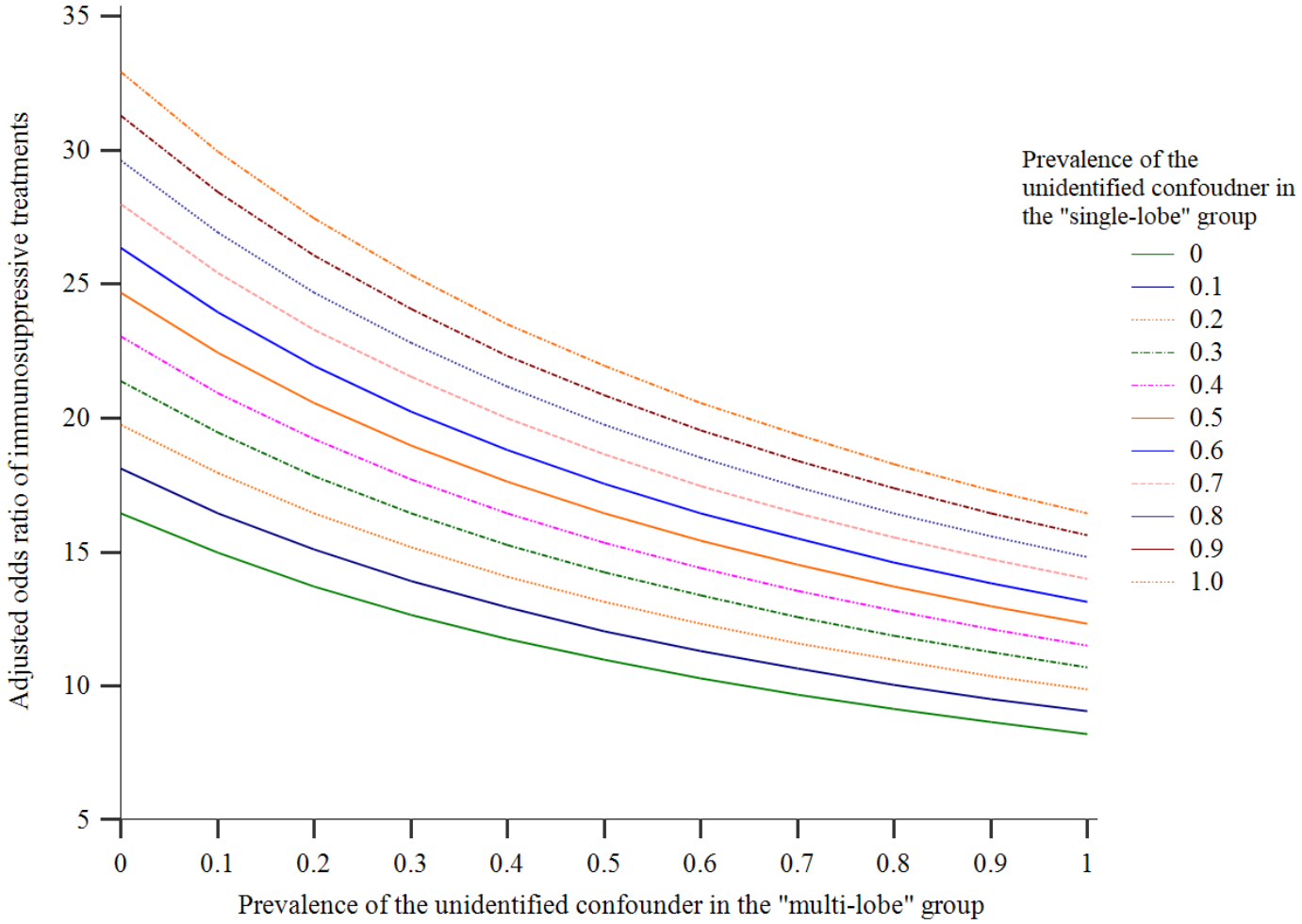

(S2d) Sensitivity analysis shows that, regardless of the various ratios of prevalence of the potentially unidentified confounder among the patient groups, the multivariable logistic regression model remained valid such that having multi-lobe involvement on the computed tomographic images persisted as a predictor of subsequent immunosuppressive treatments.

Note: For sensitivity analysis, the adjusted odds ratios were derived from ordinary logistic regression analysis, using the R function “glm’ and controlling for such covariables as sex, age, body heights and weights, smoking status, Charlson comorbidity indices, **and** aetiologies. The sensitivity analysis was performed using the R package “obsSens”. The multiple line graph was plotted using MedCal.

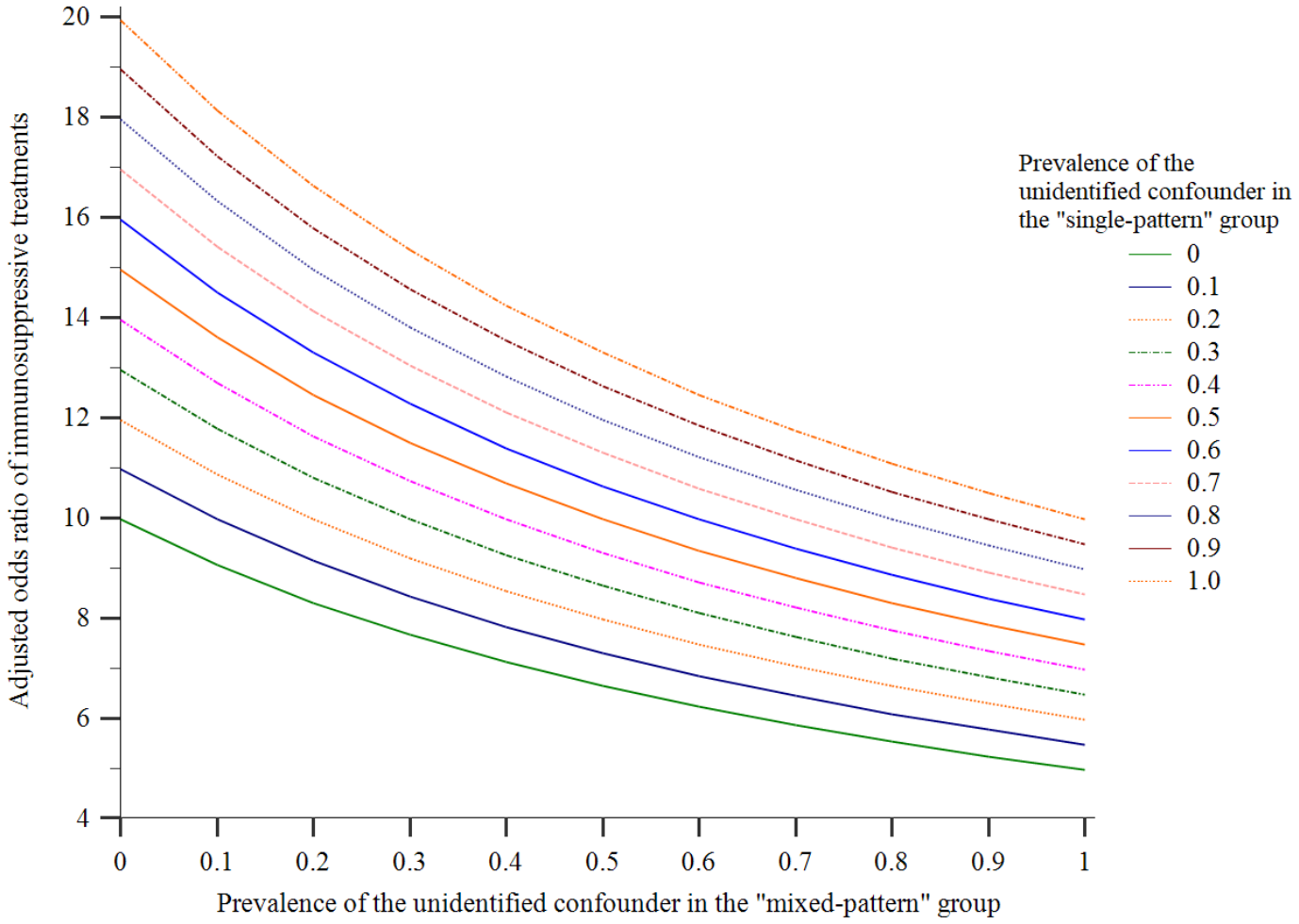

(S2e) Sensitivity analysis shows that, regardless of the various ratios of prevalence of the potentially unidentified confounder among the patient groups, the multivariable logistic regression model remained valid such that having mixed radiographic patterns on the computed tomographic images persisted as a predictor of subsequent immunosuppressive treatments.

Note: For sensitivity analysis, the adjusted odds ratios were derived from ordinary logistic regression analysis, using the R function “glm’ and controlling for such covariables as sex, age, body heights and weights, smoking status, Charlson comorbidity indices, **and** aetiologies. The sensitivity analysis was performed using the R package “obsSens”. The multiple line graph was plotted using MedCal.

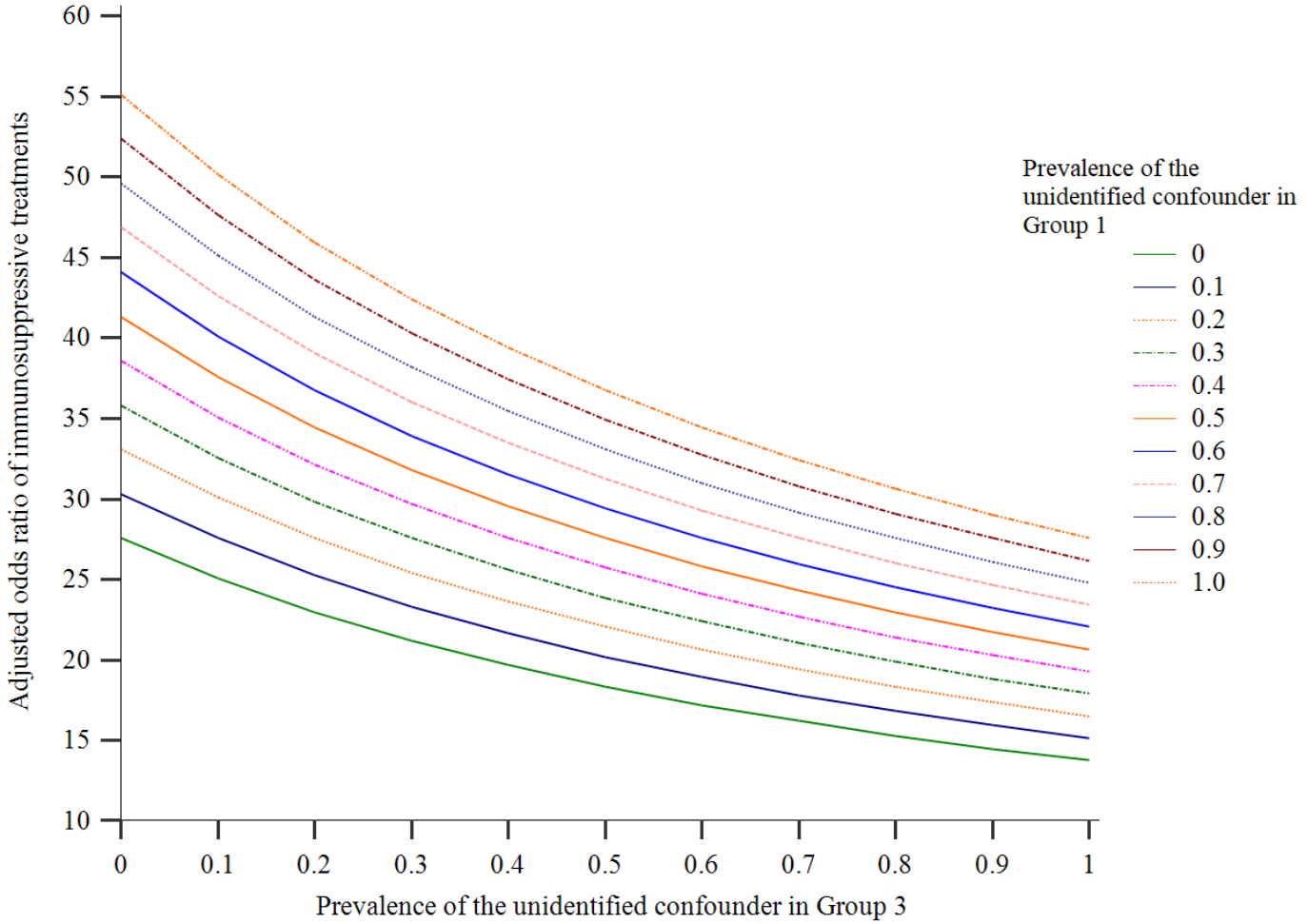

(S2f) Sensitivity analysis shows that, regardless of the various ratios of prevalence of the potentially unidentified confounder among the patient groups, the multivariable logistic regression model remained valid such that patients classified as Group 3 still had an increased odds (relative to Group 1) of subsequent immunosuppressive treatments.

Note 1: Groups are based on the combined assessment of the extent and patterns of involvement on CT images: Group 1, single-lobe and single-pattern; Group 2, single-lobe and mixed-pattern or multi-lobe and single-pattern; Group 3, multi-lobe and mixed-pattern.

Note 2: For sensitivity analysis, the adjusted odds ratios were derived from ordinary logistic regression analysis, using the R function “glm’ and controlling for such covariables as sex, age, body heights and weights, smoking status, Charlson comorbidity indices, **and** aetiologies. The sensitivity analysis was performed using the R package “obsSens”. The multiple line graph was plotted using MedCal

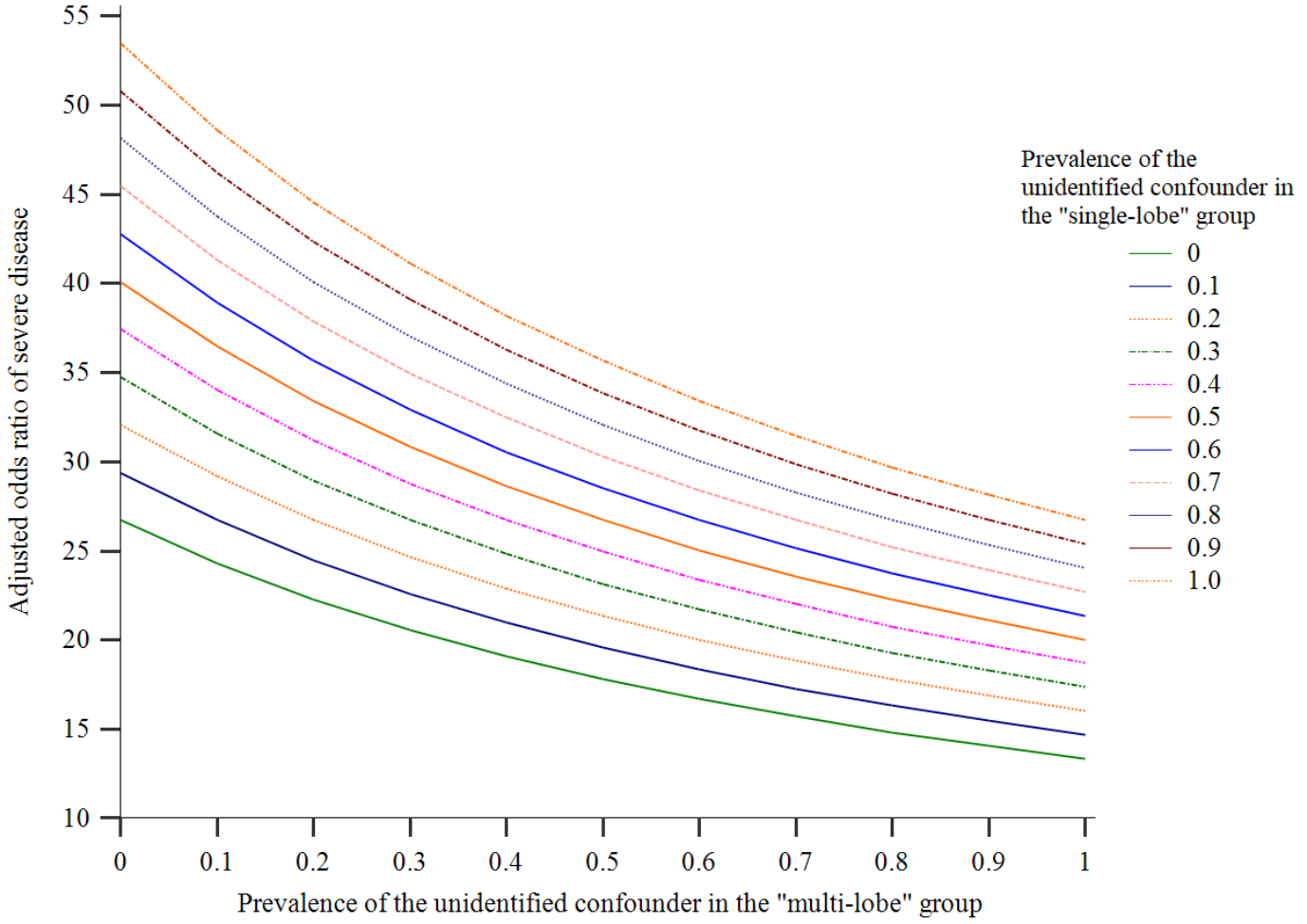

(S2g) Sensitivity analysis shows that, regardless of the various ratios of prevalence of the potentially unidentified confounder among the patient groups, the multivariable logistic regression model remained valid such that having multi-lobe involvement on the computed tomographic images persisted as a predictor of severe disease.

Note: For sensitivity analysis, the adjusted odds ratios were derived from ordinary logistic regression analysis, using the R function “glm’ and controlling for such covariables as sex, age, body heights and weights, smoking status, Charlson comorbidity indices, **and** aetiologies. The sensitivity analysis was performed using the R package “obsSens”. The multiple line graph was plotted using MedCal.

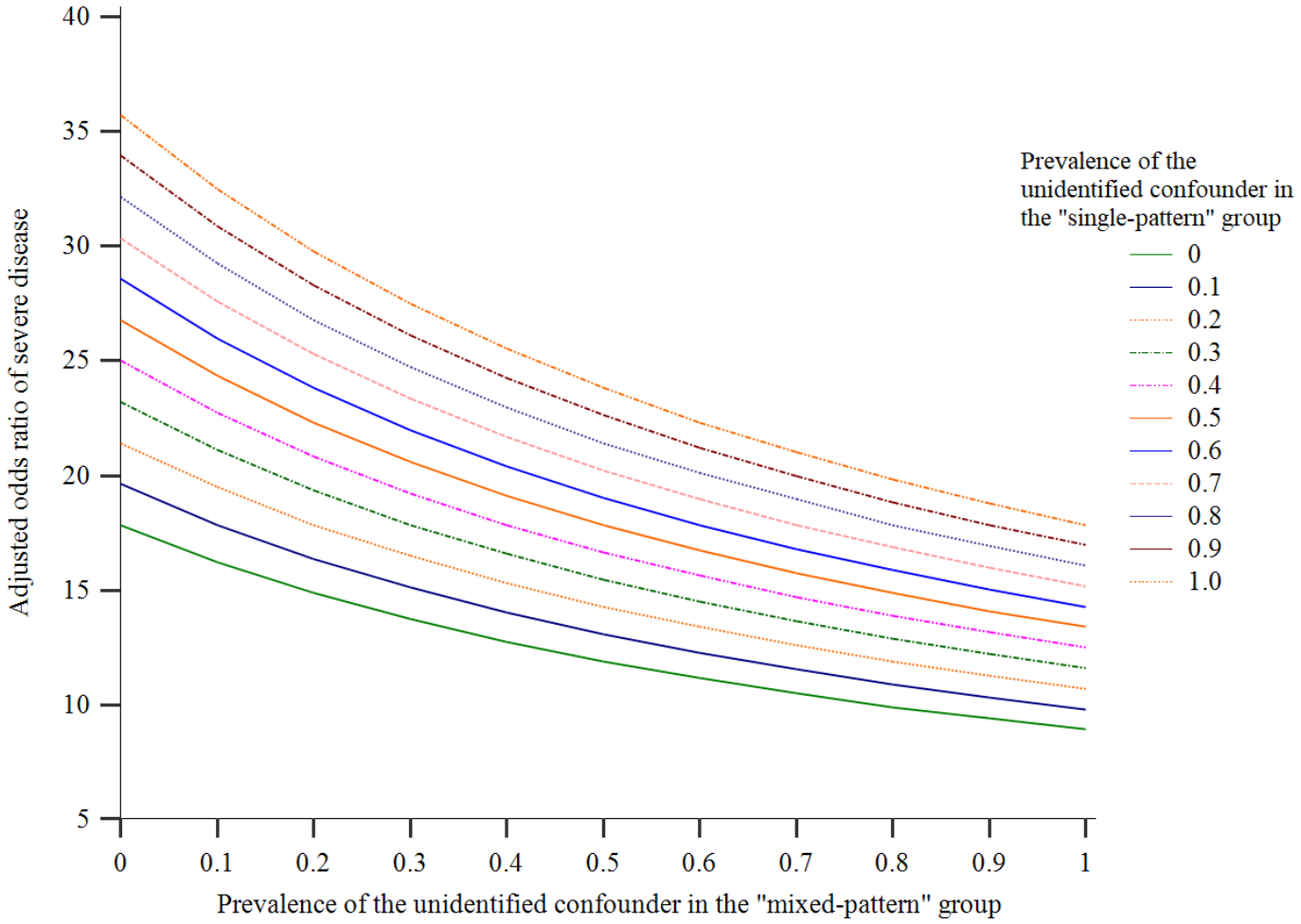

(S2h) Sensitivity analysis shows that, regardless of the various ratios of prevalence of the potentially unidentified confounder among the patient groups, the multivariable logistic regression model remained valid such that having mixed radiographic patterns on the computed tomographic images persisted as a predictor of severe disease.

Note: For sensitivity analysis, the adjusted odds ratios were derived from ordinary logistic regression analysis, using the R function “glm’ and controlling for such covariables as sex, age, body heights and weights, smoking status, Charlson comorbidity indices, **and** aetiologies. The sensitivity analysis was performed using the R package “obsSens”. The multiple line graph was plotted using MedCal.

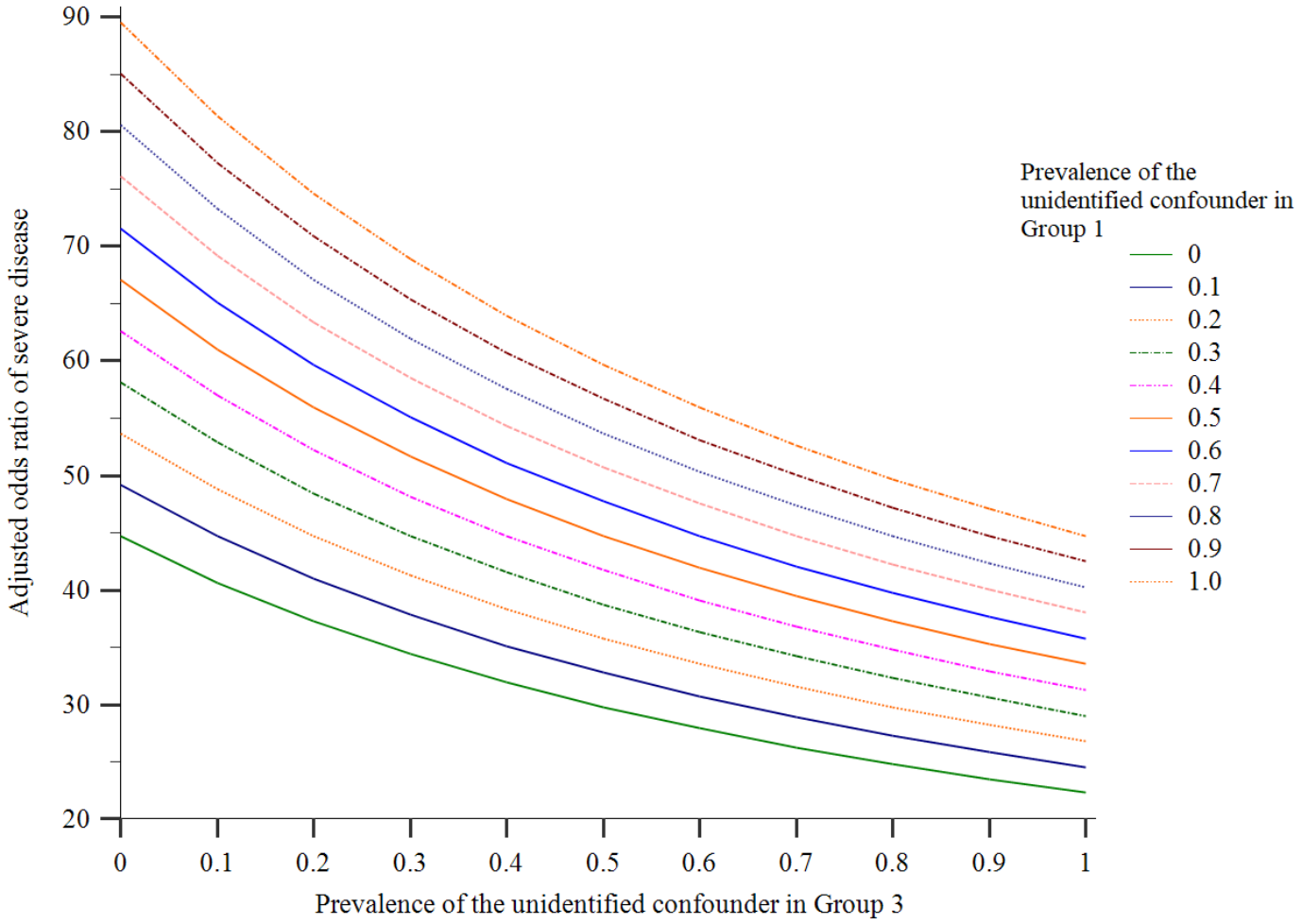

(S2i) Sensitivity analysis shows that, regardless of the various ratios of prevalence of the potentially unidentified confounder among the patient groups, the multivariable logistic regression model remained valid such that patients classified as Group 3 still had an increased odds (relative to Group 1) of severe disease.

Note 1: Groups are based on the combined assessment of the extent and patterns of involvement on CT images: Group 1, single-lobe and single-pattern; Group 2, single-lobe and mixed-pattern or multi-lobe and single-pattern; Group 3, multi-lobe and mixed-pattern.

Note 2: For sensitivity analysis, the adjusted odds ratios were derived from ordinary logistic regression analysis, using the R function "glm' and controlling for such covariables as sex, age, body heights and weights, smoking status, Charlson comorbidity indices, **and** aetiologies. The sensitivity analysis was performed using the R package "obsSens". The multiple line graph was plotted using MedCal

Supplemental Figure S3 Results from the analyses involving **only** patients with ***cryptogenic*** organizing pneumonia (N = 130)

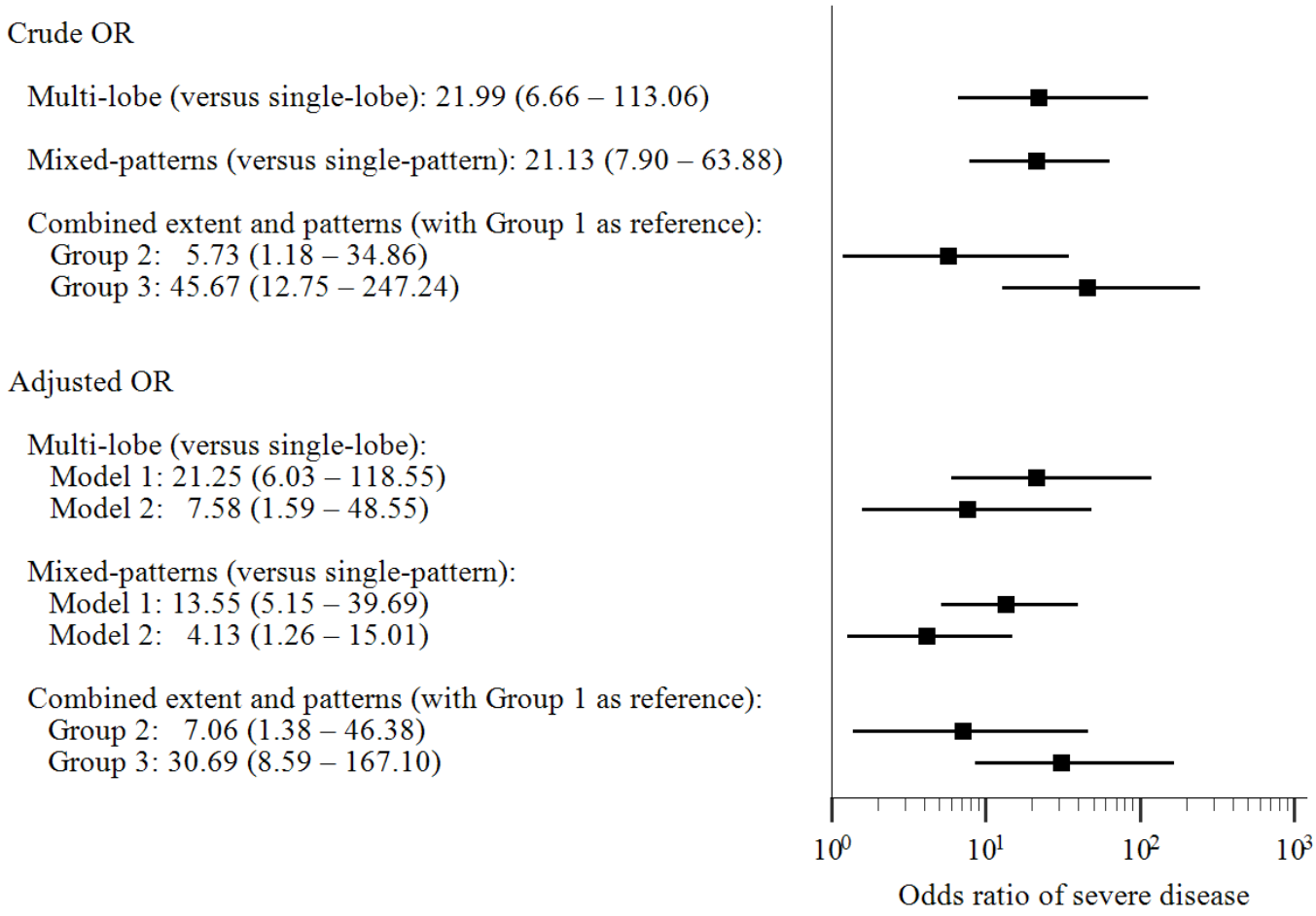

(S3a) Forest plot of the crude and adjusted odds ratios (OR, derived from univariate and multivariable Firth's logistic regression analysis) of severe disease for different computed tomographic (CT) radiographic features, involving **only** patients with ***cryptogenic*** organizing pneumonia (N = 130).
Note: Groups are based on the combined assessment of the extent and patterns of involvement on CT images: Group 1, single-lobe and single-pattern; Group 2, single-lobe and mixed-pattern or multi-lobe and single-pattern; Group 3, multi-lobe and mixed-pattern. In Model 1, either extent of involvement or patterns on CT was *separately* included (together with other covariables) in the multivariable Firth's logistic regression analysis. In Model 2, *both* extent of involvement and patterns on CT were *simultaneously* included (together with other covariables) in the multivariable Firth's logistic regression analysis.

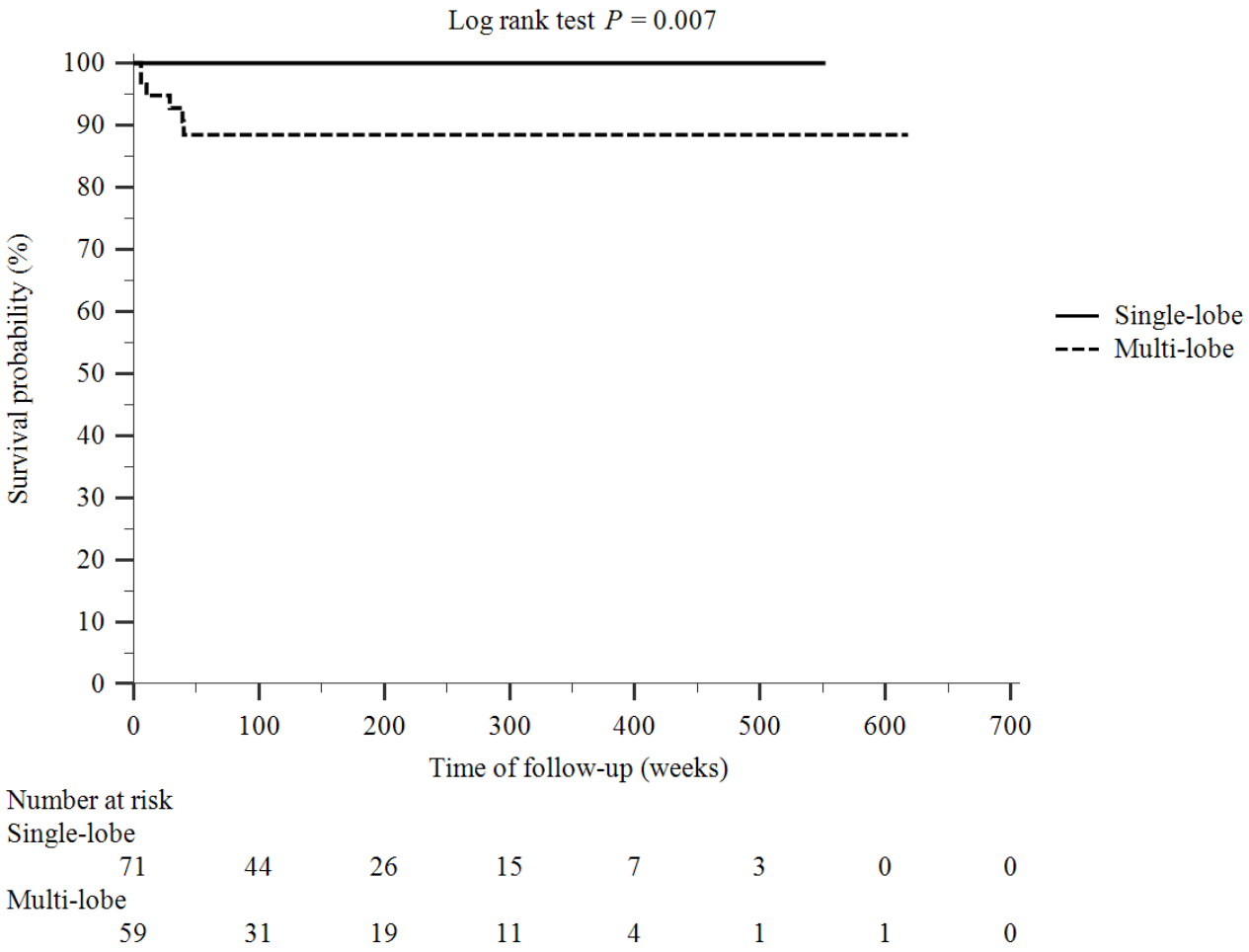

(S3b) Kaplan-Meier survival analyses between the "single-lobe" and "multi-lobe" groups, involving **only** patients with ***cryptogenic*** organizing pneumonia (N = 130).

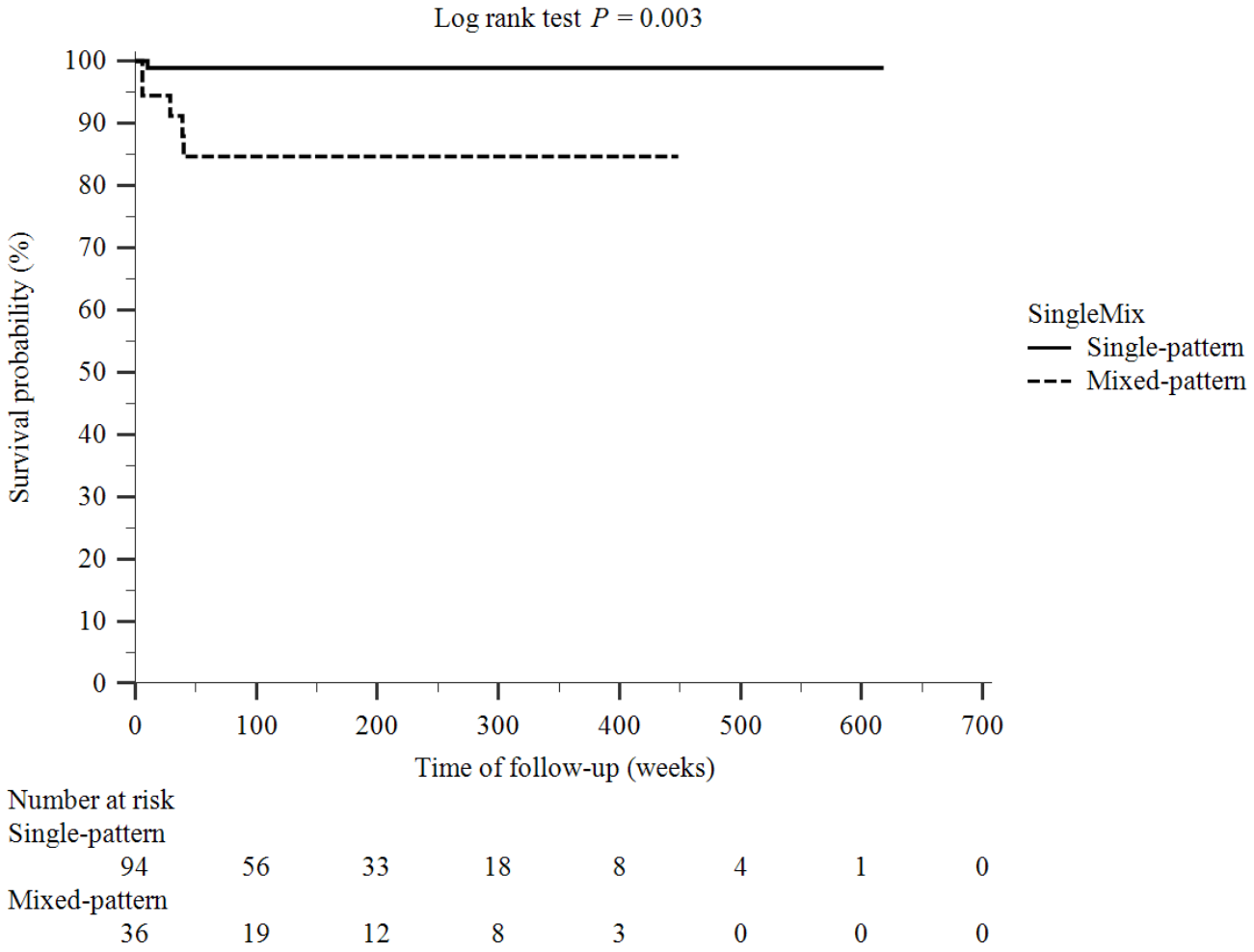

(S3c) Kaplan-Meier survival analyses between the "single-pattern" and "multi-pattern" groups, involving **only** patients with ***cryptogenic*** organizing pneumonia (N = 130).

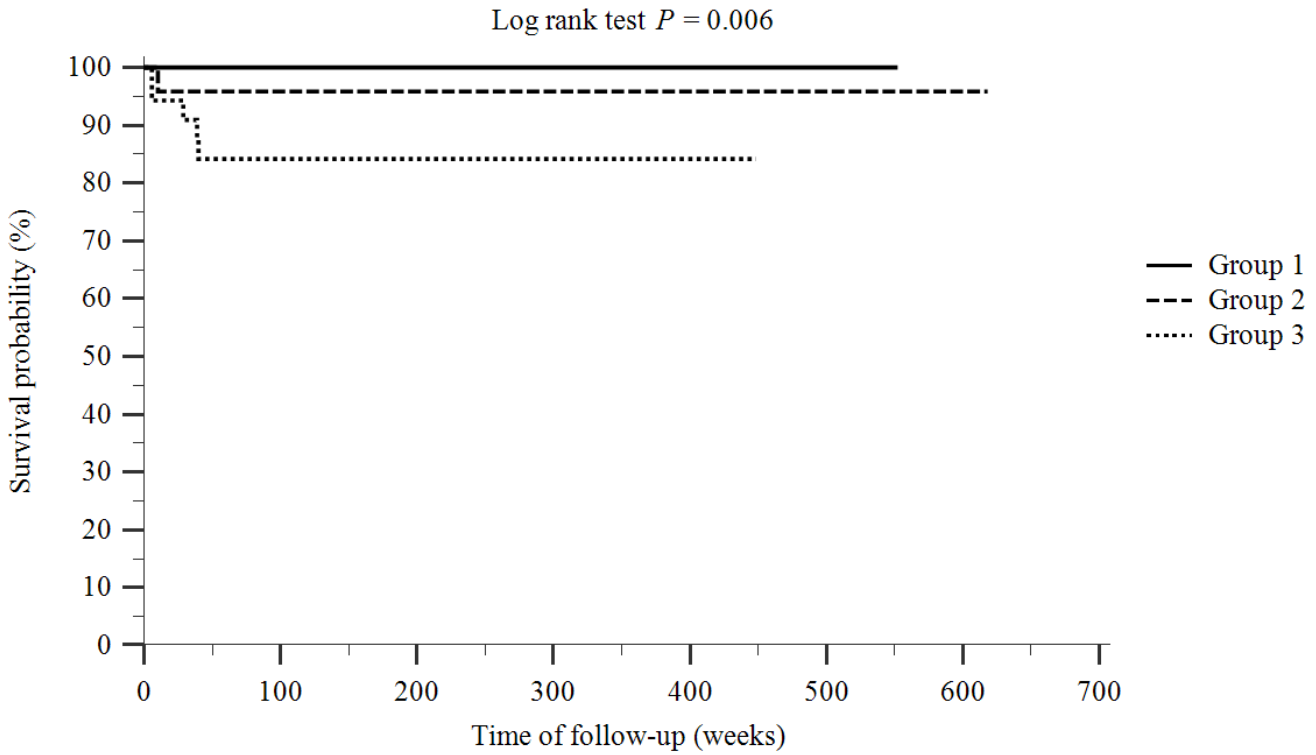

Number at risk							
Group Group 1							
70	43	25	15	7	3	0	0
Group Group 2							
25	14	9	3	1	1	1	0
Group Group 3							
35	18	11	8	3	0	0	0

(S3d) Kaplan-Meier survival analyses among Groups 1, 2, and 3, involving **only** patients with ***cryptogenic*** organizing pneumonia (N = 130).

Note: Groups are based on the combined assessment of the extent and patterns of involvement on computed tomographic images: Group 1, single-lobe and single-pattern; Group 2, single-lobe and mixed-pattern or multi-lobe and single-pattern; Group 3, multi-lobe and mixed-pattern.

Supplemental Document 1: The Protocols on Patient Inclusion / Exclusion, Diagnostic Verification and Classification, and Outcome Determination

Institutional Review Board Approval Number: B-ER-111-038

Part A: Inclusion and exclusion criteria

Inclusion criteria:

1. Age 20 ≥ years old.
2. Patients with the diagnosis of "organizing pneumonia" who were diagnosed, treated, and followed at National Cheng Kung University Hospital (NCKUH) – the diagnosis is presented in the electronic medical database in the form of typed medical terms or compatible International Classification of Disease (ICD) codes (ICD-9-CM 516.36 or ICD-10-CM J84.116).

Exclusion criteria:

1. Age < 20 years old.
2. Incomplete data or incomplete follow-up in the electronic medical database of NCKUH.
3. No baseline computed tomography of the chest upon the diagnosis of organizing pneumonia.
4. No histologic confirmation of the organizing pneumonia.
5. Presentation not compatible with organizing pneumonia in the clinical, laboratory, and/or histological domains (see Part B).

Part B: Verification of the diagnosis "organizing pneumonia"

Clinical domain:

1. All the event-relevant inpatient and outpatient electronic medical records were reviewed.
2. Initial manifestation
   - Compatible with organizing pneumonia: nonproductive cough, fever, malaise, fatigue, weight loss, resting and/or exertional dyspnea, respiratory insufficiency
   - Incompatible with organizing pneumonia: shock, copious/purulent sputum, massive hemoptysis, orthopnea or other symptoms/signs suggesting cardiogenic pulmonary congestion/edema
3. **Not** organizing pneumonia if an alternative diagnosis (ex. infectious pneumonia) was later made by the treating physician in the follow-ups as documented in the electronic medical records.

Laboratory domain:

1. All the event-relevant blood, serological, microbiological, histological test results in the electronic medical records were reviewed.
2. Leukocytosis and elevation in the levels (if available) of LDH, CRP, ESR, ferritin was acceptable and did not necessarily indicate infectious pneumonia.
3. **Not** organizing pneumonia if positive findings from any of the following tests (available at NCKUH) that were considered causally relevant and explanatory to the event:
   - Common bacterial/fungal/mycobacterial cultures of sputum and/or lavage fluid and/or lung tissue;
   - Viral isolation from sputum and/or lavage fluid;
   - *Pneumocystis carinii*-PCR TB-PCR, Aspergillus antigen of sputum and/or lavage fluid;
   - TB-PCR of lung tissue;
   - Serological tests for Mycoplasma, *Legionella pneumophila,* S*treptococcus pneumonia*, Aspergillus antigen, rickettsial infection, EBV, CMV;
   - Viral load of CMV.

Histological domain:

1. All the surgical/procedure notes and records of tissue sampling, relevant radiographic images, pathology reports, and histological slides were reviewed by the authors including the two pathologists and the thoracic surgeon.
2. Acceptable methods of histologic sampling: transbronchial forceps or cryoprobe biopsy, sonography-guided percutaneous needle biopsy, CT-guided percutaneous needle biopsy, surgical / video-assisted thoracoscopic biopsy.
3. Essential histological features of organizing pneumonia must be present:
   - preserved alveolar architecture – some degree of interstitial fibrosis is acceptable, but **not** extensive fibrosis or evident alveolar distortion or honeycombing changes;
   - Masson bodies;
   - mild-to-moderate degree of interstitial infiltrate by chronic inflammatory cells; formation of some germinal centers are acceptable in patients with underlying connective tissue diseases
4. **Not** organizing pneumonia if any of the following histological features present:
   - ongoing infection: dense neutrophilic infiltration with/without direct or indirect identification of microbial presence; cytopathic features suggesting viral infection;
   - bronchiole-centered or bronchiole-obliterative process;
   - caseous / necrotizing / non-necrotizing granuloma;

- vasculitis;
- neoplasm;
- alveolar hemorrhage;
- alveolar proteinosis;
- alveolar aggregates of foamy macrophages;
- dense eosinophilic infiltration;
- the predominant pattern is suggestive of other interstitial lung disease.

Part C: Classification of organizing pneumonia

1. The organizing pneumonia was classified as **secondary** organizing pneumonia if meeting any of the following criteria that was considered causally relevant:
   - Drug-related - documentation in the electronic medical records of the use of any of the following agent within 3 months of OP onset: amiodarone, amphotericin B, dronedarone, interferons, chemotherapeutic (anti-cancer) agents (but **excluding** any form of corticosteroids), immune checkpoint inhibitors, methotrexate, mTOR-inhibitors (sirolimus, everolimus), sulfasalazine, tacrolimus, tyrosine kinase inhibitors
   - Radiation therapy-related – documentation in the electronic medical records of radiation therapy involving pertinent lung fields within 6 months of OP onset.
   - Post-transplantation – documentation of solid-organ or hematological transplantation in the electronic medical records within 2 years of OP onset PLUS compatible histological findings.
   - Connective tissue disease (CTD)-related:
     - Documented diagnosis of an underlying CTD (with or without the identity granted by Taiwan's of Registry Catastrophic Diseases), or
     - a CTD was newly diagnosed / highly suspected during or following the onset of OP, with supporting serologies / auto-antibodies and/or documented symptomology and/or documented physical findings and/or positive results from other pertinent tests (ex. Schirmer's test by ophthalmologists, salivary gland scintigraphy, biopsy of minor salivary gland, biopsy of skeletal muscle, electromyography…etc.)
     - Consultation to rheumatologists if necessary.
2. The organizing pneumonia was classified as **cryptogenic** if none of the above-listed secondary etiology could be identified after thorough review of the electronic medical records.
3. Disagreement regarding classification was solved by direct discussion and consensus among the authors.

Part D: Outcome determination

1. For outcome determination, serial electronic medical data, images, and records in the following domains were reviewed, starting from the date of diagnosis to patients' death or the defined end of the study period (December 31, 2021).
   - Radiographic domain:
     - serial CT images were reviewed, compared, and correlated with findings from the clinical domain, until stable state of the radiographic findings (note: 101 patients had at least one follow-up CT scan);
     - for those without subsequent CT scans, serial chest radiographs were reviewed, compared, and correlated with findings from the clinical domain, until stable state of the radiographic findings.
   - Clinical domain:
     - All inpatient and outpatient electronic medical records were reviewed
     - Records of admission, oxygen supplement (serial changes in device, flow rate, duration), mechanical ventilation support (device, FiO_2, duration) – OP related or other potentially explanatory alternative etiology?
     - Documentation of changes / sable state / recurrence of respiratory symptoms – OP related or other potentially explanatory alternative etiology?
     - Changes (dosage, type, numbers) in the prescription of respiratory medication – antitussive agents, mucolytic agents, bronchodilators – OP related or other potentially explanatory alternative etiology?
     - Changes (dosage, type, numbers) in the prescription of corticosteroids and/or non-steroid immunosuppressants – OP related or other potentially explanatory alternative etiology?
     - Death – date and documented cause – OP related or other potentially explanatory alternative etiology?
2. Based on the integrated assessment of findings from the radiographic and clinical domains, the following outcomes were defined:
   - "Improvement"
     - radiographic domain: resolution of OP-related lesions > 50% (with or without decrement in radiodensity) on serial images **without** re-emergence;
     - clinical domain: symptomatic alleviation with/without decrement in the number and dosage of symptom-relieving medication and/or decrement in the number and dosage of immunosuppressants and/or decrement in non-pharmacological management (oxygen supplementation,

mechanical ventilatory support…etc).

- "Persistent disease"
  - Radiographic domain: steadiness of OP-related lesions (with or without migration) or a diminishment <50% on serial images
  - Clinical domain - persistence or limited change in: clinical symptoms, the number and dosage of symptom-relieving medication, the number and dosage of immunosuppressants, and non-pharmacological management (oxygen supplementation, mechanical ventilatory support…etc).
- "Recurrence"
  - Radiographic domain: re-emergence or enlargement of OP-related lesions (with or without migration) on serial images following an initial "improvement" (as defined above).
  - Clinical domain: escalation in symptoms, escalation in pharmacological and/or non-pharmacological management - without any alternative explanation; documentation of "recurrence" by the treating physician
- "Death" – only OP-related death is included for further analysis.
- "Need of supplemental oxygen" – need of supplemental oxygen via any mode to correct hypoxemia during the follow-up.
  - Not including the elective supplemental oxygen use immediately before or after lung biopsy.
- "Use of mechanical ventilation" – need of either non-invasive or invasive positive-pressure mechanical ventilation to treat OP-related respiratory failure.
  - Not including mechanical ventilation during general anesthesia for surgical lung biopsy.

3. Changes in pulmonary function tests were **not** included as essential criteria for the determination of outcomes, because not all patients had baseline pulmonary function tests (86 had forced vital capacity or FVC, 71 had total lung capacity or TLC, 20 had diffusion capacity of the lung for carbon monoxide or D_{LCO}), and only 27 patients had a follow-up pulmonary spirometry in the stable state for comparison.
   - For those 27 patients having follow-up tests, serial changes in forced vital capacity (FVC) were calculated and used as supporting data.
4. Disagreement regarding outcome assignment is solved by direct discussion and consensus among the authors.